Title

Optimizing Nervous System-Specific Gene Targeting with Cre Driver Lines: Prevalence of Germline Recombination and Influencing Factors.

Journal

Neuron, 106(1)

ISSN

0896-6273

Authors

Luo, Lin
Ambrozkiewicz, Mateusz C
Benseler, Fritz
et al.

Publication Date

2020-04-01

DOI

10.1016/j.neuron.2020.01.008

Peer reviewed

NeuroResource

Neuron

Optimizing Nervous System-Specific Gene Targeting with Cre Driver Lines: Prevalence of Germline Recombination and Influencing Factors

Highlights

- Most mouse Cre driver lines tested exhibited variable rates of germline recombination
- Germline recombination exhibits parental sex bias and target locus selectivity
- Similar principles apply to multiple organisms and recombinase systems
- Guidelines are provided for detecting and minimizing unwanted germline recombination

Authors

Lin Luo, Mateusz C. Ambrozkiewicz, Fritz Benseler, ..., Huda Yahya Zoghbi, Hiroshi Kawabe, Ann Marie Craig

Correspondence

kawabe@em.mpg.de (H.K.), acraig@mail.ubc.ca (A.M.C.)

In Brief

Luo et al. report variable rates of germline recombination in commonly used mouse Cre driver lines, influenced by sex of Cre-carrying parents and target loci. Guidelines are provided to optimize cell-type-specific recombination in genetically targeted organisms expressing site-specific recombinases.

Luo et al., 2020, Neuron *106*, 1–29
April 8, 2020
https://doi.org/10.1016/j.neuron.2020.01.008

CellPress

Please cite this article in press as: Luo et al., Optimizing Nervous System-Specific Gene Targeting with Cre Driver Lines: Prevalence of Germline Recombination and Influencing Factors, Neuron (2020), https://doi.org/10.1016/j.neuron.2020.01.008

Neuron
NeuroResource

Optimizing Nervous System-Specific Gene Targeting with Cre Driver Lines: Prevalence of Germline Recombination and Influencing Factors

Lin Luo,[1] Mateusz C. Ambrozkiewicz,[2,3] Fritz Benseler,[2] Cui Chen,[4] Emilie Dumontier,[5] Susanne Falkner,[6] Elisabetta Furlanis,[6] Andrea M. Gomez,[6] Naosuke Hoshina,[7] Wei-Hsiang Huang,[8,9] Mary Anne Hutchison,[10] Yu Itoh-Maruoka,[11] Laura A. Lavery,[12,13] Wei Li,[4] Tomohiko Maruo,[11,14,15] Junko Motohashi,[16] Emily Ling-Lin Pai,[17,18] Kenneth A. Pelkey,[19] Ariane Pereira,[20] Thomas Philips,[21] Jennifer L. Sinclair,[22] Jeff A. Stogsdill,[23,24] Lisa Traunmüller,[6] Jiexin Wang,[25] Joke Wortel,[26] Wenjia You,[25,27,28] Nashat Abumaria,[4,29] Kevin T. Beier,[30] Nils Brose,[2]

(Author list continued on next page)

[1]Djavad Mowafaghian Centre for Brain Health and Department of Psychiatry, University of British Columbia, 2211 Wesbrook Mall, Vancouver, BC V6T 2B5, Canada
[2]Department of Molecular Neurobiology, Max Planck Institute of Experimental Medicine, Hermann-Rein-Strasse 3, 37075 Göttingen, Germany
[3]Institute of Cell Biology and Neurobiology, Charité-Universitätsmedizin Berlin, corporate member of Freie Universität Berlin, Humboldt-Universität zu Berlin, and Berlin Institute of Health, Charitéplatz 1, 10117 Berlin, Germany
[4]State Key Laboratory of Medical Neurobiology and MOE Frontiers Center for Brain Science, Institutes of Brain Science, Fudan University, Shanghai 200032, China
[5]Department of Neurology & Neurosurgery, Montreal Neurological Institute, McGill University, Montreal, QC H3A 2B4, Canada
[6]Biozentrum of the University of Basel, Basel, Switzerland
[7]F.M. Kirby Neurobiology Center, Department of Neurology, Boston Children's Hospital, Harvard Medical School, Boston, MA 02115, USA
[8]Department of Biology, Howard Hughes Medical Institute, Stanford University, Stanford, CA 94305, USA
[9]Centre for Research in Neuroscience, Department of Neurology and Neurosurgery, The Research Institute of the McGill University Health Centre, Montreal, QC H3G 1A4, Canada
[10]Synapse and Neural Circuit Research Unit, National Institute of Neurological Disorders and Stroke, National Institutes of Health, Bethesda, MD 20892, USA
[11]Division of Pathogenetic Signaling, Department of Biochemistry and Molecular Biology, Kobe University Graduate School of Medicine, 1-5-6 Minatojima-minamimachi, Chuo-ku, Kobe, Hyogo 650-0047, Japan
[12]Department of Molecular and Human Genetics, Jan and Dan Duncan Neurological Research Institute at Texas Children's Hospital, Houston, TX 77003, USA
[13]Howard Hughes Medical Institute, Baylor College of Medicine, Houston, TX 77030, USA
[14]Department of Biochemistry, Tokushima University Graduate School of Medical Sciences, 3-18-15, Kuramoto-cho, Tokushima 770-8503, Japan

(Affiliations continued on next page)

SUMMARY

The Cre-loxP system is invaluable for spatial and temporal control of gene knockout, knockin, and reporter expression in the mouse nervous system. However, we report varying probabilities of unexpected germline recombination in distinct Cre driver lines designed for nervous system-specific recombination. Selective maternal or paternal germline recombination is showcased with sample Cre lines. Collated data reveal germline recombination in over half of 64 commonly used Cre driver lines, in most cases with a parental sex bias related to Cre expression in sperm or oocytes. Slight differences among Cre driver lines utilizing common transcriptional control elements affect germline recombination rates. Specific target loci demonstrated differential recombination; thus, reporters are not reliable proxies for another locus of interest. Similar principles apply to other recombinase systems and other genetically targeted organisms. We hereby draw attention to the prevalence of germline recombination and provide guidelines to inform future research for the neuroscience and broader molecular genetics communities.

INTRODUCTION

Advances in modern neuroscience research rely on genetically targeted animal models incorporating site-specific recombinase technology to achieve gene manipulations in a spatially and temporally controlled manner. Among all genetic tools, the Cre-loxP system has arguably been the most frequently used approach since its first discovery in bacteriophage P1 (Sternberg

Harold A. Burgess,[22] Constance L. Cepko,[27,28] Jean-François Cloutier,[5] Cagla Eroglu,[31] Sandra Goebbels,[32] Pascal S. Kaeser,[25] Jeremy N. Kay,[20] Wei Lu,[10] Liqun Luo,[8] Kenji Mandai,[11,15] Chris J. McBain,[19] Klaus-Armin Nave,[32] Marco A.M. Prado,[33,34] Vania F. Prado,[33,34] Jeffrey Rothstein,[21] John L.R. Rubenstein,[17,18] Gesine Saher,[32] Kenji Sakimura,[35] Joshua R. Sanes,[36] Peter Scheiffele,[6] Yoshimi Takai,[11] Hisashi Umemori,[7] Matthijs Verhage,[26] Michisuke Yuzaki,[16] Huda Yahya Zoghbi,[12,13] Hiroshi Kawabe,[2,11,37,*] and Ann Marie Craig[1,38,*]

[15]Department of Biochemistry, Kitasato University School of Medicine, 1-15-1 Kitasato, Minami-ku, Sagamihara, Kanagawa 252-0374, Japan
[16]Department of Physiology, Keio University School of Medicine, 35 Shinanomachi, Shinjuku-ku, Tokyo 160-8582, Japan
[17]Nina Ireland Laboratory of Developmental Neurobiology, Department of Psychiatry, UCSF Weill Institute for Neurosciences, University of California, San Francisco, San Francisco, CA 94158, USA
[18]Neuroscience Graduate Program, University of California, San Francisco, San Francisco, CA 94158, USA
[19]Section on Cellular and Synaptic Physiology, Eunice Kennedy Shriver National Institute of Child Health and Human Development, National Institutes of Health, Bethesda, MD 20892, USA
[20]Department of Neurobiology and Department of Ophthalmology, Duke University School of Medicine, Durham, NC 27710, USA
[21]Department of Neurology and Brain Science Institute, Johns Hopkins University School of Medicine, Baltimore, MD 21205, USA
[22]Division of Developmental Biology, Eunice Kennedy Shriver National Institute of Child Health and Human Development, Bethesda, MD 20892, USA
[23]Department of Cell Biology, Duke University Medical Center, Durham, NC 27710, USA
[24]Department of Stem Cell and Regenerative Biology, Harvard University, Cambridge, MA 02139, USA
[25]Department of Neurobiology, Harvard Medical School, Boston, MA 02115, USA
[26]Department of Functional Genomics and Department of Clinical Genetics, Center for Neurogenomics and Cognitive Research (CNCR), VU University Amsterdam and University Medical Center Amsterdam, de Boelelaan 1085, 1081 HV Amsterdam, the Netherlands
[27]Departments of Genetics, Harvard Medical School, Boston, MA 02115, USA
[28]Howard Hughes Medical Institute, Harvard Medical School, Boston, MA 02115, USA
[29]Department of Laboratory Animal Science, Shanghai Medical College, Fudan University, Shanghai 200032, China
[30]Department of Physiology and Biophysics, Center for the Neurobiology of Learning and Memory, University of California, Irvine, Irvine, CA 92697, USA
[31]Department of Cell Biology, Department of Neurobiology, and Duke Institute for Brain Sciences, Regeneration Next Initiative, Duke University Medical Center, Durham, NC 27710, USA
[32]Department of Neurogenetics, Max Planck Institute of Experimental Medicine, Hermann-Rein-Strasse 3, 37075 Göttingen, Germany
[33]Robarts Research Institute, Department of Anatomy and Cell Biology, and Department of Physiology and Pharmacology, Schulich School of Medicine & Dentistry, University of Western Ontario, London, ON N6A 5B7, Canada
[34]Brain and Mind Institute, The University of Western Ontario, London, ON N6A 5B7, Canada
[35]Department of Cellular Neurobiology, Brain Research Institute, Niigata University, Niigata 951-8585, Japan
[36]Center for Brain Science and Department of Molecular and Cellular Biology, Harvard University, Cambridge, MA 02138, USA
[37]Department of Gerontology, Laboratory of Molecular Life Science, Institute of Biomedical Research and Innovation, Foundation for Biomedical Research and Innovation at Kobe, 2-2 Minatojima-minamimachi Chuo-ku, Kobe, Hyogo 650-0047, Japan
[38]Lead Contact
*Correspondence: kawabe@em.mpg.de (H.K.), acraig@mail.ubc.ca (A.M.C.)
https://doi.org/10.1016/j.neuron.2020.01.008

and Hamilton, 1981) and development for genetic manipulations in mammalian cells (Sauer and Henderson, 1988) and in transgenic mice (Gu et al., 1994; Tsien et al., 1996a). Cre recombinase recognizes 34 base pair loxP sites, mediating deletion of DNA fragments between two loxP sites of the same orientation, or flipping of DNA fragments between two inverted loxP sites. Manipulation of genetic material flanked by loxP sites, in floxed genes, has been facilitated by the large-scale generation of mouse Cre driver lines with diverse expression patterns in the nervous system and mice with floxed target genes and reporters (Daigle et al., 2018; Gerfen et al., 2013; Gondo, 2008; Taniguchi et al., 2011). Thus, the Cre-loxP system has become a mainstay for conditional gene knockout (KO), knockin (KI), and reporter gene expression in mice, and recently in rats (Bäck et al., 2019; Witten et al., 2011). However, several caveats have been noted, including Cre-mediated toxicity and metabolic phenotypes due to illegitimate recombination, mosaic and/or inconsistent recombination activity, genetic background effects, and unexpected expression of Cre in undesirable cell types (Gil-Sanz et al., 2015; Harno et al., 2013; Heffner et al., 2012; Murray et al., 2012; Schmidt et al., 2000; Tachibana et al., 2018; Wojcinski et al., 2019).

A particularly under-appreciated and limiting caveat in terms of major undesirable consequences is unintentional germline recombination. When Cre expression and associated recombinase activity occur in germline cells, the Cre-mediated excision of the floxed allele will occur in all cells instead of in the intended region- and cell-type-specific pattern. A recent review describes how unexpected germline recombination could happen and how to detect such events (Song and Palmiter, 2018), but information about affected Cre driver lines has been scarce, with only a few sporadic reports (Choi et al., 2014; Kobayashi and Hensch, 2013; Liput, 2018; Zhang et al., 2013). Awareness of potential germline recombination in Cre driver lines designed to be nervous system specific is essential for correct genotyping and data interpretation. Furthermore, information about parental sex effects on germline recombination and comparisons among related Cre driver lines could guide optimal breeding schemes to save researchers valuable time and resources. Yet, such a meta-analysis has been lacking.

Please cite this article in press as: Luo et al., Optimizing Nervous System-Specific Gene Targeting with Cre Driver Lines: Prevalence of Germline Recombination and Influencing Factors, Neuron (2020), https://doi.org/10.1016/j.neuron.2020.01.008

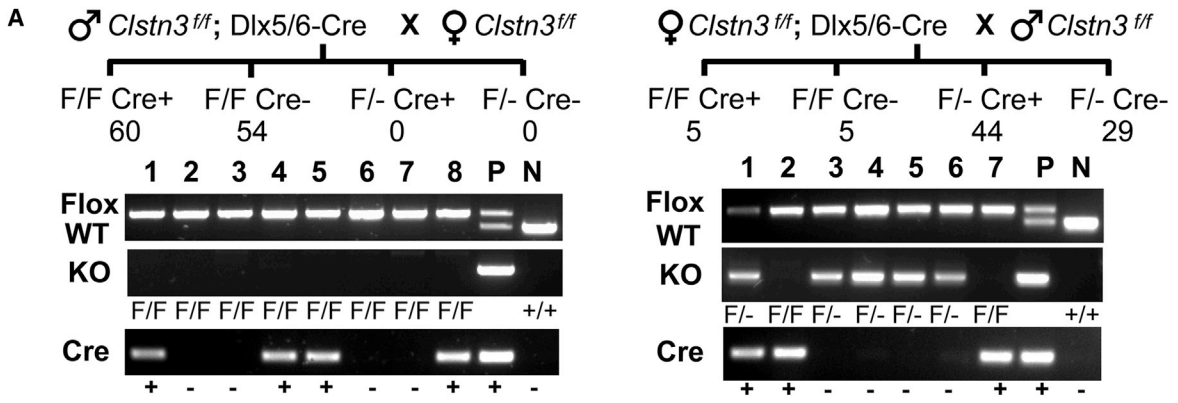

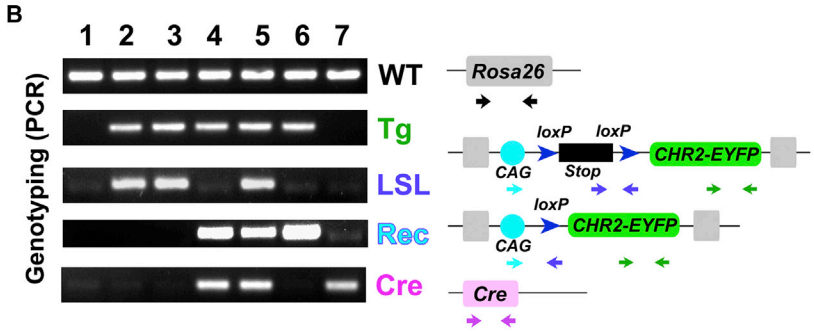

$Rosa^{LSL\text{-}tg/+}$; Dlx5/6-Cre X $Rosa^{+/+}$

Genotype	Pup number (Mendelian prediction)	
	Cre from Female	Cre from Male
LSL-tg/+, Cre+	9 (17.25)	20 (18.75)
LSL-tg/+, Cre-	12 (17.25)	13 (18.75)
L-tg/+, Cre+	12 (0)	0 (0)
L-tg/+, Cre-	6 (0)	0 (0)
+/+, Cre+	16 (17.25)	23 (18.75)
+/+, Cre-	14 (17.25)	19 (18.75)
total	69	75

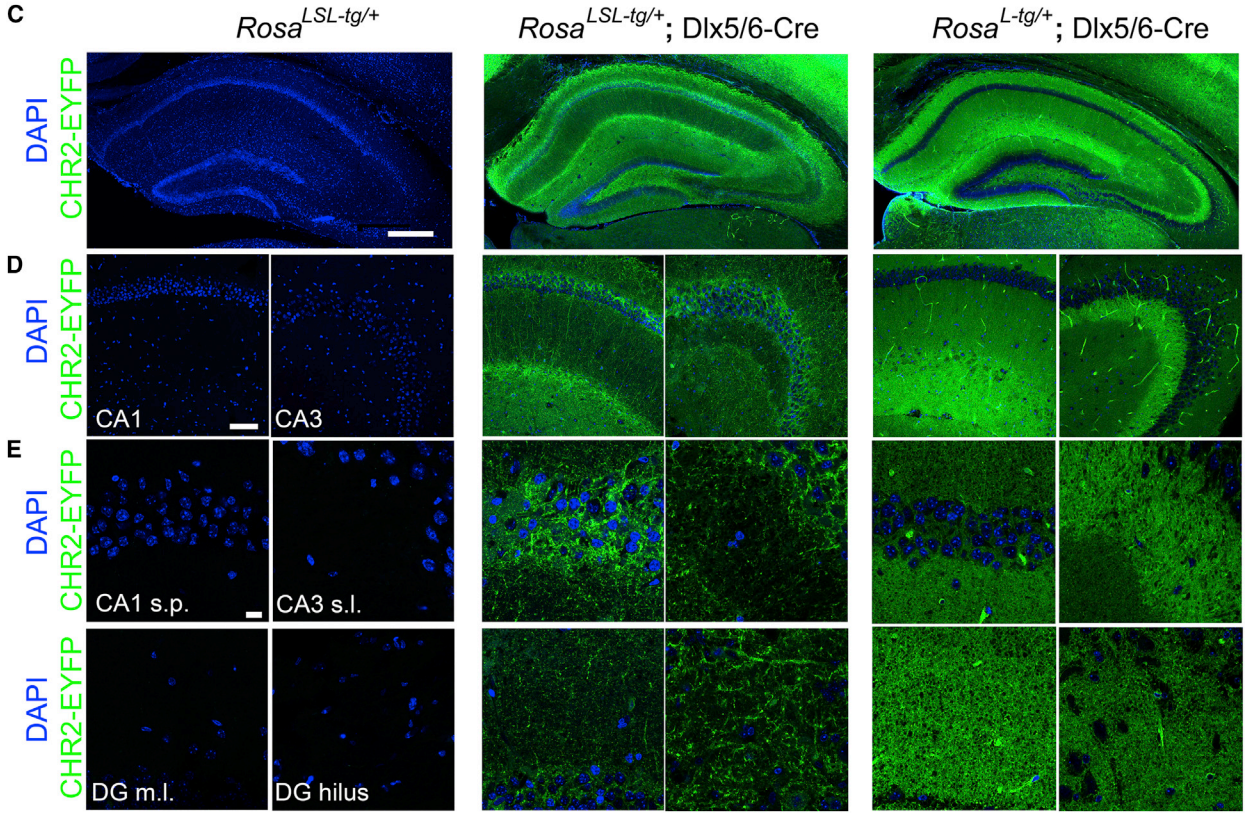

(legend on next page)

In this report, we used two Cre lines, Dlx5/6-Cre and Gpr26-Cre, expressing Cre recombinase in distinct neuronal populations, as examples to demonstrate undesirable germline recombination occurring selectively in the female or male Cre-carrying parents, respectively. To generate a more comprehensive resource, we compiled information on germline recombination frequencies from a total of 64 different Cre driver lines generally used for nervous system-specific genetic manipulations. We anticipate that our short report will serve as a collective resource to guide the optimal usage of Cre driver lines.

RESULTS AND DISCUSSION

Maternal Germline Recombination in Dlx5/6-Cre Driver Mice

The Dlx5/6-Cre line (Tg(dlx5a-cre)1Mekk) (Zerucha et al., 2000) has been used in over 70 papers to specifically target forebrain interneurons (Mouse Genome Informatics [MGI] database; Bult et al., 2019). We combined this transgene with the *Clstn3*$^{f/f}$ (B6-*Clstn3*^{tm1Amcr}/J) allele (Pettem et al., 2013) and then crossed *Clstn3*$^{f/f}$; Dlx5/6-Cre with *Clstn3*$^{f/f}$ mice to generate experimental conditional KO animals. We genotyped the offspring with three sets of primers: the first for the *Clstn3* floxed and wild-type (WT) alleles, the second for the Cre-recombined *Clstn3* KO allele, and the third for Cre. We expected to observe only the *Clstn3* floxed allele and no KO allele regardless of Cre. Yet, 88% (73/83) of the offspring expressed a *Clstn3* KO allele when the female parent carried Cre, suggesting germline deletion. In contrast, none of the 114 offspring we tested had the KO allele when the Cre recombinase was transmitted from the male parent (Figure 1A). Counting Cre-negative offspring to rule out any potential direct effects of Cre in the offspring, all (54) offspring from paternal Cre crosses were *Clstn3*$^{f/f}$ but 85.3% (29/34) of the offspring from maternal Cre crosses were *Clstn3*$^{f/-}$. These results indicate that a high fraction of female mice carrying the Dlx5/6-Cre and floxed genes apparently expressed Cre in the germ cells resulting in maternal germline recombination and that this unexpected germline deletion could be circumvented by transmitting Cre strictly paternally.

To test whether this maternal germline recombination is floxed locus specific, we crossed the Dlx5/6-Cre with an Ai32 reporter line (B6;129S-*Gt(ROSA)26Sor*$^{tm32(CAG-COP4*H134R/EYFP)Hze}$/J) (Madisen et al., 2012). The Ai32 mouse line contains a LoxP-stop-LoxP-EYFP-channelrhodopsin2 (ChR2) cassette at the *Rosa 26* locus. To distinguish the reporter allele before and after recombination, we designed a primer set targeting the loxP-stop-loxP-EYFP region, with the forward primer annealing to the stop cassette that would be deleted by Cre recombinase. Thus, PCR product with these primers is present in the tail tissue of transgenic mice without Cre-dependent recombination ("LSL-tg" in Figure 1B) and absent in mice with germline recombination ("L-tg" in Figure 1B). When female *Rosa*$^{LSL\text{-}tg/+}$; Dlx5/6-Cre mice were crossed with male WT mice, 46.2% (18/39) of offspring with the transgene had a recombined L-tg allele instead of the original LSL-tg, indicating germline Cre-recombination (Figure 1B). In contrast, no recombined allele was detected when male *Rosa*$^{LSL\text{-}tg/+}$; Dlx5/6-Cre mice were crossed with female WT mice (0/33 offspring with the transgene). This germline recombination activity in female but not male germ cells is consistent with the finding from the *Clstn3*$^{f/f}$ crosses. However, the recombination frequencies differed (33.3% for *Rosa*$^{LSL\text{-}tg}$ and 85.3% for *Clstn3*^{f} per target allele for Cre-negative mice, assuming no recombination in the zygote, which was verified as discussed below).

To support the PCR results with Dlx5/6-Cre and the Ai32 reporter, we assessed germline versus forebrain interneuron-specific Cre recombination by fluorescence imaging for the Cre-dependent expression of EYFP-ChR2; Figures 1C–1E). *Rosa*$^{LSL\text{-}tg/+}$ mice showed no EYFP signal above background levels. *Rosa*$^{LSL\text{-}tg/+}$; Dlx5/6-Cre mice showed a pattern of EYFP-ChR2 consistent with expression in axons and dendrites of interneurons, as expected. For example, the signal was strong in the hippocampal CA1 and CA3 stratum pyramidale regions that are rich in inhibitory inputs but weak in the CA3 stratum lucidum that is rich in excitatory synapses. The germline-recombined *Rosa*$^{L\text{-}tg/+}$; Dlx5/6-Cre offspring showed a broad EYFP-ChR2 expression pattern spanning all brain regions, consistent with expression in all cell types, neurons, glia cells, and blood vessels (Figures 1C–1E). Note that the excitation laser power for the EYFP channel used to image the germline Cre-recombined *Rosa*$^{L\text{-}tg/+}$; Dlx5/6-Cre mouse hippocampus was only 15% of that for the other two genotypes in Figures 1C–1E. Cre-negative *Rosa*$^{L\text{-}tg/+}$mice showed the same phenotype as *Rosa*$^{L\text{-}tg/+}$; Dlx5/6-Cre (data not shown).

Mosaic Cre Expression in Genotyping Tissue

Of note, the presence of Cre-recombined alleles in the tissue used for PCR genotyping could be due to limited Cre expression and recombination in peripheral nerve or non-neural cell types in

Figure 1. Dlx5/6-Cre Mice Show Maternal Germline Recombination

(A) Pedigree and sample genotyping results of *Clstn3*$^{f/f}$ crosses with Dlx5/6-Cre transmitted from either the male or female parent. F/F Cre^{+} indicates *Clstn3*$^{f/f}$; Dlx5/6-Cre. F/F Cre^{-} indicates *Clstn3*$^{f/f}$ without Cre. F/– Cre^{+} indicates *Clstn3*$^{f/-}$; Dlx5/6-Cre in which recombination has occurred (this labeling is used for simplicity, but some of these mice may be F/– Cre^{+} and some may be F/F Cre^{+} genotypes because mosaic recombination was observed in tail tissue used for genotyping). F/– Cre^{-} indicates *Clstn3*$^{f/-}$ without Cre in which recombination has occurred. P and N indicate controls (multiple mice were used for P). The numbers below genotypes indicate the total number of offspring obtained with that genotype.

(B) Representative genotyping results and numbers of offspring from Ai32 *Gt(ROSA)26Sor*$^{tm32(CAG-COP4*H134R/EYFP)Hze}$/J reporter and Dlx5/6-Cre crosses. LSL-tg indicates the CAG promoter and lox-stop-lox sequences before the transgene channelrhodopsin-2(H134R)-EYFP (CHR2-EYFP) on the *Rosa* locus. L-tg indicates the transgene after germline recombination by Cre resulting in global transgene expression. Genotypes of the animals are 1, +/+ and Cre^{-}; 2 and 3, LSL-tg/+ and Cre^{-}; 4, L-tg/+ and Cre^{+}; 5, LSL-tg/+ and Cre^{+} (showing some mosaic recombination); 6, L-tg/+ and Cre^{-}; 7, +/+ and Cre^{+}.

(C–E) Tiled images of the hippocampus (C) and sample CA1 and CA3 regions (D) showing CHR2-EYFP transgene expression and DAPI nuclear stain for selected offspring from (B). (E) Higher-magnification images are shown for hippocampal CA1 stratum pyramidale (s.p.), CA3 stratum lucidum (s.l.), dentate gyrus molecular layer (DG m.l.), and dentate gyrus hilus regions. Note that the laser power used for the EYFP channel in the far right panel for images from *Rosa26*$^{L\text{-}tg/+}$;Dlx5/6-Cre mice was only 15% of that for the rest. Scale bars, 500 μm (C), 100 μm (D), and 20 μm (E).

Please cite this article in press as: Luo et al., Optimizing Nervous System-Specific Gene Targeting with Cre Driver Lines: Prevalence of Germline Recombination and Influencing Factors, Neuron (2020), https://doi.org/10.1016/j.neuron.2020.01.008

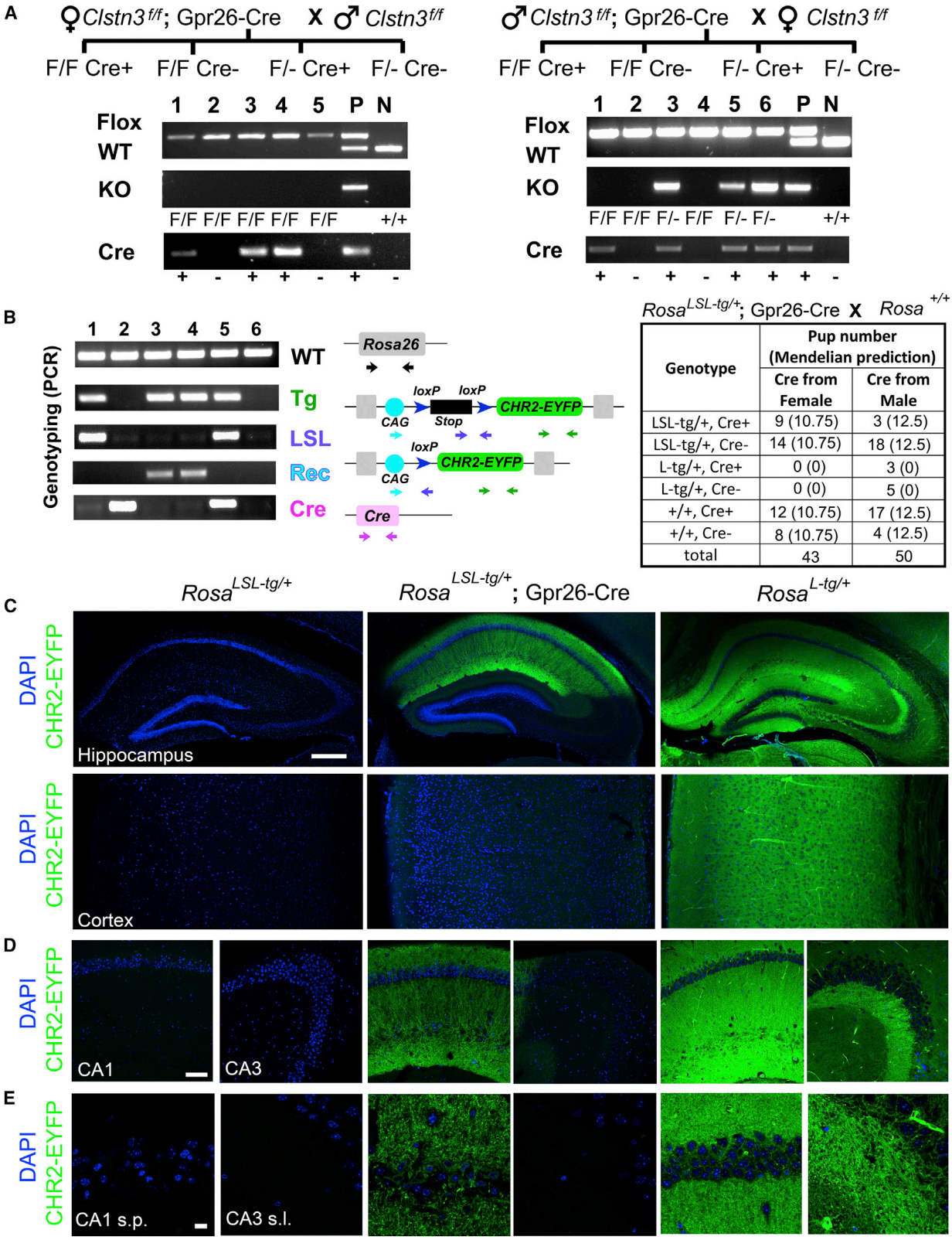

$Rosa^{LSL\text{-}tg/+}$; Gpr26-Cre X $Rosa^{+/+}$

Genotype	Pup number (Mendelian prediction)	
	Cre from Female	Cre from Male
LSL-tg/+, Cre+	9 (10.75)	3 (12.5)
LSL-tg/+, Cre-	14 (10.75)	18 (12.5)
L-tg/+, Cre+	0 (0)	3 (0)
L-tg/+, Cre-	0 (0)	5 (0)
+/+, Cre+	12 (10.75)	17 (12.5)
+/+, Cre-	8 (10.75)	4 (12.5)
total	43	50

(legend on next page)

the genotyping tissue rather than germline recombination. This phenomenon typically involves mosaic rather than ubiquitous recombination, as indicated by the presence of both intact floxed and recombined products from one target allele. Such mosaic recombination occurred in the tail tissue used for PCR genotyping of Ai32 *Rosa*$^{LSL\text{-}tg/+}$; Dlx5/6-Cre mice. For example, in Figure 1B, lane 5 shows bands for both the recombined *Rosa*$^{L\text{-}tg/+}$and the non-recombined *Rosa*$^{LSL\text{-}tg/+}$ forms for a single *Rosa*$^{LSL\text{-}tg}$ locus, indicating a mouse genotype of *Rosa*$^{LSL\text{-}tg/+}$ with some local recombination. Such mosaic recombination was observed in 22/26 *Rosa*$^{LSL\text{-}tg/+}$; Dlx5/6-Cre offspring whereas no *Rosa*$^{LSL\text{-}tg/+}$ Cre-negative offspring (0/20) showed any recombined *Rosa*$^{L\text{-}tg/+}$ product. For mice with two target alleles, it can be difficult based solely on PCR genotyping of the target locus to distinguish germline ubiquitous recombination at one allele from somatic mosaic recombination. A definitive approach to distinguish germline recombination from such local mosaic recombination is the detection of the recombined allele in Cre-negative offspring. Another definitive approach is cellular resolution imaging for the expression of RNA or protein products from both the recombined and non-recombined loci. Additionally, germline recombination is likely to display a parental sex bias, as was the case for most lines reported here, whereas mosaic recombination is typically independent of sex except in some situations involving epigenetic modification.

The use of cells that developmentally diverge considerably from nerve cells for PCR genotyping, such as blood cells, may help distinguish between germline versus local recombination. For example, in offspring from crossing female Emx1-Cre;*Wwp1*$^{f/f}$;*Wwp2*$^{f/f}$ with male *Wwp1*$^{f/f}$;*Wwp2*$^{f/f}$ mice, recombination at *Wwp2* alleles was observed in tail tissue of most Cre-positive (14/15) but not Cre-negative (0/16) mice. PCR from blood revealed no recombination in any offspring (0/14), altogether indicating that the recombination observed in tail tissue was due to mosaic rather than germline recombination. However, this approach is not universally useful, as the *Rosa*$^{LSL\text{-}tg/+}$; Dlx5/6-Cre mice showed mosaic recombination in blood as well as in tail tissue.

Paternal Germline Recombination in Gpr26-Cre Driver Mice

Given the experience with Dlx5/6-Cre and the recommendations on the Jackson Labs website—"For many *cre* strains, but not all, using *cre*-positive males for breeding avoids potential germline deletion of your *loxP*-flanked allele." (https://www.jax.org/news-and-insights/jax-blog/2016/may/are-your-cre-lox-mice-deleting-what-you-think-they-are)—we adopted a general breeding strategy of transmitting Cre recombinase paternally. However, we found that Gpr26-Cre showed selective paternal germline recombination.

Gpr26-Cre (Tg(Gpr26-cre)KO250Gsat/Mmucd) was generated by the GENSAT project (http://gensat.org/index.html) and displays abundant expression in the hippocampal CA1 region and sparse expression in other brain regions, including layer V cortex and thalamus (Gerfen et al., 2013; Harris et al., 2014). We chose this line for its specific expression in CA1 pyramidal neurons (Figure 2), which actually turned out to be only in the deep sublayer (near stratum oriens) but not the superficial sublayer of CA1 stratum pyramidale in our characterization (data not shown; Figure 2C). In order to delete *Clstn3* in the CA1 region conditionally, we crossed *Clstn3*$^{f/f}$; Gpr26-Cre and *Clstn3*$^{f/f}$ mice and genotyped offspring by PCR. As shown by the presence of KO PCR bands in Figure 2A, we observed Cre-mediated recombination in the tail tissue when male *Clstn3*$^{f/f}$; Gpr26-Cre were crossed with female *Clstn3*$^{f/f}$ but not vice versa. Further germline transmission of this KO allele and the absence of local recombination in tail tissue confirmed selective paternal germline recombination of floxed *Clstn3.*

To test whether selective paternal germline recombination also occurs with another target floxed locus, we crossed Gpr26-Cre mice with the Ai32 reporter line and assessed genotypes of F2 progeny by PCR using tail tissue and by imaging of EYFP-ChR2 in brain sections. When male *Rosa*$^{LSL\text{-}tg/+}$; Gpr26-Cre mice were crossed with WT females, 27.6% (8/29) of the offspring with the transgene had only a recombined allele regardless of the presence of Cre, indicating germline recombination. In contrast, when Cre was transmitted through the female parent, the loxP-stop-loxP sequences remained largely intact (Figure 2B; no ubiquitous germline recombination was observed but 2/17 *Rosa*$^{LSL\text{-}tg/+}$; Gpr26-Cre mice showed mosaic recombination in tail tissue). As expected, *Rosa*$^{LSL\text{-}tg/+}$mice showed no EYFP signal above background levels and *Rosa*$^{LSL\text{-}tg/+}$; Gpr26-Cre mice expressed EYFP-ChR2 prominently in the hippocampal CA1 region with weak expression in the cortex (Figures 2C–2E). In contrast, for animals with germline recombination, i.e., *Rosa*$^{L\text{-}tg/+}$ mice, EYFP-ChR2 was expressed globally. In the hippocampus, *Rosa*$^{LSL\text{-}tg/+}$; Gpr26-Cre mice had strong EYFP-ChR2 expression in the CA1 stratum radiatum and oriens

Figure 2. Gpr26-Cre Mice Show Paternal Germline Recombination

(A) Pedigree and sample genotyping results of *Clstn3*$^{f/f}$ crosses with Gpr26-Cre from either the male or female parent. F/F Cre^{+} indicates *Clstn3*$^{f/f}$;Gpr26-Cre. F/F Cre^{-} indicates *Clstn3*$^{f/f}$ without Cre. F/− Cre^{+} indicates *Clstn3*$^{f/-}$;Gpr26-Cre in which recombination has occurred. This was confirmed to be germline deletion by the absence of a KO band in tail tissue from *Clstn3*$^{f/f}$;Gpr26-Cre mice (n = 46 mice generated from maternal Cre crosses) indicating the absence of local recombination in the tissue used for genotyping and by transmission of the KO allele to offspring. F/− Cre^{-} indicates *Clstn3*$^{f/-}$ without Cre in which recombination has occurred. P and N indicate controls (multiple mice were used for P).

(B) Representative genotyping results and numbers of offspring from Ai32 *Gt(ROSA)26Sor*$^{tm32(CAG\text{-}COP4*H134R/EYFP)Hze}$/J reporter and Gpr26-Cre crosses. LSL-tg indicates the CAG promoter and lox-stop-lox sequences before the transgene channelrhodopsin-2(H134R)-EYFP (CHR2-EYFP) on the *Rosa* locus. L-tg indicates the transgene after germline recombination by Cre resulting in global transgene expression. Genotypes of the animals are 1, LSL-tg/+ and Cre^{-}; 2, +/+ and Cre^{+}; 3 and 4, L-tg/+ and Cre^{-}; 5, LSL-tg/+ and Cre^{+}; 6, +/+ and Cre^{-}.

(C–E) Tiled images of the hippocampus and cortex (C) and sample CA1 and CA3 regions (D) showing CHR2-EYFP transgene expression and DAPI nuclear stain for selected offspring from (B). Higher-magnification images are shown for hippocampal CA1 stratum pyramidale (s.p.) and CA3 stratum lucidum (s.l.) (E). Note that the laser power used for the EYFP channel in the far right panel for images from *Rosa*$^{tg/+}$ mice was only 15% of that for the rest. Scale bars, 500 μm (C), 100 μm (D), and 20 μm (E).

layers but not in CA3, while *Rosa*$^{L\text{-}tg/+}$ mice showed EYFP-ChR2 expression in both regions in a pattern consistent with expression in all cell types (Figures 2C–2E).

Germline Recombination in Mouse Cre Driver Lines Designed for Cell-Type-Specific Expression

As significant germline recombination happened in both Dlx5/6-Cre and Gpr26-Cre lines designed for recombination in specific neuron types, we wondered about the prevalence of this phenomenon in other Cre lines. To the best of our knowledge, there are only a handful of papers focused on germline recombination in Cre driver lines intended for nervous system-specific recombination (Kobayashi and Hensch, 2013; Liput, 2018; Weng et al., 2008; Zhang et al., 2013) and several other papers that mention this issue, typically in the methods (Table 1). Lines reported to undergo significant germline recombination include the widely used Nestin-Cre, GFAP-Cre, CaMKIIα-Cre, and Synapsin1-Cre lines (Choi et al., 2014; Rempe et al., 2006; Zhang et al., 2013), which collectively have been used in over 1,500 published papers according to the MGI database (Bult et al., 2019). Furthermore, in these data collected from the literature, most (9/10) of the Cre driver lines tested showed a parental sex effect. We suspect that these data represent the tip of an iceberg, as for the majority of Cre driver lines information has not been readily available on either the extent of germline recombination or parental sex bias.

A comprehensive resource of relevant information on Cre driver lines could be invaluable to mitigate undesired germline recombination by serving as a guide for choosing among similar Cre lines and for designing optimal breeding schemes. We thus pooled information to present new combined data on germline recombination rates and parental sex effects for Cre driver lines for neuroscience research. The collective data from all previously published and unpublished sources are reported in Table 1.

Of the 64 Cre driver lines analyzed, over half (64.1%) exhibited some germline recombination. The mosaic nature of germline deletion for most of the Cre driver lines renders the genotype of individual offspring to be unpredictable. Furthermore, of the 29 Cre driver lines for which sufficient information is available on parental sex effects, the majority (82.8%) showed a sex bias, with 62.1% demonstrating germline recombination solely or selectively through the male parent and 20.1% solely or selectively through the female parent. Only 17.2% showed nearly equal rates of germline recombination in male and female parents. These findings highlight the importance of assessing potential germline recombination for every mouse and the value of tracking parental sex bias toward optimizing breeding schemes to minimize unwanted germline recombination.

Recombination in Germline Cells

As discussed in the introduction, Cre activity in the germline cells of the ovary or testes mediates germline recombination. Relevant to the Cre driver lines chosen as examples here, native Gpr26 is expressed in the testes (Jones et al., 2007), consistent with the selective paternal germline recombination of Gpr26-Cre. However, native Dlx5 and Dlx6 are expressed in both the ovary and testes (Bouhali et al., 2011; Nishida et al., 2008); yet, only maternal germline recombination was observed for Dlx5/6-Cre. Moreover, expression in the ovary or testes may not reflect expression by germline cells, and the Cre driver lines may not reproduce native expression patterns. Recent scRNA-seq data from male germline cells (Lukassen et al., 2018a, 2018b) circumvents the former limitation. Yet, even restricting analyses to KI Cre driver lines, expression levels of the native driver genes at these KI loci in male germline cells showed no apparent relation to whether the Cre driver line mediated paternal germline recombination (Figure S1). Circumventing the second limitation, that Cre expression may not be adequately reflected by the native driver gene expression, the Cre portal of the MGI database (Bult et al., 2019; Heffner et al., 2012) reports Cre recombinase activity patterns for many lines. For the majority (75%) of the 16 Cre driver lines with information about reproductive system germline cell activity in the MGI database, the data were consistent with our findings on germline recombination in Table 1. For 3 cases, germline cell Cre activity was reported but recombination was not observed; for example, ChAT-Cre was positive for Cre recombinase activity in oocytes (MGI) yet did not exhibit maternal germline recombination at any of several target loci (Table 1). Tg(Grik4-cre)G32-4Stl and Sst-IRES-Cre were listed as negative for Cre recombinase activity in germline cells yet showed some germline recombination, although for Sst-IRES-Cre only at one of six target loci, thus consistent with the MGI data for most target loci. Among the 30 other lines that showed germline recombination in Table 1, the MGI database did not list any as negative for Cre recombinase activity in germline cells, although several were listed as negative either in the testes or ovary. Thus, a conservative interpretation of the MGI database Cre recombinase activity may be helpful to predict the occurrence of germline recombination. Basing predictions for germline recombination at the majority of target loci on Cre activity in germ cells yields good measures with precision 0.700, recall 0.875, accuracy 0.750, diagnostic odds ratio 11.67, and F_1 score 0.778 (from 16 lines: 7 true positive, 5 true negative, 3 false positive, and 1 false negative).

In principle, one would expect mice expressing Cre recombinase fused with the estrogen receptor (CreER) to lack germline recombination unless they are exposed to tamoxifen to activate the CreER. Indeed, of the 7 driver lines studied here that express CreER or the improved version CreERT2 (Feil et al., 1997), 85.7% did not show germline recombination. However, Tg(hs799-cre/ERT2,-GFP)405Jlr showed maternal germline recombination in the absence of tamoxifen administration (Table 1). This mouse line exhibits some tamoxifen-independent activity of CreERT2, possibly associated with high expression of the CreERT2 allele (Silberberg et al., 2016). Such tamoxifen-independent activity can also lead to an age-dependent increase in cell-specific recombination; for example, untreated Tg(Plp1-cre/ERT)3Pop mice showed increasing recombination in oligodendrocytes with age (Traka et al., 2016). Thus, it is not safe to assume that CreER driver lines lack germline recombination.

Recombination in Zygotes

Our data in Table 1 focus on germline recombination occurring when the Cre driver and the target locus are together in the male or female germline cells of F1 mice, resulting in the transmission of a recombined allele to F2 mice. It is also possible

Table 1. Prevalence of Germline Recombination in Mouse Cre Driver Lines Designed for Nervous System-Specific Recombination

Cre line Common Name	Full Cre Line Name/ Source	Target Gene/ Reporter	Breeding Strategy[a]	Germline Recombination Efficiency, Cre from Father[b]	Germline Recombination Efficiency, Cre from Mother[b]	Germline Recombindation Efficiency, Parental Sex Effects Unknown[b]	Reference/ Associated Publication[c]	Contributors[d]
799-CreER-IRES-GFP	Tg(hs799-cre/ERT2,-GFP)405Jlr	*Mafb*$^{tm1.1Good}$	H	0 (from >20 litters)	observed (from >20 litters)	–	Pai et al., 2019; Silberberg et al., 2016	Emily Ling-Lin Pai, John L.R. Rubenstein
	Tg(hs799-cre/ERT2,-GFP)405Jlr	*Maf*$^{tm2.1Cbm}$	H	0 (from >20 litters)	observed (from >20 litters)	–	Pai et al., 2019; Silberberg et al., 2016	Emily Ling-Lin Pai, John L.R. Rubenstein
	Tg(hs799-cre/ERT2,-GFP)405Jlr	Ai14[e]	H	0 (from >20 litters)	observed (from >20 litters)	–	Pai et al., 2019; Silberberg et al., 2016	Emily Ling-Lin Pai, John L.R. Rubenstein
A2a-Cre	B6-Tg(Adora2a-Cre) KG139GSat	Ai14[e]	E or G	0 (from >3 years breeding)	0 (from >3 years breeding)	–	–	Kevin T. Beier
	B6.FVB(Cg)-Tg (Adora2a-cre) KG139Gsat/ Mmucd/GENSAT	*Gt(ROSA) 26Sor*$^{tm2(CAG-tdTomato)Fawa}$	F	0 (0/15)	ND	–	–	Hisashi Umemori
Bhlhb5-Cre	*Bhlhe22*$^{tm3.1(cre)Meg}$	Ai9[e]	B	0 (from >10 litters)	0 (from >10 litters)	–	–	Wenjia You, Constance L. Cepko
CaMKIIα-Cre	Tg(Camk2a-cre) 159Kln	*Fdft1*^{tm1Kan}	C	16.2% (12/74)	6.3% (3/48)	–	Fünfschilling et al., 2012; Minichiello et al., 1999	Gesine Saher, Klaus A. Nave
CaMKIIα-Cre	Tg(Camk2a-cre)93Kln	*Gnao1*	B	72.1% (31/43)	ND	–	Choi et al., 2014	–
	Tg(Camk2a-cre)93Kln	B6;129S4-*Gt(ROSA) 26Sor*^{tm1Sor}/J	B	98.5% (64/65)	ND	–	Choi et al., 2014	–
CaMKIIα-Cre	B6.Cg-Tg(Camk2a-cre)2Szi/J	*Lepr*$^{tm1.1Chua}$	A	observed	0	–	McMinn et al., 2005	–
	B6.Cg-Tg(Camk2a-cre)2Szi/J	*Chat/Slc18a3*$^{tm1.2Vpra}$	A or C	observed	ND	–	de Castro et al., 2009	–
CaMKIIα-Cre (T29-1)	Tg(Camk2a-cre) T29-1Stl	*Khdrbs3*$^{tm1.1Schei}$/J	C	31.3% (5/16)	0% (0/7)	–	–	Elisabetta Furlanis, Lisa Traunmüller, Peter Scheiffele
	Tg(Camk2a-cre) T29-1Stl	*Rpl22*$^{tm1.1Psam}$/J	C	21.4% (6/28)	0% (0/21)	–	–	Elisabetta Furlanis, Lisa Traunmüller, Peter Scheiffele
	Tg(Camk2a-cre) T29-1Stl	*Trpm7*^{tm1Clph}	C	25.0% (33/132)	ND	–	Liu et al., 2018b	Cui Chen, Wei Li, Nashat Abumaria

(*Continued on next page*)

Table 1. *Continued*

Cre line Common Name	Full Cre Line Name/ Source	Target Gene/ Reporter	Breeding Strategy[a]	Germline Recombination Efficiency, Cre from Father[b]	Germline Recombination Efficiency, Cre from Mother[b]	Germline Recombindation Efficiency, Parental Sex Effects Unknown[b]	Reference/ Associated Publication[c]	Contributors[d]
Chat-Cre	B6;129S6-*Chat*$^{tm2(cre)Lowl}$/J	*Megf10*$^{tm1c(KOMP)Jrs}$	A or C	0 (from 16 litters)	0 (from 15 litters)	–	Ray et al., 2018	Ariane Pereira, Jeremy N. Kay
	B6;129S6-*Chat*$^{tm2(cre)Lowl}$/J	*Tgfb3*^{tm1Moaz}	A or C	0 (from 33 litters)	0 (from 35 litters)	–	Ray et al., 2018	Ariane Pereira, Jeremy N. Kay
	B6;129S6-*Chat*$^{tm2(cre)Lowl}$/J	ROSA$^{mT/mG5}$	A or C	0 (from 17 litters)	0 (from 19 litters)	–	Ray et al., 2018	Ariane Pereira, Jeremy N. Kay
	B6;129S6-*Chat*$^{tm2(cre)Lowl}$/J	Ai14[e]	A or C	0 (from 15 litters)	0 (from 9 litters)	–	Ray et al., 2018	Ariane Pereira, Jeremy N. Kay
Cux2-Cre	B6.Cg-*Cux2*$^{tm2.1(cre)Mull}$	Ai9[e]	B	–	–	observed	Gil-Sanz et al., 2015	–
	B6.Cg-*Cux2*$^{tm2.1(cre)Mull}$	*Gt(ROSA) 26Sor*$^{tm1(CAG-lacZ,-EGFP)Glh}$/J	B	–	–	observed	Gil-Sanz et al., 2015	–
Cux2-CreERT2	B6.Cg-*Cux2*$^{tm3.1(cre/ERT2)Mull}$/ Mmmh	*Rpl22*$^{tm1.1Psam}$/J	B	ND	0 (0/15)	–	–	Susanne Falkner, Peter Scheiffele
	B6.Cg-*Cux2*$^{tm3.1(cre/ERT2)Mull}$/ Mmmh	*Rpl22*$^{tm1.1Psam}$/J	E	0 (0/23)	0 (0/23)	–	–	Susanne Falkner, Peter Scheiffele
CX3CR1-CreER	*Cx3cr1*$^{tm2.1(cre/ERT2)Litt}$/ WganJ	*Syk*$^{tm1.2Tara}$	E	0 (from 32 litters)	0 (from 26 litters)	–	Puñal et al., 2019	Ariane Pereira, Jeremy N. Kay
	Cx3cr1$^{tm2.1(cre/ERT2)Litt}$/ WganJ	*Gt(ROSA) 26Sor*$^{tm1(HBEGF)Awai}$/J	A or C	0 (from 8 litters)	0 (from 6 litters)	–	Puñal et al., 2019	Ariane Pereira, Jeremy N. Kay
	Cx3cr1$^{tm2.1(cre/ERT2)Litt}$/ WganJ	*Csf1r*$^{tm1.2Jwp}$/J	A or C	0 (from 10 litters)	0 (from 8 litters)	–	Puñal et al., 2019	Ariane Pereira, Jeremy N. Kay
D2-Cre	Tg(Drd2-cre) ER44Gsat/ Mmucd	*Chat/Slc18a3*$^{tm1.2Vpra}$	C	0 (0/55)	0 (0/44)	–	Guzman et al., 2011	Marco A.M. Prado, Vania F. Prado
DAT-Cre	*Slc6a3*$^{tm1.1(cre)Bkmn}$/J	*Gria1*^{tm2Rsp}	A or C	0 (from >3 years breeding)	ND	–	Hutchison et al., 2018	Mary Anne Hutchison, Wei Lu
	Slc6a3$^{tm1.1(cre)Bkmn}$/J	*Gria2*^{tm3Rsp}	A or C	0 (from >3 years breeding)	ND	–	Hutchison et al., 2018	Mary Anne Hutchison, Wei Lu
	Slc6a3$^{tm1.1(cre)Bkmn}$/J	*Gria3*^{tm1Rsp}	A or C	0 (from >3 years breeding)	ND	–	Hutchison et al., 2018	Mary Anne Hutchison, Wei Lu
	Slc6a3$^{tm1.1(cre)Bkmn}$/J	*Grin1*^{tm2Stl}	A or C	0 (from >3 years breeding)	ND	–	Hutchison et al., 2018	Mary Anne Hutchison, Wei Lu

(*Continued on next page*)

Table 1. ***Continued***

Cre line Common Name	Full Cre Line Name/ Source	Target Gene/ Reporter	Breeding Strategy[a]	Germline Recombination Efficiency, Cre from Father[b]	Germline Recombination Efficiency, Cre from Mother[b]	Germline Recombindation Efficiency, Parental Sex Effects Unknown[b]	Reference/ Associated Publication[c]	Contributors[d]
	Slc6a3$^{tm1.1(cre)Bkmn}$/J	Ai14[e]	A or C	0 (from >3 years breeding)	ND	–	Hutchison et al., 2018	Mary Anne Hutchison, Wei Lu
	B6.SJL-*SLc6a3*$^{tm1.1(cre)Bkmn}$/J	Ai14[e]	E or G	0 (from >6 years breeding)	0 (from >6 years breeding)	–	–	Kevin T. Beier
	B6.SJL-*SLc6a3*$^{tm1.1(cre)Bkmn}$/J	*Gt(ROSA) 26Sor*$^{tm2(CAG-tdTomato)Fawa}$	E, F	0 (0/26)	0 (0/15)	–	–	Hisashi Umemori
	B6.SJL-*SLc6a3*$^{tm1.1(cre)Bkmn}$/J	*Rims1*^{tm3Sud}/J	A or C	0 (from >1 year of breeding)	0 (from >1 year of breeding)	–	Liu et al., 2018a	Jiexin Wang, Pascal S. Kaeser
	B6.SJL-*SLc6a3*$^{tm1.1(cre)Bkmn}$/J	*Rims2*$^{tm1.1Sud}$/J	A or C	0 (from >1 year of breeding)	0 (from >1 year of breeding)	–	Liu et al., 2018a	Jiexin Wang, Pascal S. Kaeser
	B6.SJL-*SLc6a3*$^{tm1.1(cre)Bkmn}$/J	Ai34[e]	A or C	0 (from >19 litters)	0 (from >14 litters)	–	Liu et al., 2018a	Jiexin Wang, Pascal S. Kaeser
Dlx5/6-Cre	B6-Tg(dlx5a-cre) 1Mekk/J	*Prox1*^{tm2Gco}	B	0 or less than female	observed	–	Miyoshi et al., 2015	–
	B6-Tg(dlx5a-cre) 1Mekk/J	*Clstn3*^{tm1Amcr}/J	C	0 (0/52)	85.3% (29/34) of Cre negative offspring	–	–	Lin Luo, Ann Marie Craig
	B6-Tg(dlx5a-cre) 1Mekk/J	Ai32[e]	B	0 (0/33)	33.3% (6/18) of Cre negative offspring	–	–	Lin Luo, Ann Marie Craig
DlxI12B-Cre	*Tg(I12b–cre)1Jlr*	*Mafb*$^{tm1.1Good}$	H	observed (from >10 litters)	ND	–	Potter et al., 2009	Emily Ling-Lin Pai, John L.R. Rubenstein
	Tg(I12b–cre)1Jlr	*Maf*$^{tm2.1Cbm}$	H	observed (from >10 litters)	ND	–	Potter et al., 2009	Emily Ling-Lin Pai, John L.R. Rubenstein
	Tg(I12b–cre)1Jlr	Ai14[e]	H	observed (from >10 litters)	ND	–	Potter et al., 2009	Emily Ling-Lin Pai, John L.R. Rubenstein
Drd1-Cre	B6-Tg(Drd1-Cre) EY262GSat	Ai14[e]	E or G	0 (from >3 years breeding)	0 (from >3 years breeding)	–	–	Kevin T. Beier
	B6.FVB(Cg)-Tg(Drd1-cre)EY262Gsat/Mmucd/ GENSAT	*Gt(ROSA) 26Sor*$^{tm2(CAG-tdTomato)Fawa}$	F	0 (0/20)	ND	–	–	Hisashi Umemori

(*Continued on next page*)

Table 1. *Continued*

Cre line Common Name	Full Cre Line Name/ Source	Target Gene/ Reporter	Breeding Strategy[a]	Germline Recombination Efficiency, Cre from Father[b]	Germline Recombination Efficiency, Cre from Mother[b]	Germline Recombindation Efficiency, Parental Sex Effects Unknown[b]	Reference/ Associated Publication[c]	Contributors[d]
E3-CreN	*Grin2c*$^{tm2(icre)Mwa}$	*Cacna1a*^{tm1Kano}	C	41.2% (7/17) of Cre negative offspring	0 (0/20)	–	–	Junko Motohashi, Michisuke Yuzaki
Emx1-Cre	*Emx1*$^{tm1(cre)Ito}$	B6.129(FVB)$^{-}$ *Gabra1*^{tm1Geh}/J	A	36%	36%	–	Zeller et al., 2008	–
Emx1-Cre	B6.129S2-*Emx1*$^{tm1(cre)Krj}$/J	*Syngap1*$^{tm1.1Geno}$	Not specified	observed	0 or less than male	–	Ozkan et al., 2014	–
	B6.129S2-*Emx1*$^{tm1(cre)Krj}$/J	Ai93[e]	Not specified	–	–	observed	Steinmetz et al., 2017	–
	B6.129S2-*Emx1*$^{tm1(cre)Krj}$/J	*Wwp2*$^{tm1.1Hkb}$	C	33.3% (4/12) of Cre negative offspring	0 (0/20)	–	Ambrozkiewicz et al., 2018	Mateusz C. Ambrozkiewicz, Fritz Benseler, Nils Brose, Hiroshi Kawabe
	B6.129S2-*Emx1*$^{tm1(cre)Krj}$/J	*Rai1*$^{tm2.1Luo}$/J	A	40.5% (64/158)	ND	–	–	Wei-Hsiang Huang, Liqun Luo
En1-Cre	*En1*$^{tm2(cre)Wrst}$/J	*Chat/Slc18a3*$^{tm1.2Vpra}$	A or C	54.6% (95/174 including 17 Cre negative offspring)	36.2% (54/149 including 3 Cre negative offspring)	–	Janickova et al., 2017	Marco A.M. Prado, Vania F. Prado
Foxd1-Cre	B6;129S4-*Foxd1*$^{tm1(GFP/cre)Amc}$/J	Ai9[e]	B	0 (from >7 litters)	0 (from >7 litters)	–	–	Wenjia You, Constance L. Cepko
Foxg1-Cre	129(Cg)-*Foxg1*$^{tm1(cre)Skm}$/J	*Gt(ROSA)26Sor*^{tm1Sor}	B	68.8% (11/16)	ND	–	Weng et al., 2008	–
Gad2-IRES-Cre	B6.Cg-*Gad2*$^{tm2(cre)Zjh}$/J	*stxbp1*^{tm1Mver}	E or G	–	–	~50% (from >17 litters)	Kovacevic et al., 2018	Matthijs Verhage
	B6N.Cg-*Gad2*$^{tm2(cre)Zjh}$/J	*Rai1*$^{tm2.1Luo}$/J	A	0 (0/26)	ND	–	–	Wei-Hsiang Huang, Liqun Luo
	B6-*Gad2*$^{tm2(cre)Zjh}$/J	Ai14[e]	E or G	0 (from >6 years breeding)	0 (from >6 years breeding)	–	–	Kevin T. Beier
GFAP-Cre	Tg(GFAP-cre)25Mes	*Gja1*^{tm1Kwi}	C	16.7% (7/42) of Cre negative offspring	50% (8/16) of Cre negative offspring	–	Zhang et al., 2013	–
	Tg(GFAP-cre)25Mes	*Epas1*^{tm1Mcs}/J	A or C	50% (9/18)	42.9% (6/14)	–	–	Ariane Pereira, Jeremy N. Kay
GFAP-Cre	B6.Cg-Tg(Gfap-cre) 77.6Mvs/2J	*Slc16a1*$^{lox/lox}$	C	observed (100% from a few litters)	<1% (from >35 litters)	–	–	Thomas Phillips, Jeffrey Rothstein

(*Continued on next page*)

Table 1. ***Continued***

Cre line Common Name	Full Cre Line Name/ Source	Target Gene/ Reporter	Breeding Strategy[a]	Germline Recombination Efficiency, Cre from Father[b]	Germline Recombination Efficiency, Cre from Mother[b]	Germline Recombindation Efficiency, Parental Sex Effects Unknown[b]	Reference/ Associated Publication[c]	Contributors[d]
GLAST-CreERT2	Tg(Slc1a3-cre/ERT) 1Nat/J	*Nlgn2*$^{tm1.1Sud}$/J	A	–	–	0 (0/160)	Stogsdill et al., 2017	Jeff Stogsdill, Cagla Eroglu
	Tg(Slc1a3-cre/ERT) 1Nat/J	*Gt(ROSA) 26Sor*$^{tm14(CAG-tdTomato)Hze}$/J	A	–	–	0 (0/160)	Stogsdill et al., 2017	Jeff Stogsdill, Cagla Eroglu
Gpr26-Cre	B6-Tg(Gpr26-cre) KO250Gsat/ Mmucd	*Clstn3*^{tm1Amcr}/J	C	observed	0 (0/92)	–	–	Lin Luo, Ann Marie Craig
	B6-Tg(Gpr26-cre) KO250Gsat/ Mmucd	Ai32[e]	B	27.6% (8/29 including 5 Cre negative offspring)	0 (0/23)	–	–	Lin Luo, Ann Marie Craig
Grik4-Cre	B6-Tg(Grik4-cre) G32-4Stl/J	*Khdrbs3*$^{tm1.1Schei}$/J	E	–	–	37.5% (12/32)	–	Lisa Traunmüller, Andrea Gomez, Peter Scheiffele
	B6-Tg(Grik4-cre) G32-4Stl/J	*Khdrbs3*$^{tm1.1Schei}$/J	C	0% (0/42)	ND	–	–	Lisa Traunmüller, Andrea Gomez, Peter Scheiffele
	B6-Tg(Grik4-cre) G32-4Stl/J	*Rpl22*$^{tm1.1Psam}$/J	C	0% (0/10)	ND	–	–	Lisa Traunmüller, Andrea Gomez, Peter Scheiffele
	B6-Tg(Grik4-cre) G32-4Stl/J	*Fgf22*$^{tm1a(EUCOMM)Hmgu}$	A, B, C, F, G	–	–	0 (0/16)	Terauchi et al., 2017	Hisashi Umemori
Grik4-Cre	*Grik4*$^{tm1(cre)Ksak}$	*Grin2b*^{tm1Ksak}	Not specified	–	–	observed	Akashi et al., 2009	–
	Grik4$^{tm1(cre)Ksak}$	Ai9[e]	D	71.4% (5/7) of Cre negative offspring	48.3% (14/29) of Cre negative offspring	–	–	Yu Itoh-Maruoka, Tomohiko Maruo, Kenji Sakimura, Kenji Mandai, Yoshimi Takai
	Grik4$^{tm1(cre)Ksak}$	*Grik2*$^{tm1.1\ Ksak}$	C	95% (38/40) of Cre negative offspring	0 (0/31)	–	–	Junko Motohashi, Michisuke Yuzaki
Htr3a-Cre	Tg(Htr3a-cre) NO152Gsat/ Mmucd	Ai14[e]	multiple	–	–	~20%–50% (from >60 litters)	–	Kenneth Pelkey, Chris J. McBain
Isl1-Cre	*Isl1*$^{tm1(cre)Sev}$/J	*Ptf1a*^{tm3Cvw}	A	0 (from 2 litters)	0 (from 2 litters)	–	–	Ariane Pereira, Jeremy N. Kay

(*Continued on next page*)

Table 1. *Continued*

Cre line Common Name	Full Cre Line Name/ Source	Target Gene/ Reporter	Breeding Strategy[a]	Germline Recombination Efficiency, Cre from Father[b]	Germline Recombination Efficiency, Cre from Mother[b]	Germline Recombindation Efficiency, Parental Sex Effects Unknown[b]	Reference/ Associated Publication[c]	Contributors[d]
Klf3-CreERT2	B6;129P-*Klf3*$^{tm1(cre/ERT2)Pzg}$/J	Ai9[e]	B	0 (from >15 litters)	0 (from >15 litters)	–	–	Wenjia You, Constance L. Cepko
Nestin-Cre	Tg(Nes-cre)1Kln/J	*Gja1*^{tm8Kwi}	Not specified	–	–	28.6% (4/14) of Cre negative offspring	Zhang et al., 2013	–
	Tg(Nes-cre)1Kln/J	Ai34[e]	B	12.5% (1/8)	20% (2/10)	–	–	Jiexin Wang, Pascal S. Kaeser
	Tg(Nes-cre)1Kln/J	*Rai1*$^{tm2.1Luo}$/J	A	79.1% (117/148)	ND	–	Huang et al., 2016, 2018	Wei-Hsiang Huang, Liqun Luo
Nestin-Cre	Tg(Nes-cre)1Atp	*Runx1*^{tm1Buch}	D	–	–	observed in Cre negative offspring	Buchholz et al., 2000	–
	Tg(Nes-cre)1Atp	*Fgf8*$^{tm1.3Mrt}$	A	~100%	observed	–	Dubois et al., 2006; Trumpp et al., 1999	–
	Tg(Nes-cre)1Atp	*Ntf3*^{tm2Jae}	F	~100%	ND	–	Bates et al., 1999	–
	Tg(Nes-cre)1Atp	*Smad4*$^{tm2.1Cxd}$	A	~100%	0 or less than male	–	Zhou et al., 2003	–
	Tg(Nes-cre)1Atp	*Rb1*^{tm3Tyj}	A	~100%	ND	–	MacPherson et al., 2003	v
NEX-Cre	*Neurod6*$^{tm1(cre)Kan}$	*Wwp1*$^{tm1.1Hkb}$	C	0 (0/30)	0 (0/30)	–	–	Hiroshi Kawabe
	Neurod6$^{tm1(cre)Kan}$	*Wwp2*$^{tm1.1Hkb}$	C	0 (0/30)	0 (0/30)	–	–	Hiroshi Kawabe
	Neurod6$^{tm1(cre)Kan}$	*Gt(ROSA)26Sor*^{tm1Sor}	multiple	0 (from >5 litters)	0 (from >5 litters)	–	Goebbels et al., 2006	Sandra Goebbels, Klaus A. Nave
Ngn2-CreER	*Neurog2*$^{tm1(cre/Esr1*)And}$	Ai9[e]	B	0 (from >25 litters)	0 (from >25 litters)	–	–	Wenjia You, Constance L. Cepko
Nkx2.1-Cre	C57BL/6J-Tg(Nkx2-1-cre)2Sand/J	RCE:loxp[e]	multiple	–	–	~10%–30% (from >60 litters)	–	Kenneth Pelkey, Chris J. McBain
	C57BL/6J-Tg(Nkx2-1-cre)2Sand/J	Ai14[e]	multiple	–	–	~10%–30% (from >60 litters)	–	Kenneth Pelkey, Chris J. McBain
	C57BL/6J-Tg(Nkx2-1-cre)2Sand/J	*Chat/Slc18a3*$^{tm1.2Vpra}$	C	5.4% (12/224)	12.5% (24/192 including 5 Cre negative offspring)	–	Kolisnyk et al., 2017	Marco A.M. Prado, Vania F. Prado
	B6.CD1-Tg(Nkx2-1-cre)2Sand	*Mafb*$^{tm1.1Good}$	H	observed (from >100 litters)	observed (from >100 litters)	–	Pai et al., 2019	Emily Ling-Lin Pai, John L.R. Rubenstein

(*Continued on next page*)

Table 1. ***Continued***

Cre line Common Name	Full Cre Line Name/ Source	Target Gene/ Reporter	Breeding Strategy[a]	Germline Recombination Efficiency, Cre from Father[b]	Germline Recombination Efficiency, Cre from Mother[b]	Germline Recombindation Efficiency, Parental Sex Effects Unknown[b]	Reference/ Associated Publication[c]	Contributors[d]
	B6.CD1-Tg(Nkx2-1-cre)2Sand	*Maf*$^{tm2.1Cbm}$	H	observed (from >100 litters)	observed (from >100 litters)	–	Pai et al., 2019	Emily Ling-Lin Pai, John L.R. Rubenstein
	B6.CD1-Tg(Nkx2-1-cre)2Sand	Ai14[e]	H	observed (from >100 litters)	observed (from >100 litters)	–	Pai et al., 2019	Emily Ling-Lin Pai, John L.R. Rubenstein
Ntsr1-Cre	B6.FVB(Cg)-Tg(Ntsr1-cre) GN220Gsat/Mmucd	Ai93[e]	Not specified	–	–	observed	Steinmetz et al., 2017	–
	B6.Cg-Tg(Ntsr1-cre) GN220Gsat/Mmucd	*Rpl22*$^{tm1.1Psam}$/J	C	ND	0 (0/21)	–	–	Susanne Falkner, Peter Scheiffele
	B6.Cg-Tg(Ntsr1-cre) GN220Gsat/Mmucd	*Rpl22*$^{tm1.1Psam}$/J	E	–	–	8.1% (3/37)	–	Susanne Falkner, Peter Scheiffele
Nos1-Cre	*Nos1*$^{tm1(cre)Mgmj}$	*Lepr*$^{tm1.1Chua}$	C	ND	observed	–	Rupp et al., 2018	–
Pcp2/L7-Cre	B6.129-Tg(Pcp2-cre) 2Mpin/J	Tsc1$^{tm1.1Djk}$	A or E	–	–	~5%	Tsai et al., 2012	–
	B6.129-Tg(Pcp2-cre) 2Mpin/J	*Adgrb3*^{tm1Ksak}	C	84% (63/75) of Cre negative offspring	0 (0/90)	–	Kakegawa et al., 2015	Junko Motohashi, Michisuke Yuzaki
	B6.129-Tg(Pcp2-cre) 2Mpin/J	*Atg*^{tm1Myok}	C	14.3% (3/21) of Cre negative offspring	0 (0/50)	–	Nishiyama et al., 2007	Junko Motohashi, Michisuke Yuzaki
	B6.129-Tg(Pcp2-cre) 2Mpin/J	PhotonSABER-LSL	C	69% (58/84) of Cre negative offspring	0 (0/256)	–	Kakegawa et al., 2018	Junko Motohashi, Michisuke Yuzaki
Pcp2/L7-Cre	B6.129-*Pcp2*$^{tm1(cre)Nobs}$	*Rpl22*$^{tm1.1Psam}$/J	C	0 (0/11)	ND	–	–	Elisabetta Furlanis, Peter Scheiffele
	B6.129-*Pcp2*$^{tm1(cre)Nobs}$	*Rpl22*$^{tm1.1Psam}$/J	G	0 (0/4)	0 (0/4)	–	–	Elisabetta Furlanis, Peter Scheiffele
Pou4f2-Cre	*Pou4f2*$^{tm1(cre)Bnt}$/J	Ai9[e]	B	~100%	0	–	Simmons et al., 2016	–
Pvalb-2A-Cre	B6.Cg-*Pvalb*$^{tm1.1(cre)Aibs}$/J	B6.129S4-*Clock*^{tm1Rep}/J	F	50% (24/48)	<5%	–	Kobayashi and Hensch, 2013	–
Pvalb-IRES-Cre	B6.129P2-*Pvalb*$^{tm1(cre)Arbr}$/J	*Khdrbs3*$^{tm1.1Schei}$/J	D	ND	0 (0/23)	–	–	Elisabetta Furlanis, Lisa Traunmüller, Peter Scheiffele

(*Continued on next page*)

Table 1. ***Continued***

Cre line Common Name	Full Cre Line Name/ Source	Target Gene/ Reporter	Breeding Strategy[a]	Germline Recombination Efficiency, Cre from Father[b]	Germline Recombination Efficiency, Cre from Mother[b]	Germline Recombindation Efficiency, Parental Sex Effects Unknown[b]	Reference/ Associated Publication[c]	Contributors[d]
	B6.129P2-*Pvalb*$^{tm1(cre)Arbr}$/J	*Rpl22*$^{tm1.1Psam}$/J	A	ND	0 (0/19)	–	–	Elisabetta Furlanis, Lisa Traunmüller, Peter Scheiffele
	B6.129P2-*Pvalb*$^{tm1(cre)Arbr}$/J	*Rpl22*$^{tm1.1Psam}$/J	B	0 (0/24)	ND	–	–	Elisabetta Furlanis, Lisa Traunmüller, Peter Scheiffele
	B6.129P2-*Pvalb*$^{tm1(cre)Arbr}$/J	*Rpl22*$^{tm1.1Psam}$/J	F	0 (0/11)	ND	–	–	Elisabetta Furlanis, Lisa Traunmüller, Peter Scheiffele
	B6.129P2-*Pvalb*$^{tm1(cre)Arbr}$/J	*Rpl22*$^{tm1.1Psam}$/J	E	0 (0/16)	0 (0/16)	–	–	Elisabetta Furlanis, Lisa Traunmüller, Peter Scheiffele
	B6.129P2-*Pvalb*$^{tm1(cre)Arbr}$/J	*Rpl22*$^{tm1.1Psam}$/J	G	0 (0/3)	0 (0/3)	–	–	Elisabetta Furlanis, Lisa Traunmüller, Peter Scheiffele
	B6.129P2-*Pvalb*$^{tm1(cre)Arbr}$/J	*Trpm7*^{tm1Clph}	C	0 (0/57)	ND	–	–	Cui Chen, Wei Li, Nashat Abumaria
Rbp4-Cre	Tg(Rbp4-cre) KL100Gsat/ Mmucd	Ai93[e]	Not specified	–	–	observed	Steinmetz et al., 2017	–
	B6.Cg-Tg(Rbp4-cre) KL100Gsat/Mmucd	*Rpl22*$^{tm1.1Psam}$/J	E	0 (0/14)	0 (0/14)	–	–	Susanne Falkner, Peter Scheiffele
	B6.Cg-Tg(Rbp4-cre) KL100Gsat/Mmucd	*Rpl22*$^{tm1.1Psam}$/J	B	ND	0 (0/16)	–	–	Susanne Falkner, Peter Scheiffele
	B6.FVB(Cg)-Tg(Rbp4-cre)KL100Gsat/Mmucd/ GENSAT	*Gt(ROSA) 26Sor*$^{tm2(CAG-tdTomato)Fawa}$	F	26.7% (4/15)	ND	–	–	Naosuke Hoshina, Hisashi Umemori
Rgs9-Cre	*Rgs9*$^{tm1(cre)Yql}$	*Cnr1*$^{tm1.2Ltz}$	Not specified	–	–	observed	Davis et al., 2018	–
	Rgs9$^{tm1(cre)Yql}$	B6.Cg-*Rem2*$^{tm3551(T2A-mkate2)Arte}$	A	7.6%	55.1%	–	Liput, 2018	–
Rorb-Cre	B6.129S-*Rorb*$^{tm1.1(cre)Hze}$/J	Ai93[e]	Not specified	–	–	observed	Steinmetz et al., 2017	–
	B6.129S-*Rorb*$^{tm1.1(cre)Hze}$/J	*Rpl22*$^{tm1.1Psam}$/J	E	0 (0/17)	0 (0/17)	–	–	Susanne Falkner, Peter Scheiffele
	B6.129S-*Rorb*$^{tm1.1(cre)Hze}$/J	*Rpl22*$^{tm1.1Psam}$/J	G	0 (0/22)	0 (0/22)	–	–	Susanne Falkner, Peter Scheiffele

(*Continued on next page*)

Table 1. ***Continued***

Cre line Common Name	Full Cre Line Name/ Source	Target Gene/ Reporter	Breeding Strategy[a]	Germline Recombination Efficiency, Cre from Father[b]	Germline Recombination Efficiency, Cre from Mother[b]	Germline Recombindation Efficiency, Parental Sex Effects Unknown[b]	Reference/ Associated Publication[c]	Contributors[d]
	B6.129S-*Rorb*$^{tm1.1(cre)Hze}$/J	*Rpl22*$^{tm1.1Psam}$/J	C	ND	0 (0/20)	–	–	Susanne Falkner, Peter Scheiffele
Scnn1a-Cre	B6;C3-Tg(Scnn1a-cre)2Aibs/J	*Rpl22*$^{tm1.1Psam}$/J	A	0 (0/17)	ND	–	–	Elisabetta Furlanis, Peter Scheiffele
	B6;C3-Tg(Scnn1a-cre)2Aibs/J	*Rpl22*$^{tm1.1Psam}$/J	C	0 (0/17)	ND	–	–	Elisabetta Furlanis, Peter Scheiffele
Scx-Cre	Tg(Scx-GFP/cre)1Stzr	Ai9[e]	B	0 (from >10 litters)	0 (from >10 litters)	–	–	Wenjia You, Constance L. Cepko
SERT-Cre	B6.129(Cg)-*Slc6a4*$^{tm1(cre)Xz}$/J	*Lepr*$^{tm1.1Chua}$	C	–	–	~100%	Lam et al., 2011	–
	B6.129(Cg)-*Slc6a4*$^{tm1(cre)Xz}$/J	*Stxbp1*^{tm1Mver}	A	observed (from >20 litters)	observed (from >20 litters)	–	Dudok et al., 2011	Matthijs Verhage
Sim1-Cre	Tg(Sim1-cre)1Lowl/J	*Rai1*$^{tm2.1Luo}$/J	A	0 (0/95)	ND	–	–	Wei-Hsiang Huang, Liqun Luo
Six3-Cre	Tg(Six3-cre)69Frty/GcoJ	*Isl1*$^{tm1.1Whk}$	A	1/1	2/3	–	Ray et al., 2018	Ariane Pereira, Jeremy N. Kay
	Tg(Six3-cre)69Frty/GcoJ	*Syk*$^{tm1.2Tara}$	A	1/1	1/2	–	Ray et al., 2018	Ariane Pereira, Jeremy N. Kay
	Tg(Six3-cre)69Frty/GcoJ	*Tgfb3*^{tm1Moaz}	A	1/2	3/4	–	Ray et al., 2018	Ariane Pereira, Jeremy N. Kay
	Tg(Six3-cre)69Frty/GcoJ	*Flrt2*$^{tm1c(EUCOMM)Wtsi}$	A	3/3	4/4	–	Ray et al., 2018	Ariane Pereira, Jeremy N. Kay
	Tg(Six3-cre)69Frty/GcoJ	*Ptf1a*^{tm3Cvw}	A	1/1	1/1	–	Ray et al., 2018	Ariane Pereira, Jeremy N. Kay
	Tg(Six3-cre)69Frty/GcoJ	*Pcdhg*^{tm2Xzw}	multiple	observed	observed	–	Ing-Esteves et al., 2018	Joshua R. Sanes
	Tg(Six3-cre)69Frty/GcoJ	Pcdha^{em1Jrs}	multiple	observed	observed	–	Ing-Esteves et al., 2018	Joshua R. Sanes
	Tg(Six3-cre)69Frty/GcoJ	*Chat/Slc18a3*$^{tm1.2Vpra}$	A or C	51.9.% (177/341 including 58 Cre negative offspring)	100% (12/12 including 4 Cre negative offspring)	–	Martyn et al., 2012	Marco A.M. Prado, Vania F. Prado
Sox10-Cre	Tg(Sox10-cre)1Wdr	*Gria2*^{tm3Rsp}	F	observed	0	–	Kougioumtzidou et al., 2017	–

(*Continued on next page*)

Table 1. *Continued*

Cre line Common Name	Full Cre Line Name/ Source	Target Gene/ Reporter	Breeding Strategy[a]	Germline Recombination Efficiency, Cre from Father[b]	Germline Recombination Efficiency, Cre from Mother[b]	Germline Recombindation Efficiency, Parental Sex Effects Unknown[b]	Reference/ Associated Publication[c]	Contributors[d]
	Tg(Sox10-cre)1Wdr	*Gjb2*^{tm1Ugds}	Not specified	observed	0 or less than male	–	Crispino et al., 2011; Takada et al., 2014	–
	B6;CBA-Tg(Sox10-cre) 1Wdr/J	*Slc16a1*$^{lox/lox}$	C	ND	0 (from >35 litters)	–	–	Thomas Phillips, Jeffrey Rothstein
Sst-IRES-Cre	B6-*Sst*$^{tm2.1(cre)Zjh}$	Ai9[e]	multiple	–	–	<5%	–	Elisabetta Furlanis, Lisa Traunmüller, Peter Scheiffele
	B6-*Sst*$^{tm2.1(cre)Zjh}$	*Khdrbs3*$^{tm1.1Schei}$/J	E	0 (0/5)	0 (0/5)	–	–	Elisabetta Furlanis, Lisa Traunmüller, Peter Scheiffele
	B6-*Sst*$^{tm2.1(cre)Zjh}$	*Khdrbs3*$^{tm1.1Schei}$/J	C	0 (0/16)	0 (0/10)	–	–	Elisabetta Furlanis, Lisa Traunmüller, Peter Scheiffele
	B6-*Sst*$^{tm2.1(cre)Zjh}$	*Rpl22*$^{tm1.1Psam}$/J	E	0 (0/26)	0 (0/26)	–	–	Elisabetta Furlanis, Lisa Traunmüller, Peter Scheiffele
	B6-*Sst*$^{tm2.1(cre)Zjh}$	*Rpl22*$^{tm1.1Psam}$/J	C	0 (0/12)	0 (0/2)	–	–	Elisabetta Furlanis, Lisa Traunmüller, Peter Scheiffele
	B6;129S4;CD1-*Sst*$^{tm2.1(cre)Zjh}$	*Mafb*$^{tm1.1Good}$	H	0 (from >60 litters)	0 (from >60 litters)	–	Pai et al., 2019	Emily Ling-Lin Pai, John L.R. Rubenstein
	B6;129S4;CD1-*Sst*$^{tm2.1(cre)Zjh}$	*Maf*$^{tm2.1Cbm}$	H	0 (from >60 litters)	0 (from >60 litters)	–	Pai et al., 2019	Emily Ling-Lin Pai, John L.R. Rubenstein
	B6;129S4;CD1-*Sst*$^{tm2.1(cre)Zjh}$	Ai14[e]	H	0 (from >60 litters)	0 (from >60 litters)	–	Pai et al., 2019	Emily Ling-Lin Pai, John L.R. Rubenstein
Synapsin1-Cre	B6.Cg-Tg(Syn1-cre)671Jxm/J	*Prkar2b*^{tm3Gsm}	F	observed	0 or less than male	–	Zheng et al., 2013	–
	B6.Cg-Tg(Syn1-cre)671Jxm/J	*Hif1a*^{tm1Rsjo}	C	63%	0	–	Zheng et al., 2013	–
	B6.Cg-Tg(Syn1-cre)671Jxm/J	*Erc2*$^{tm1.1Sud}$/J	A	ND	0 (0/39)	–	–	Jiexin Wang, Pascal S. Kaeser
Thy1-CreER	Tg(Thy1-cre/ERT2,-EYFP) HGfng/PyngJ	*Fgf22*$^{tm1a(EUCOMM)Hmgu}$	A, B, C, D, E, F	–	–	0 (0/27)	–	Hisashi Umemori
VAChT.Cre.Fast	B6;129^{-} Tg(SLC18A3-cre)KMisa/0	*Chat/Slc18a3*$^{tm1.2Vpra}$	A or C	6.1% (7/115)	1.3% (1/76)	–	–	Marco A.M. Prado, Vania F. Prado

(*Continued on next page*)

Table 1. ***Continued***

Cre line Common Name	Full Cre Line Name/ Source	Target Gene/ Reporter	Breeding Strategy[a]	Germline Recombination Efficiency, Cre from Father[b]	Germline Recombination Efficiency, Cre from Mother[b]	Germline Recombindation Efficiency, Parental Sex Effects Unknown[b]	Reference/ Associated Publication[c]	Contributors[d]
VGAT/VIAAT-Cre	*Slc32a1*$^{tm2(cre)Lowl}$/J	*Rai1*$^{tm2.1Luo}$/J	A	0 (0/103)	ND	–	–	Wei-Hsiang Huang, Liqun Luo
VGAT/VIAAT-Cre	B6.FVB-Tg(Slc32a1-cre) 2.1Hzo/FrkJ/	*Dnmt3a*$^{tm3.1Enl}$	A or F	60.9% (14/23)	0.7% (from >100 mice)	–	–	Laura Lavery, Huda Y. Zoghbi
VGluT1-IRES2-Cre-D	*Slc17a7*$^{tm1.1(cre)Hze}$/J	Ai34[e]	A, F, H	33.3% (10/30)	38.5% (5/13)	–	–	Jiexin Wang, Pascal S. Kaeser
	B6;129S-*Slc17a7*$^{tm1.1(cre)Hze}$/J	*Rai1*$^{tm2.1Luo}$/J	A	0 (0/20)	ND	–	–	Wei-Hsiang Huang, Liqun Luo
VGluT2-IRES-cre	*Slc17a6*$^{tm2(cre)Lowl}$/J	*Rai1*$^{tm2.1Luo}$/J	A	0 (0/142)	ND	–	–	Wei-Hsiang Huang, Liqun Luo
	Slc17a6$^{tm2(cre)Lowl}$/J	Ai14[e]	E or G	0 (from >3 years breeding)	0 (from >3 years breeding)	–	–	Kevin T. Beier
VGluT3-Cre	Tg(Slc17a8-icre) 1Edw/SealJ	*Chat/Slc18a3*$^{tm1.2Vpra}$	C	1.9% (5/265 including 2 Cre negative offspring)	1.9% (1/52)	–	–	Marco A.M. Prado, Vania F. Prado
	Tg(Slc17a8-icre) 1Edw/SealJ	Ai14[e]	multiple	–	–	~30% (from >60 litters)	–	Kenneth Pelkey, Chris J. McBain
VIP-Cre	B6-*Vip*$^{tm1(cre)Zjh}$/J	*Khdrbs3*$^{tm1.1Schei}$/J	C	0 (0/22)	ND	–	–	Lisa Traunmüller, Peter Scheiffele
	B6-*Vip*$^{tm1(cre)Zjh}$/J	*Khdrbs3*$^{tm1.1Schei}$/J	E	0 (0/7)	0 (0/7)	–	–	Lisa Traunmüller, Peter Scheiffele
	B6-*Vip*$^{tm1(cre)Zjh}$/J	*Rpl22*$^{tm1.1Psam}$/J	E	0 (0/31)	0 (0/31)	–	–	Lisa Traunmüller, Peter Scheiffele
	B6-*Vip*$^{tm1(cre)Zjh}$/J	Ai9[e]	multiple	–	–	<10%	–	Lisa Traunmüller, Peter Scheiffele
Wnt1-Cre	B6.Cg-*H2afv*$^{Tg(Wnt1-cre)11Rth}$	*Gt(ROSA)26Sor*^{tm1Sor}	B	0 (0/8)	0 (0/6)	–	Weng et al., 2008	–
	B6.Cg-*H2afv*$^{Tg(Wnt1-cre)11Rth}$	*Neo1*$^{tm1.1Jfcl}$	F	0 (0/37)	ND	–	–	Emilie Dumontier, Jean-François Cloutier

ND, not determined. See also Figure S1 and Table S1.

[a]Breeding strategy: A: Target$^{f/+}$; Cre driver X Target$^{f/f}$; B: Target$^{f/+}$; Cre driver X Target$^{+/+}$; C: Target$^{f/f}$; Cre driver X Target$^{f/f}$; D: Target$^{f/f}$; Cre driver X Target$^{+/+}$; E: Target$^{f/+}$; Cre driver ⊗; F: Target$^{f/+}$; Cre driver X Target$^{f/+}$; G: Target$^{f/f}$; Cre driver ⊗; H: Target$^{f/f}$; Cre driver X Target$^{f/+}$.

[b]The numbers (x/y) indicate that x offspring with germline recombination were found from y offspring with the target locus in cumulative data from multiple litters. ND indicates not determined.

[c]Where no contributors are listed, the information is from the reference. Where contributors are listed, the associated publication reported findings from the crosses, but not information about germline recombination.

[d]Contributors providing information on germline recombination. Please contact the Lead Contact for the electronic addresses of principal investigators.

[e]Ai9: B6.Cg-Gt(ROSA)26Sor$^{tm9(CAG-tdTomato)Hze}$/J; Ai14: B6.Cg-Gt(ROSA)26Sor$^{tm14(CAG-tdTomato)Hze}$/J; Ai32: B6;129S-Gt(ROSA)26Sor$^{tm32(CAG-COP4*H134R/EYFP)Hze}$/J; Ai93: B6;129S6-Igs7$^{tm93.1(tetO-GCaMP6f)Hze}$/J; ROSA$^{mT/mG}$: Gt(ROSA)26Sor$^{tm4(ACTB-tdTomato,-EGFP)Luo}$/J; RCE:loxp: Gt(ROSA)26Sor$^{tm1.1(CAG-EGFP)Fsh}$/Mmjax; Ai34: 129S-Gt(ROSA)26Sor$^{tm34.1(CAG-Syp/tdTomato)Hze}$/J.

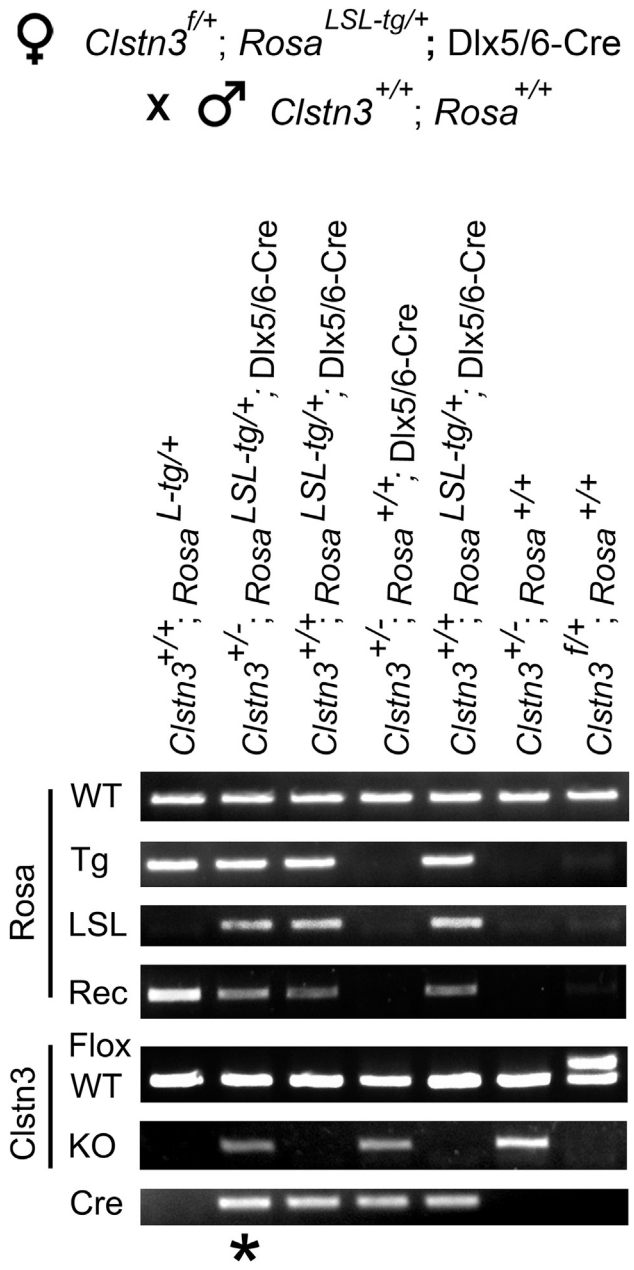

Figure 3. Differential Recombination at Two Target Loci

Breeding scheme and genotyping result from tail tissue for a litter from crossing female *Clstn3*$^{f/+}$;*Rosa*$^{LSL\text{-}tg/+}$; Dlx5/6-Cre with male WT mice. In one offspring (*), ubiquitous recombination happened at the *Clstn3*$^{f/+}$ locus but not at the Ai32 *Rosa*$^{LSL\text{-}tg/+}$ locus implying differential activity of Cre at these target loci in the female germ cells. This mouse exhibited mosaic deletion in tail tissue at the *Rosa* locus as indicated by the presence of WT, LSL, and Rec PCR bands (see Figure 1B for a diagram).

for recombination to occur directly in the F1 zygote when the Cre driver is inherited from one parent and the target locus from the other parent, resulting in global recombination and also germline transmission of the recombined allele. Indeed, this occurs with deleter (Tg(CMV-cre)1Cgn) and EIIa-Cre (Tg(EIIa-cre) C5379Lmgd) mouse lines commonly used in crosses with floxed mice to generate lines with global recombination (Lakso et al., 1996; Schwenk et al., 1995). In F1 mice crossing EIIa-Cre with a floxed target, half of the mice showed global recombination resulting from Cre activity in the one-cell zygote and half showed mosaic recombination (Lakso et al., 1996). Furthermore, virtually all floxed loci undergo global recombination in F1 offspring of females carrying Vasa-Cre (Tg(Ddx4-cre)1Dcas), even in offspring lacking Cre, due to apparent perdurance of Cre protein in the zygote (Gallardo et al., 2007). However, global recombination was not commonly observed in our F1 mice combining Cre drivers and target loci. For example, we observed no recombination in tail tissue of F1 mice from Dlx5/6-Cre X Ai32 crosses (0/9 with maternal Cre) or Gpr26-Cre X Ai32 crosses (0/19 with paternal Cre) despite global recombination in some F2 mice (Figures 1 and 2). Furthermore, in the crosses described in Figures 1A and 2A, recombination in the F2 zygote would likely affect both *Clstn3*$^{f/f}$ alleles, yet recombination was only observed for one of the two alleles, suggesting that recombination occurred in germline cells of F1 mice but not in F2 zygotes. Similarly, in the publications discussed here reporting global recombination in F2 mice resulting from germline recombination in F1 mice, global recombination was not observed in F1 mice where analyzed (Simmons et al., 2016; Weng et al., 2008). Thus, recombination can occur in zygotes combining a Cre driver and a target locus but the prevalence appears to be considerably lower than in germline cells carrying both the Cre driver and the target locus.

Comparisons among Related Cre Driver Lines

Different Cre driver lines with some common transcriptional regulatory elements frequently behaved differently regarding germline recombination. Perhaps the most interesting comparison is for the pairs of Cre driver lines targeting common transcriptional regulatory elements by both random transgenic insertion and KI approaches. For one such pair, Grik4-Cre, germline recombination was observed with both approaches. For the other two such pairs, Pcp2/L7-Cre and VGAT/VIAAT-Cre, germline recombination was observed for the transgenic line but not the KI line. While we cannot rule out differences related to target locus selectivity (see below), intrinsic differences between these related Cre driver lines seems likely. Potential factors contributing to germline recombination in the transgenic lines include ectopic expression due to a limited regulatory region, genetic and epigenetic effects of the transgene insertion site, and high expression due to multi-copy integration (although the latter would not apply to the Pcp2/L7-Cre transgenic line, which was generated through embryonic stem cells to avoid multi-copy integration (Barski et al., 2000).

Differences in germline recombination were observed even among Cre driver lines generated using similar strategies. Both Nestin-Cre transgenic lines showed germline recombination but with some differences in frequencies. The four CaMKII-Cre transgenic lines were generated with similar targeting strategies (Dragatsis and Zeitlin, 2000; Minichiello et al., 1999; Rios et al., 2001; Tsien et al., 1996a). While all four CaMKII-Cre lines showed paternal germline recombination, two lacked maternal germline recombination, one had a low rate, and the last was not tested maternally. Comparing the two lines generated with exactly

Table 2. Prevalence of Germline Recombination in Zebrafish Cre Driver Lines that Show Nervous System Recombination

Cre Line Common Name	Full Cre Line Name/ Source	Target Gene/ Reporter	Breeding Strategy[a]	Germline Recombination Efficiency, Cre from Father[b]	Germline Recombination Efficiency, Cre from Mother[b]	Reference/ Associated Publication[c]	Contributors[d]
y492-Cre	Et(REX2-SCP1-Ocu.Hbb2:Cre-2A-Cerulean)y492	Tg(actb2:LOXP-EGFP-LOXP-LY-TagRFPT)y272	A	4.8% (3/63)	0% (0/134)	Tabor et al., 2019	Jennifer Sinclair, Harold Burgess
y547-Cre	Et(REX2-SCP1-Ocu.Hbb2:Cre)y547	Tg(actb2:LOXP-EGFP-LOXP-LY-TagRFPT)y272	B	82.3% (51/62)	38.1% (8/21)	Tabor et al., 2019	Jennifer Sinclair, Harold Burgess
y549-Cre	Et(REX2-SCP1-Ocu.Hbb2:Cre)y549	Tg(actb2:LOXP-EGFP-LOXP-LY-TagRFPT)y272	B	0% (0/58)	6.7% (2/30)	Tabor et al., 2019	Jennifer Sinclair, Harold Burgess
y559-Cre	Et(REX2-SCP1-Ocu.Hbb2:Cre)y559	Tg(actb2:LOXP-EGFP-LOXP-LY-TagRFPT)y272	B	3.4% (3/89)	2.4% (1/42)	Tabor et al., 2019	Jennifer Sinclair, Harold Burgess
y546-Cre	Et(REX2-SCP1-Ocu.Hbb2:Cre-2A-Cerulean)y546	Tg(actb2:LOXP-EGFP-LOXP-LY-TagRFPT)y272	B	51.1% (23/45)	6.2% (4/64)	Tabor et al., 2019	Jennifer Sinclair, Harold Burgess
y555-Cre	Et(REX2-SCP1-Ocu.Hbb2:Cre)y555	Tg(actb2:LOXP-EGFP-LOXP-LY-TagRFPT)y272	A	3.2% (3/95)	0% (0/64)	Tabor et al., 2019	Jennifer Sinclair, Harold Burgess

[a]Breeding strategy: A: Target$^{f/f}$; Cre driver X Target$^{+/+}$; B: Target$^{f/+}$; Cre driver X Target$^{+/+}$.
[b]The numbers (x/y) indicate that x offspring with germline recombination were found from y offspring with the target locus in cumulative data from multiple clutches.
[c]The associated publication reported the generation and characterization of the Cre driver lines but not detailed information about germline recombination.
[d]Contributors providing information on germline recombination. Please contact the Lead Contact for electronic addresses of principal investigators.

the same strategy (Minichiello et al., 1999; Rios et al., 2001), Tg(Camk2a-cre)93Kln showed stronger overall Cre expression than Tg(Camk2a-cre)159Kln (Tolson et al., 2010) and a higher rate of paternal germline recombination. Differences were also observed between the two Emx1-Cre KI lines and between the two GFAP-Cre lines. In both cases, one line showed roughly equal paternal and maternal germline recombination and the other only paternal germline recombination. In comparing the two Pvalb-Cre KI lines, Pvalb-IRES-Cre did not exhibit germline recombination in multiple crosses from different labs, while Pvalb-2A-Cre showed germline recombination through both parents. These findings are consistent with the stronger overall Cre activity in Pvalb-2A-Cre mice than in Pvalb-IRES-Cre mice (Madisen et al., 2010) and detection of Cre activity in spermatids of Pvalb-2A-Cre but not Pvalb-IRES-Cre mice (Kobayashi and Hensch, 2013). Using tools such as an IRES to attenuate Cre expression may be beneficial to reduce germline recombination for KI driver lines where Cre expression in germ cells is lower than that in the nervous system. Song and Palmiter (2018) reported success in reducing germline recombination by generating a new Cre driver line with attenuated Cre expression by altering the codons, removing a nuclear localization signal, or adding destabilizing signals.

Target Locus Selectivity

The germline recombination prevalence could also depend on the specific target locus. Among the Cre driver lines crossed with multiple target loci, 81.6% (31/38) showed consistent results for all target loci in terms of occurrence of germline recombination and parental sex bias where known. Quantitative data for multiple targets were available for nine of these lines, of which the majority (six) showed target-specific differences. In addition to Dlx5/6-Cre as mentioned above, Tg(Camk2a-cre)93Kln, Tg(Nes-cre)1Kln, Tg(Pcp2-cre)2Mpin, Tg(Six3-cre)69Frty, and Tg(Slc17a8-icre)1Edw showed substantial locus-dependent differences in germline recombination rates. For example, Tg(Pcp2-cre)2Mpin generated Cre-negative germline-recombined offspring at rates of 14.3%, 69.0%, or 84.0% at different floxed loci. Furthermore, 15.8% (6/38) of the Cre driver lines showed germline recombination at some target loci but not others. In most (5/6) cases, recombination occurred for reporter genes at the *Rosa26* locus but not for other floxed target genes. Another line showed target-consistent germline recombination with paternal Cre but recombined only at the *Rosa26* locus with maternal Cre. Thus, overall, the majority of Cre driver lines behaved consistently in terms of the presence of germline recombination events and parental sex effects at different target loci, but the target loci influenced recombination rates over a wide range. Target locus-specific differences in recombination could be due to differences in the length of loxP-flanked sequences, chromosomal location, epigenetic modification, and accessibility reflected by transcriptional activity in germ cells (Liu et al., 2013; Long and Rossi, 2009; Zheng et al., 2000). Indeed, the *Rosa26* locus, which we found particularly prone to germline recombination, is widely used for gene targeting because it supports strong ubiquitous expression and appears to lack gene silencing effects (Soriano, 1999).

These findings dispel the common belief that a reporter can be used as a readout of recombination at another target locus. For example, using the Ai32 *Rosa*$^{LSL\text{-}tg}$ locus as a reporter for Dlx5/6-Cre-mediated recombination would have missed nearly half the instances of germline recombination seen at the *Clstn3*^{f} locus. Conversely, the Ai9 *Rosa*$^{LSL\text{-}tg}$ reporter locus showed germline

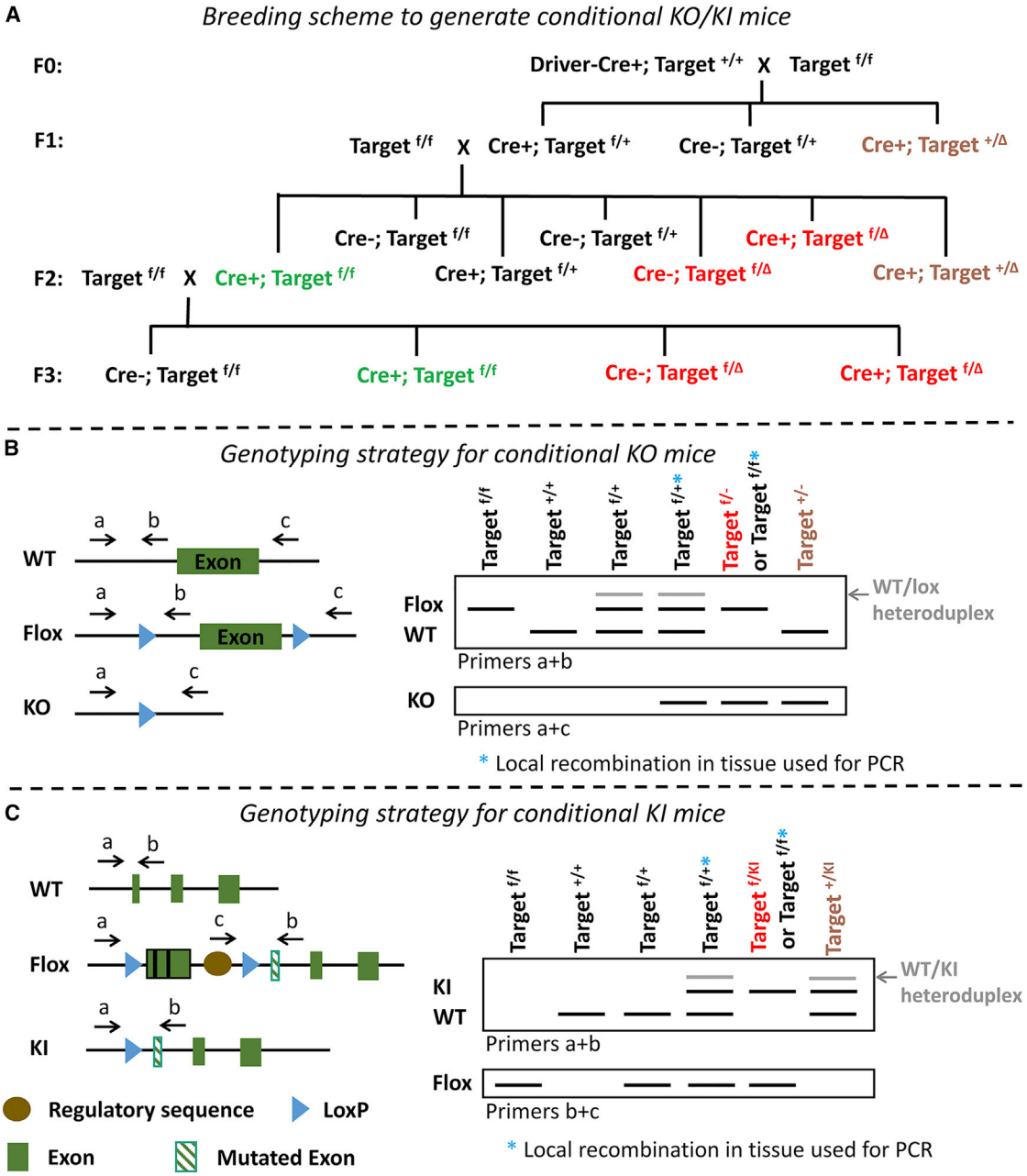

Figure 4. Breeding and Genotyping Strategies for Conditional KO/KI Mice

(A) A recommended breeding scheme is outlined. Target$^{\Delta}$ indicates a target allele that has undergone recombination in male or female germline cells (red) or more rarely in zygotes (brown); thus, Target^{-} or Target^{KI}. Target$^{f/+}$ instead of Target$^{f/f}$ mice can be used for the F0 cross, reducing the frequency of generating Cre^{+}; Target$^{f/+}$ mice for the F1 cross. Routine use of F2 crosses to generate experimental mice is recommended to minimize required animal numbers, but F1 crosses can also be used. It is recommended that F1 crosses using both male and female Cre^{+}; Target$^{f/+}$ mice be established and the resultant germline recombination rates be tracked in offspring. Then male or female Cre^{+}; Target$^{f/f}$ mice can be used for the F2 crosses, depending on which sex gave the lowest germline recombination rate in the F1 crosses. It is important that Cre^{+}; Target$^{f/f}$ mice (green experimental mice) be validated by immunostaining or *in situ* hybridization for the target protein/RNA in the region of interest to confirm consistent recombination in the expected cell type. Cre^{-}; Target$^{f/f}$ mice can be used as controls; separate breeding of congenic Cre^{+}; Target$^{+/+}$ and WT controls is also recommended. "Cre^{+}" refers to mice with one allele of the Cre transgene. In these recommended breeding schemes, Cre^{+} mice are not bred to Cre^{+} mice as this would result in a subset of offspring have 2 alleles of the Cre driver gene. This scenario can be problematic. For random insertion transgenic Cre drivers, it is typically not possible to differentiate among mice with one or two Cre driver alleles by PCR genotyping, leading to unknown variation in Cre expression levels upon subsequent breeding of these mice (which could result in further variability in germline recombination rates). For KI Cre driver lines, it is generally possible to differentiate among mice with one or two Cre driver alleles. However, homozygous insertion of the Cre driver may result in deleterious effects not seen with heterozygous Cre drivers, due to possible disruption of the native gene at the random or

(legend continued on next page)

recombination by Sst-IRES-Cre and VIP-Cre not seen at multiple other target loci. While we focus here on undesirable germline recombination, this caveat likely applies more generally, that cell-type-specific recombination at one locus cannot be inferred from recombination at a different locus. Indeed, in the example discussed above crossing female Emx1-Cre;*Wwp1*$^{f/f}$;*Wwp2*$^{f/f}$ with male *Wwp1*$^{f/f}$;*Wwp2*$^{f/f}$ mice, mosaic recombination in tail tissue occurred frequently at the *Wwp2* locus with little or none at the *Wwp1* locus. Strategies to amplify Cre expression may help to achieve recombination at all floxed target loci in Cre positive cells. For example, in mice intercrossed with the *Tg(iSuRe-Cre)* line, which both amplifies Cre expression and uses MbTomato as a reporter of recombination, MbTomato-positive cells were recombined at other floxed loci with high confidence (Fernández-Chacón et al., 2019).

To demonstrate directly the differential sensitivity of target loci to Cre-mediated germline recombination, we assayed offspring from female Dlx5/6-Cre; Ai32 *Rosa*$^{LSL\text{-}tg/+}$; *Clstn3*$^{f/+}$ mice crossed with WT. In this small sample, germline recombination occurred more frequently at the *Clstn3*$^{f/+}$ locus than at the Ai32 *Rosa*$^{LSL\text{-}tg/+}$ locus, as expected from the difference in frequencies reported in Table 1. Importantly, one mouse showed germline recombination at the *Clstn3*^{f} locus but not at the Ai32 *Rosa*$^{LSL\text{-}tg}$ locus (Figure 3, lane 2), implying differential recombination in the maternal germ cells. In this case, using Ai32 as a reporter to assess whether recombination occurred at the locus of interest (*Clstn3*^{f}) would be misleading.

Broader Implications—Other Recombinase Systems and Organisms

The principles discussed here apply to all genetically targeted recombinase systems, including lox variants, Flp-frt, and Dre-rox systems. For example, the En1-Dre KI mouse line shows variable paternal germline recombination (Nouri and Awatramani, 2017). Moreover, the problem of unwanted recombination may be compounded by intersectional strategies involving multiple recombinases. For example, if the desired gene expression requires the cell-specific expression of both Cre and Flp introduced from different driver lines, then germline recombination by Cre will result in gene expression regulated only by Flp, and vice versa. Such intersectional strategies constitute a powerful tool for achieving exquisite cellular specificity in gene targeting (Huang and Zeng, 2013) but require vigilant monitoring to ensure the desired cell-specific expression.

Furthermore, while we focus here on mouse models, the same issues apply to all genetically targeted organisms using site-specific recombinase systems. Similar unwanted germline recombination with a parental sex bias was observed in the rat tyrosine hydroxylase-Cre line (Liu et al., 2016). In this case, recombination occurred in F2 offspring when the Cre driver and the target locus were together in the female germline cells (18/18, including Cre-negative offspring) but not in the male germline cells (0/19) and not in F1 zygotes. Similar unwanted germline recombination was also observed in zebrafish Cre enhancer trap driver lines with differential expression patterns in the brain (Table 2; Tabor et al., 2019). Among the 6 lines surveyed here, 2 showed only paternal germline deletion, 1 only maternal, and 2 with a strong paternal bias. Thus, zebrafish Cre driver lines show varied rates of germline recombination with a parental sex bias, similar to mouse Cre driver lines.

Alternatives to complement genetic strategies to achieve spatially and temporally controlled recombination exist, notably viral vectors to deliver recombinase-dependent expression cassettes to Cre driver lines or to deliver recombinases to floxed target lines. This is a powerful and commonly used approach that circumvents any potential for germline recombination but has other limitations. Perhaps the most serious limitation is animal to animal variability in recombination efficiency and targeted brain regions due to differences in viral vector injection sites. In addition, the small capacity of adeno-associated viral vectors, which are mostly commonly used in the nervous system, limits the potential for cell-type specificity. Despite ongoing improvements through engineering transcriptional control elements and capsids (Bedbrook et al., 2018), viral vectors are unlikely to achieve the highest specificity and reproducibility possible with genetic methods.

Guidelines

We recommend researchers to consider the following suggestions when using Cre driver lines:

1. Always genotype every animal for the WT, floxed, and recombined alleles at the target locus of interest. This is the only way to ensure all the animals have their expected genotypes. If recombined alleles are observed, concerns of leaky Cre expression in tail or ear tissue could be addressed by testing Cre-negative animals. Beyond the focus here on reducing unwanted germline recombination, the differential sensitivity of distinct target loci to Cre recombinase implies that cell-type-specific recombination patterns must also be confirmed at the locus of interest and not just at a separate reporter locus. Thus, validation by *in situ* hybridization and/

targeted insertion site. An exception may apply to targeted insertion Cre driver lines shown to have normal native gene expression; then, if one wanted to maximize Cre expression level, one might breed Cre^{+} with Cre^{+} mice and select those with 2 Cre alleles for further breeding.
(B and C) Recommended genotyping strategies are diagrammed for conditional KO and KI mice, assuming a mini-gene strategy was used for conditional KI. Genotyping should also be done for the presence of the Cre driver gene (as in Figures 1 and 2, not shown here). The black PCR bands are diagnostic, and the gray bands are additional heteroduplexes that may appear. Potential PCR products that are too large to be generated under typical conditions are not diagrammed here, but these may be generated under some conditions (B with a+c primers for WT and Flox alleles, and C with a+b primers for Flox allele). For mice with one target allele, the presence of Flox, WT, and KO/KI bands indicates the occurrence of local recombination in the tissue used for genotyping rather than ubiquitous germline recombination (Target$^{f/+*}$). For mice with two target alleles, the presence of Flox and KO/KI bands indicates either germline recombination (Target$^{f/-}$ or Target$^{f/KI}$) or local recombination in the tissue used for genotyping (Target$^{f/f*}$). The additional absence of a Cre driver identifies such mice to be Target$^{f/-}$ or Target$^{f/KI}$, but such Cre^{+} mice would have to be bred further, or local recombination in genotyping tissue ruled out, to determine whether the recombination is germline.

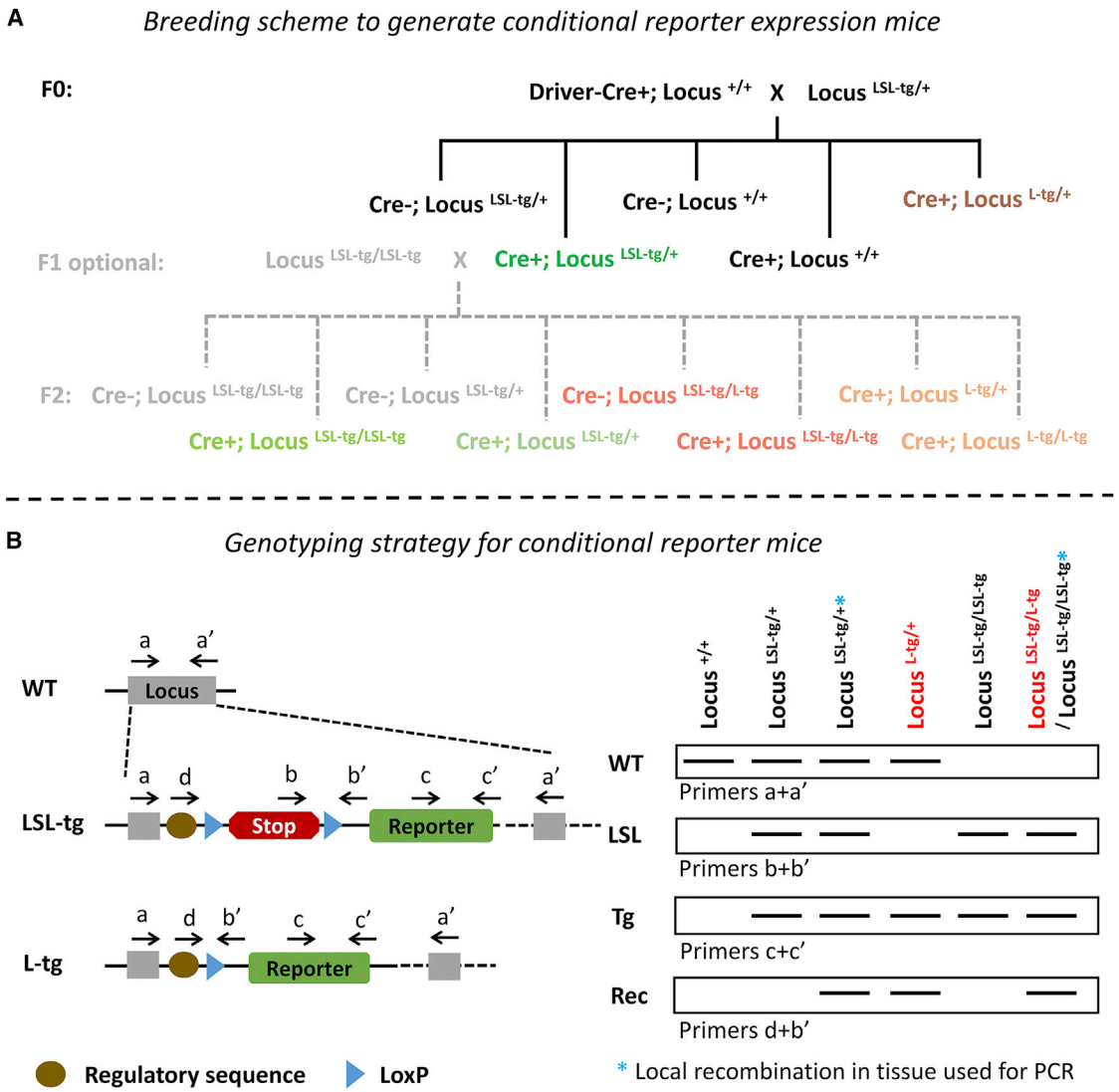

Figure 5. Breeding and Genotyping Strategy for Conditional Reporter Mice

(A) For conditional reporter mice, it is simplest to breed F0 mice and study F1 Cre^{+};$Locus^{LSL\text{-}tg/+}$ mice. Thus, the Cre driver gene and target locus are not together in the germline so unwanted global recombination could only occur by recombination in the zygote, which is not as common as in germline cells. It is important that Cre^{+};$Locus^{LSL\text{-}tg/+}$ mice (green, experimental mice) be validated by immunostaining or *in situ* hybridization for the transgene protein/RNA in the region of interest to confirm consistent recombination in the expected cell type. The optional F1 breeding scheme could be used to increase reporter expression level in Cre^{+}; $Locus^{LSL\text{-}tg/LSL\text{-}tg}$ mice, but this also results in possible germline recombination. If F1 crosses are performed, both male and female Cre^{+}; $Locus^{LSL\text{-}tg/+}$ mice should be used initially to track resultant germline recombination rates so that the sex resulting in the lowest germline recombination rate can be used in further F1 crosses. $Locus^{LSL\text{-}tg+}$ indicates a lox-stop-lox-transgene cassette that expresses the transgene upon Cre-mediated recombination, but our recommendation applies to other Cre-dependent loci such as those using a flip excision or double-inverted orientation mechanism. $Locus^{L\text{-}tg+}$ indicates a globally recombined locus resulting from recombination in male or female germline cells (red) or more rarely in the zygote (brown). "Cre^{+}" refers to mice with one allele of the Cre transgene (see Figure 4 legend).

(B) A recommended genotyping strategy is diagrammed for conditional reporter mice. Only the first four lanes depicting PCR bands are relevant to F1 mice in the above breeding scheme. Genotyping should also be done for the presence of the Cre driver gene (as in Figures 1 and 2, not shown here). Potential PCR products that are too large to be generated under typical conditions are not diagrammed here, but these may be generated under some conditions (with a+a′ primers for LSL-tg and L-tg alleles, and d+b′ primers for the LSL-tg allele). For mice with one target allele, the presence of WT, LSL, Tg, and Rec bands indicates the occurrence of local recombination in the tissue used for genotyping rather than ubiquitous germline recombination ($Locus^{LSL\text{-}tg/+*}$). For mice with two target alleles, the presence of LSL, Tg, and Rec bands indicates either germline recombination ($Locus^{LSL\text{-}tg/L\text{-}tg}$) or local recombination in the tissue used for genotyping ($Locus^{LSL\text{-}tg/LSL\text{-}tg*}$). The additional absence of a Cre driver identifies such mice to be $Locus^{LSL\text{-}tg/L\text{-}tg}$, but such Cre^{+} mice would have to be bred further or local recombination in genotyping tissue ruled out to determine whether the recombination is germline.

or immunostaining for the target of interest in the region of interest is important to confirm cell-type specificity and efficiency of local recombination.

2. If there are multiple Cre driver lines that could give the desired Cre expression pattern, check for information on germline recombination rates. Check the MGI database for recombinase activity in male or female germline cells, as such activity is a good predictor of germline recombination. If such information is lacking, typically KI driver lines tend to have lower undesirable germline recombination than random insertion transgenic driver lines, and tools that attenuate Cre expression such as an IRES can reduce germline recombination.
3. Choose an optimal breeding strategy to reduce or avoid germline recombination. If information on germline recombination frequencies is not available, test breeding strategies with Cre recombinase transmitted exclusively through the male parent or the female parent. Given the parental sex effects observed here for the majority of Cre driver lines, there is often one better way to mitigate or even avoid undesired germline recombination altogether. Detailed strategies for breeding and genotyping are suggested in Figures 4 and 5.
4. In publishing a paper using Cre driver lines, clearly indicate that all WT, floxed, and recombined alleles were assessed by genotyping, report the frequencies of germline recombination and parental sex bias, and indicate how cell-type-specific recombination at the target locus was assessed. Deposit new information on frequencies of germline recombination and parental sex bias in the MGI database.

STAR★METHODS

Detailed methods are provided in the online version of this paper and include the following:

- KEY RESOURCES TABLE
- LEAD CONTACT AND MATERIALS AVAILABILITY
- EXPERIMENTAL MODEL AND SUBJECT DETAILS
- METHOD DETAILS
  - Brain slice imaging
- DATA AND CODE AVAILABILITY

SUPPLEMENTAL INFORMATION

Supplemental Information can be found online at https://doi.org/10.1016/j.neuron.2020.01.008.

ACKNOWLEDGMENTS

We thank Dr. Cynthia Smith from the Jackson Laboratory for her open acceptance of our data on the MGI database. We thank Dr. Timothy Murphy for his kind gift of the Ai32 mouse line. We thank Drs. Elizabeth M. Simpson, Sören Lukassen, and the University of British Columbia Dynamic Brain Circuits Cluster for discussion. Work by Lin Luo and A.M.C. was supported by Canadian Institutes of Health Research (FDN-143206) and Simons Foundation Autism Research Initiative (SFARI 608066). Work by M.C.A. and H.K. was supported by German Research Foundation (SPP1365/KA3423/1-1 and KA3423/3-1) and Japan Society for the Promotion of Science (JSPS) KAKENHI grant number 15K21769. Work by N.B. and F.B. was supported by European Research Council (ERC) Advanced Grant SYNPRIME and the German Research Foundation SFB 1286/A9 awards to N.B. Work by C.C., W. Li, and N.A. was supported by the Natural Science Foundation of China grant (81573408), Fudan University-Shanghai Institute of Materia Medica Chinese Academy of Science joint grant (FU-SIMM20174015), and the Shanghai Municipal Science and Technology Major Project (No. 2018SHZDZX01). Work by J.L.S. and H.A.B. was supported by the Intramural Research Program of the Eunice Kennedy Shriver National Institute of Child Health and Human Development. Work by K.T.B. was supported by National Institutes of Health (NIH) grant F32 DA038913 and NIH grant K99/R00 DA041445. Work by W.Y. and C.C. was supported by a Howard Hughes Medical Institute (HHMI) salary awarded to C.C. Work by E.D. and J.-F.C. was supported by the Canadian Institutes of Health Research and the Natural Sciences and Engineering Research Council of Canada (NSERC). Work by J.A.S. and C.E. was supported by NIH grants RO1DA031833 and F31NS092419. Work by J. Wang and P.S.K. was supported by NIH grants R01NS083898, R01NS103484, and R01MH113349. Work by A.P. and J.N.K. was supported by NIH grants EY024694 to J.N.K. and EY5722 to Duke University. Work by M.A.H. and W. Lu was supported by National Institute of Neurological Disorders and Stroke (NINDS) and NIH Intramural Research Program. Work by W.-H.H. and Liqun Luo was supported by HHMI, SFARI Research Award 345098, and NIH grant R01NS050580 to Liqun Luo and NIH grant 5K99HD092545-02 to W.-H.H. Work by T.M. and K.M. was supported by Japan's Ministry of Education, Culture, Sports, Science and Technology KAKENHI grant 16H06463 and JPSP KAKENHI grant 18K06503. Work by K.A.P. and C.J.M. was supported by a Eunice Kennedy Shriver National Institute of Child Health and Human Development Intramural Award. Work by S.G., G.S., and K.-A.N. was supported by ERC Advanced Grants AxoGLIA and MyeliNANO, the German Research Foundation (SPP1757), and the Max Planck Society. Work by M.A.M.P. and V.F.P. was supported by Canadian Institute of Health Research grants MOP136930, MOP89919, PJT 162431, and PJT 159781 and NSERC grant 06577-2018 RGPIN. Work by E.L.-L.P. and J.L.R.R. was supported by NIH NINDS grant R01 NS099099, National Institute of Mental Health (NIMH) grant R01 MH081880, and NIMH grant R01 MH049428. Work by J.R.S. was supported by NIH R37NS029169. Work by S.F., E.F., A.M.G., L.T., and P.S. was supported by ERC Advanced Grant SPLICECODE; Swiss National Science Foundation to P.S. and European Molecular Biology Organization EMBO ALTF-70-2015 and aALTF-760-2016 to A.M.G. Work by Y.T. was supported by JPSP KAKENHI grant 26251013. Work by H.U. was supported by NIH R01DA042744, R01MH111647, R01NS092578, and SFARI grants. Work by J. Wortel and M.V. was supported by an ERC Advanced Grant (322966) of the European Union. Work by J.M. and M.Y. was supported by Japan Science and Technology Agency (JPMJCR1854) and KAKENHI (16H06461 and 15H05772). Work by L.A.L. and H.Y.Z. was supported by NIH/NINDS grant 5R01NS057819-13 as well as HHMI to H.Y.Z.

AUTHOR CONTRIBUTIONS

Lin Luo, H.K., and A.M.C. conceived the project. All authors contributed unpublished data to Tables 1 or 2. Lin Luo and A.M.C. generated the figures, collated and analyzed the data, and wrote the manuscript with input from all authors.

DECLARATION OF INTERESTS

The authors declare no competing interests.

Received: July 25, 2019
Revised: November 12, 2019
Accepted: January 10, 2020
Published: February 5, 2020

REFERENCES

Akashi, K., Kakizaki, T., Kamiya, H., Fukaya, M., Yamasaki, M., Abe, M., Natsume, R., Watanabe, M., and Sakimura, K. (2009). NMDA receptor GluN2B (GluR ε 2/NR2B) subunit is crucial for channel function, postsynaptic

macromolecular organization, and actin cytoskeleton at hippocampal CA3 synapses. J. Neurosci. *29*, 10869–10882.

Ambrozkiewicz, M.C., Schwark, M., Kishimoto-Suga, M., Borisova, E., Hori, K., Salazar-Lázaro, A., Rusanova, A., Altas, B., Piepkorn, L., Bessa, P., et al. (2018). Polarity Acquisition in Cortical Neurons Is Driven by Synergistic Action of Sox9-Regulated Wwp1 and Wwp2 E3 Ubiquitin Ligases and Intronic miR-140. Neuron *100*, 1097–1115.

Bäck, S., Necarsulmer, J., Whitaker, L.R., Coke, L.M., Koivula, P., Heathward, E.J., Fortuno, L.V., Zhang, Y., Yeh, C.G., Baldwin, H.A., et al. (2019). Neuron-Specific Genome Modification in the Adult Rat Brain Using CRISPR-Cas9 Transgenic Rats. Neuron *102*, 105–119.

Bäckman, C.M., Malik, N., Zhang, Y., Shan, L., Grinberg, A., Hoffer, B.J., Westphal, H., and Tomac, A.C. (2006). Characterization of a mouse strain expressing Cre recombinase from the 3′ untranslated region of the dopamine transporter locus. Genesis *44*, 383–390.

Balthasar, N., Dalgaard, L.T., Lee, C.E., Yu, J., Funahashi, H., Williams, T., Ferreira, M., Tang, V., McGovern, R.A., Kenny, C.D., et al. (2005). Divergence of melanocortin pathways in the control of food intake and energy expenditure. Cell *123*, 493–505.

Barski, J.J., Dethleffsen, K., and Meyer, M. (2000). Cre recombinase expression in cerebellar Purkinje cells. Genesis *28*, 93–98.

Bates, B., Rios, M., Trumpp, A., Chen, C., Fan, G., Bishop, J.M., and Jaenisch, R. (1999). Neurotrophin-3 is required for proper cerebellar development. Nat. Neurosci. *2*, 115–117.

Bedbrook, C.N., Deverman, B.E., and Gradinaru, V. (2018). Viral Strategies for Targeting the Central and Peripheral Nervous Systems. Annu. Rev. Neurosci. *41*, 323–348.

Blitz, E., Viukov, S., Sharir, A., Shwartz, Y., Galloway, J.L., Pryce, B.A., Johnson, R.L., Tabin, C.J., Schweitzer, R., and Zelzer, E. (2009). Bone ridge patterning during musculoskeletal assembly is mediated through SCX regulation of Bmp4 at the tendon-skeleton junction. Dev. Cell *17*, 861–873.

Bouhali, K., Dipietromaria, A., Fontaine, A., Caburet, S., Barbieri, O., Bellessort, B., Fellous, M., Veitia, R.A., and Levi, G. (2011). Allelic reduction of Dlx5 and Dlx6 results in early follicular depletion: a new mouse model of primary ovarian insufficiency. Hum. Mol. Genet. *20*, 2642–2650.

Buch, T., Heppner, F.L., Tertilt, C., Heinen, T.J.A.J., Kremer, M., Wunderlich, F.T., Jung, S., and Waisman, A. (2005). A Cre-inducible diphtheria toxin receptor mediates cell lineage ablation after toxin administration. Nat. Methods *2*, 419–426.

Buchholz, F., Refaeli, Y., Trumpp, A., and Bishop, J.M. (2000). Inducible chromosomal translocation of AML1 and ETO genes through Cre/loxP-mediated recombination in the mouse. EMBO Rep. *1*, 133–139.

Bult, C.J., Blake, J.A., Smith, C.L., Kadin, J.A., and Richardson, J.E.; Mouse Genome Database Group (2019). Mouse Genome Database (MGD) 2019. Nucleic Acids Res. *47* (D1), D801–D806.

Chao, H.-T., Chen, H., Samaco, R.C., Xue, M., Chahrour, M., Yoo, J., Neul, J.L., Gong, S., Lu, H.-C., Heintz, N., et al. (2010). Dysfunction in GABA signalling mediates autism-like stereotypies and Rett syndrome phenotypes. Nature *468*, 263–269.

Chittajallu, R., Craig, M.T., McFarland, A., Yuan, X., Gerfen, S., Tricoire, L., Erkkila, B., Barron, S.C., Lopez, C.M., Liang, B.J., et al. (2013). Dual origins of functionally distinct O-LM interneurons revealed by differential 5-HT(3A)R expression. Nat. Neurosci. *16*, 1598–1607.

Choi, C.-I., Yoon, S.-P., Choi, J.-M., Kim, S.-S., Lee, Y.-D., Birnbaumer, L., and Suh-Kim, H. (2014). Simultaneous deletion of floxed genes mediated by CaMKIIα-Cre in the brain and in male germ cells: application to conditional and conventional disruption of Goα. Exp. Mol. Med. *46*, e93.

Crispino, G., Di Pasquale, G., Scimemi, P., Rodriguez, L., Galindo Ramirez, F., De Siati, R.D., Santarelli, R.M., Arslan, E., Bortolozzi, M., Chiorini, J.A., and Mammano, F. (2011). BAAV mediated GJB2 gene transfer restores gap junction coupling in cochlear organotypic cultures from deaf Cx26Sox10Cre mice. PLoS ONE *6*, e23279.

Daigle, T.L., Madisen, L., Hage, T.A., Valley, M.T., Knoblich, U., Larsen, R.S., Takeno, M.M., Huang, L., Gu, H., Larsen, R., et al. (2018). A Suite of Transgenic Driver and Reporter Mouse Lines with Enhanced Brain-Cell-Type Targeting and Functionality. Cell *174*, 465–480.

Danielian, P.S., Muccino, D., Rowitch, D.H., Michael, S.K., and McMahon, A.P. (1998). Modification of gene activity in mouse embryos in utero by a tamoxifen-inducible form of Cre recombinase. Curr. Biol. *8*, 1323–1326.

Davis, M.I., Crittenden, J.R., Feng, A.Y., Kupferschmidt, D.A., Naydenov, A., Stella, N., Graybiel, A.M., and Lovinger, D.M. (2018). The cannabinoid-1 receptor is abundantly expressed in striatal striosomes and striosome-dendron bouquets of the substantia nigra. PLoS ONE *13*, e0191436.

de Castro, B.M., De Jaeger, X., Martins-Silva, C., Lima, R.D.F., Amaral, E., Menezes, C., Lima, P., Neves, C.M.L., Pires, R.G., Gould, T.W., et al. (2009). The vesicular acetylcholine transporter is required for neuromuscular development and function. Mol. Cell. Biol. *29*, 5238–5250.

Del Toro, D., Ruff, T., Cederfjäll, E., Villalba, A., Seyit-Bremer, G., Borrell, V., and Klein, R. (2017). Regulation of Cerebral Cortex Folding by Controlling Neuronal Migration via FLRT Adhesion Molecules. Cell *169*, 621–635.

Divito, C.B., Steece-Collier, K., Case, D.T., Williams, S.-P.G., Stancati, J.A., Zhi, L., Rubio, M.E., Sortwell, C.E., Collier, T.J., Sulzer, D., et al. (2015). Loss of VGLUT3 Produces Circadian-Dependent Hyperdopaminergia and Ameliorates Motor Dysfunction and l-Dopa-Mediated Dyskinesias in a Model of Parkinson's Disease. J. Neurosci. *35*, 14983–14999.

Doetschman, T., Georgieva, T., Li, H., Reed, T.D., Grisham, C., Friel, J., Estabrook, M.A., Gard, C., Sanford, L.P., and Azhar, M. (2012). Generation of mice with a conditional allele for the transforming growth factor beta3 gene. Genesis *50*, 59–66.

Dragatsis, I., and Zeitlin, S. (2000). CaMKIIalpha-Cre transgene expression and recombination patterns in the mouse brain. Genesis *26*, 133–135.

Dubois, N.C., Hofmann, D., Kaloulis, K., Bishop, J.M., and Trumpp, A. (2006). Nestin-Cre transgenic mouse line Nes-Cre1 mediates highly efficient Cre/loxP mediated recombination in the nervous system, kidney, and somite-derived tissues. Genesis *44*, 355–360.

Dudok, J.J., Groffen, A.J.A., Toonen, R.F.T., and Verhage, M. (2011). Deletion of Munc18-1 in 5-HT neurons results in rapid degeneration of the 5-HT system and early postnatal lethality. PLoS ONE *6*, e28137.

Engblom, D., Bilbao, A., Sanchis-Segura, C., Dahan, L., Perreau-Lenz, S., Balland, B., Parkitna, J.R., Luján, R., Halbout, B., Mameli, M., et al. (2008). Glutamate receptors on dopamine neurons control the persistence of cocaine seeking. Neuron *59*, 497–508.

Feil, R., Wagner, J., Metzger, D., and Chambon, P. (1997). Regulation of Cre recombinase activity by mutated estrogen receptor ligand-binding domains. Biochem. Biophys. Res. Commun. *237*, 752–757.

Fernández-Chacón, M., Casquero-García, V., Luo, W., Francesca Lunella, F., Ferreira Rocha, S., Del Olmo-Cabrera, S., and Benedito, R. (2019). iSuRe-Cre is a genetic tool to reliably induce and report Cre-dependent genetic modifications. Nat. Commun. *10*, 2262.

Franco, S.J., Gil-Sanz, C., Martinez-Garay, I., Espinosa, A., Harkins-Perry, S.R., Ramos, C., and Müller, U. (2012). Fate-restricted neural progenitors in the mammalian cerebral cortex. Science *337*, 746–749.

Fünfschilling, U., Jockusch, W.J., Sivakumar, N., Möbius, W., Corthals, K., Li, S., Quintes, S., Kim, Y., Schaap, I.A.T., Rhee, J.-S., et al. (2012). Critical time window of neuronal cholesterol synthesis during neurite outgrowth. J. Neurosci. *32*, 7632–7645.

Furuta, Y., Lagutin, O., Hogan, B.L., and Oliver, G.C. (2000). Retina- and ventral forebrain-specific Cre recombinase activity in transgenic mice. Genesis *26*, 130–132.

Gallardo, T., Shirley, L., John, G.B., and Castrillon, D.H. (2007). Generation of a germ cell-specific mouse transgenic Cre line, Vasa-Cre. Genesis *45*, 413–417.

Gerfen, C.R., Paletzki, R., and Heintz, N. (2013). GENSAT BAC cre-recombinase driver lines to study the functional organization of cerebral cortical and basal ganglia circuits. Neuron *80*, 1368–1383.

Gil-Sanz, C., Espinosa, A., Fregoso, S.P., Bluske, K.K., Cunningham, C.L., Martinez-Garay, I., Zeng, H., Franco, S.J., and Müller, U. (2015). Lineage Tracing Using Cux2-Cre and Cux2-CreERT2 Mice. Neuron *86*, 1091–1099.

Goebbels, S., Bormuth, I., Bode, U., Hermanson, O., Schwab, M.H., and Nave, K.-A. (2006). Genetic targeting of principal neurons in neocortex and hippocampus of NEX-Cre mice. Genesis *44*, 611–621.

Gondo, Y. (2008). Trends in large-scale mouse mutagenesis: from genetics to functional genomics. Nat. Rev. Genet. *9*, 803–810.

Gong, S., Zheng, C., Doughty, M.L., Losos, K., Didkovsky, N., Schambra, U.B., Nowak, N.J., Joyner, A., Leblanc, G., Hatten, M.E., and Heintz, N. (2003). A gene expression atlas of the central nervous system based on bacterial artificial chromosomes. Nature *425*, 917–925.

Gong, S., Doughty, M., Harbaugh, C.R., Cummins, A., Hatten, M.E., Heintz, N., and Gerfen, C.R. (2007). Targeting Cre recombinase to specific neuron populations with bacterial artificial chromosome constructs. J. Neurosci. *27*, 9817–9823.

Gorski, J.A., Talley, T., Qiu, M., Puelles, L., Rubenstein, J.L.R., and Jones, K.R. (2002). Cortical excitatory neurons and glia, but not GABAergic neurons, are produced in the Emx1-expressing lineage. J. Neurosci. *22*, 6309–6314.

Gregorian, C., Nakashima, J., Le Belle, J., Ohab, J., Kim, R., Liu, A., Smith, K.B., Groszer, M., Garcia, A.D., Sofroniew, M.V., et al. (2009). Pten deletion in adult neural stem/progenitor cells enhances constitutive neurogenesis. J. Neurosci. *29*, 1874–1886.

Grimes, W.N., Seal, R.P., Oesch, N., Edwards, R.H., and Diamond, J.S. (2011). Genetic targeting and physiological features of VGLUT3+ amacrine cells. Vis. Neurosci. *28*, 381–392.

Gruber, M., Hu, C.-J., Johnson, R.S., Brown, E.J., Keith, B., and Simon, M.C. (2007). Acute postnatal ablation of Hif-2α results in anemia. Proc. Natl. Acad. Sci. USA *104*, 2301–2306.

Gu, H., Marth, J.D., Orban, P.C., Mossmann, H., and Rajewsky, K. (1994). Deletion of a DNA polymerase beta gene segment in T cells using cell type-specific gene targeting. Science *265*, 103–106.

Guzman, M.S., De Jaeger, X., Raulic, S., Souza, I.A., Li, A.X., Schmid, S., Menon, R.S., Gainetdinov, R.R., Caron, M.G., Bartha, R., et al. (2011). Elimination of the vesicular acetylcholine transporter in the striatum reveals regulation of behaviour by cholinergic-glutamatergic co-transmission. PLoS Biol. *9*, e1001194.

Hara, T., Nakamura, K., Matsui, M., Yamamoto, A., Nakahara, Y., Suzuki-Migishima, R., Yokoyama, M., Mishima, K., Saito, I., Okano, H., and Mizushima, N. (2006). Suppression of basal autophagy in neural cells causes neurodegenerative disease in mice. Nature *441*, 885–889.

Harno, E., Cottrell, E.C., and White, A. (2013). Metabolic pitfalls of CNS Cre-based technology. Cell Metab. *18*, 21–28.

Harris, J.A., Hirokawa, K.E., Sorensen, S.A., Gu, H., Mills, M., Ng, L.L., Bohn, P., Mortrud, M., Ouellette, B., Kidney, J., et al. (2014). Anatomical characterization of Cre driver mice for neural circuit mapping and manipulation. Front. Neural Circuits *8*, 76.

Hashimoto, K., Tsujita, M., Miyazaki, T., Kitamura, K., Yamazaki, M., Shin, H.-S., Watanabe, M., Sakimura, K., and Kano, M. (2011). Postsynaptic P/Q-type Ca2+ channel in Purkinje cell mediates synaptic competition and elimination in developing cerebellum. Proc. Natl. Acad. Sci. USA *108*, 9987–9992.

Hébert, J.M., and McConnell, S.K. (2000). Targeting of cre to the Foxg1 (BF-1) locus mediates loxP recombination in the telencephalon and other developing head structures. Dev. Biol. *222*, 296–306.

Heeroma, J.H., Roelandse, M., Wierda, K., van Aerde, K.I., Toonen, R.F.G., Hensbroek, R.A., Brussaard, A., Matus, A., and Verhage, M. (2004). Trophic support delays but does not prevent cell-intrinsic degeneration of neurons deficient for munc18-1. Eur. J. Neurosci. *20*, 623–634.

Heffner, C.S., Herbert Pratt, C., Babiuk, R.P., Sharma, Y., Rockwood, S.F., Donahue, L.R., Eppig, J.T., and Murray, S.A. (2012). Supporting conditional mouse mutagenesis with a comprehensive cre characterization resource. Nat. Commun. *3*, 1218.

Hippenmeyer, S., Vrieseling, E., Sigrist, M., Portmann, T., Laengle, C., Ladle, D.R., and Arber, S. (2005). A developmental switch in the response of DRG neurons to ETS transcription factor signaling. PLoS Biol. *3*, e159.

Huang, Z.J., and Zeng, H. (2013). Genetic approaches to neural circuits in the mouse. Annu. Rev. Neurosci. *36*, 183–215.

Huang, W.-H., Guenthner, C.J., Xu, J., Nguyen, T., Schwarz, L.A., Wilkinson, A.W., Gozani, O., Chang, H.Y., Shamloo, M., and Luo, L. (2016). Molecular and Neural Functions of Rai1, the Causal Gene for Smith-Magenis Syndrome. Neuron *92*, 392–406.

Huang, W.-H., Wang, D.C., Allen, W.E., Klope, M., Hu, H., Shamloo, M., and Luo, L. (2018). Early adolescent Rai1 reactivation reverses transcriptional and social interaction deficits in a mouse model of Smith-Magenis syndrome. Proc. Natl. Acad. Sci. USA *115*, 10744–10749.

Humphreys, B.D., Lin, S.-L., Kobayashi, A., Hudson, T.E., Nowlin, B.T., Bonventre, J.V., Valerius, M.T., McMahon, A.P., and Duffield, J.S. (2010). Fate tracing reveals the pericyte and not epithelial origin of myofibroblasts in kidney fibrosis. Am. J. Pathol. *176*, 85–97.

Hutchison, M.A., Gu, X., Adrover, M.F., Lee, M.R., Hnasko, T.S., Alvarez, V.A., and Lu, W. (2018). Genetic inhibition of neurotransmission reveals role of glutamatergic input to dopamine neurons in high-effort behavior. Mol. Psychiatry *23*, 1213–1225.

Ing-Esteves, S., Kostadinov, D., Marocha, J., Sing, A.D., Joseph, K.S., Laboulaye, M.A., Sanes, J.R., and Lefebvre, J.L. (2018). Combinatorial Effects of Alpha- and Gamma-Protocadherins on Neuronal Survival and Dendritic Self-Avoidance. J. Neurosci. *38*, 2713–2729.

Janickova, H., Rosborough, K., Al-Onaizi, M., Kljakic, O., Guzman, M.S., Gros, R., Prado, M.A.M., and Prado, V.F. (2017). Deletion of the vesicular acetylcholine transporter from pedunculopontine/laterodorsal tegmental neurons modifies gait. J. Neurochem. *140*, 787–798.

Jha, M.K., Lee, Y., Russell, K.A., Yang, F., Dastgheyb, R.M., Deme, P., Ament, X.H., Chen, W., Liu, Y., Guan, Y., et al. (2019). Monocarboxylate transporter 1 in Schwann cells contributes to maintenance of sensory nerve myelination during aging. Glia *68*, 161–177.

Jin, J., Desai, B.N., Navarro, B., Donovan, A., Andrews, N.C., and Clapham, D.E. (2008). Deletion of Trpm7 disrupts embryonic development and theymopoiesis without altering Mg2+ homeostasis. Science *322*, 756–760.

Jones, P.G., Nawoschik, S.P., Sreekumar, K., Uveges, A.J., Tseng, E., Zhang, L., Johnson, J., He, L., Paulsen, J.E., Bates, B., and Pausch, M.H. (2007). Tissue distribution and functional analyses of the constitutively active orphan G protein coupled receptors, GPR26 and GPR78. Biochim. Biophys. Acta *1770*, 890–901.

Kaeser, P.S., Kwon, H.-B., Chiu, C.Q., Deng, L., Castillo, P.E., and Südhof, T.C. (2008). RIM1alpha and RIM1beta are synthesized from distinct promoters of the RIM1 gene to mediate differential but overlapping synaptic functions. J. Neurosci. *28*, 13435–13447.

Kaeser, P.S., Deng, L., Chávez, A.E., Liu, X., Castillo, P.E., and Südhof, T.C. (2009). ELKS2alpha/CAST deletion selectively increases neurotransmitter release at inhibitory synapses. Neuron *64*, 227–239.

Kaeser, P.S., Deng, L., Wang, Y., Dulubova, I., Liu, X., Rizo, J., and Südhof, T.C. (2011). RIM proteins tether Ca2+ channels to presynaptic active zones via a direct PDZ-domain interaction. Cell *144*, 282–295.

Kakegawa, W., Mitakidis, N., Miura, E., Abe, M., Matsuda, K., Takeo, Y.H., Kohda, K., Motohashi, J., Takahashi, A., Nagao, S., et al. (2015). Anterograde C1ql1 signaling is required in order to determine and maintain a single-winner climbing fiber in the mouse cerebellum. Neuron *85*, 316–329.

Kakegawa, W., Katoh, A., Narumi, S., Miura, E., Motohashi, J., Takahashi, A., Kohda, K., Fukazawa, Y., Yuzaki, M., and Matsuda, S. (2018). Optogenetic Control of Synaptic AMPA Receptor Endocytosis Reveals Roles of LTD in Motor Learning. Neuron *99*, 985–998.

Kam, J.W.K., Dumontier, E., Baim, C., Brignall, A.C., Mendes da Silva, D., Cowan, M., Kennedy, T.E., and Cloutier, J.-F. (2016). RGMB and neogenin

control cell differentiation in the developing olfactory epithelium. Development *143*, 1534–1546.

Kaneda, M., Okano, M., Hata, K., Sado, T., Tsujimoto, N., Li, E., and Sasaki, H. (2004). Essential role for de novo DNA methyltransferase Dnmt3a in paternal and maternal imprinting. Nature *429*, 900–903.

Kay, J.N., Chu, M.W., and Sanes, J.R. (2012). MEGF10 and MEGF11 mediate homotypic interactions required for mosaic spacing of retinal neurons. Nature *483*, 465–469.

Kimmel, R.A., Turnbull, D.H., Blanquet, V., Wurst, W., Loomis, C.A., and Joyner, A.L. (2000). Two lineage boundaries coordinate vertebrate apical ectodermal ridge formation. Genes Dev. *14*, 1377–1389.

Kobayashi, Y., and Hensch, T.K. (2013). Germline recombination by conditional gene targeting with Parvalbumin-Cre lines. Front. Neural Circuits *7*, 168.

Kolisnyk, B., Al-Onaizi, M., Soreq, L., Barbash, S., Bekenstein, U., Haberman, N., Hanin, G., Kish, M.T., Souza da Silva, J., Fahnestock, M., et al. (2017). Cholinergic Surveillance over Hippocampal RNA Metabolism and Alzheimer's-Like Pathology. Cereb. Cortex *27*, 3553–3567.

Kougioumtzidou, E., Shimizu, T., Hamilton, N.B., Tohyama, K., Sprengel, R., Monyer, H., Attwell, D., and Richardson, W.D. (2017). Signalling through AMPA receptors on oligodendrocyte precursors promotes myelination by enhancing oligodendrocyte survival. eLife *6*, e28080.

Kovacevic, J., Maroteaux, G., Schut, D., Loos, M., Dubey, M., Pitsch, J., Remmelink, E., Koopmans, B., Crowley, J., Cornelisse, L.N., et al. (2018). Protein instability, haploinsufficiency, and cortical hyper-excitability underlie STXBP1 encephalopathy. Brain *141*, 1350–1374.

Krah, N.M., De La O, J.P., Swift, G.H., Hoang, C.Q., Willet, S.G., Chen Pan, F., Cash, G.M., Bronner, M.P., Wright, C.V., MacDonald, R.J., and Murtaugh, L.C. (2015). The acinar differentiation determinant PTF1A inhibits initiation of pancreatic ductal adenocarcinoma. eLife. Published online July 7, 2015. https://doi.org/10.7554/eLife.07125.

Lakso, M., Pichel, J.G., Gorman, J.R., Sauer, B., Okamoto, Y., Lee, E., Alt, F.W., and Westphal, H. (1996). Efficient in vivo manipulation of mouse genomic sequences at the zygote stage. Proc. Natl. Acad. Sci. USA *93*, 5860–5865.

Lam, D.D., Leinninger, G.M., Louis, G.W., Garfield, A.S., Marston, O.J., Leshan, R.L., Scheller, E.L., Christensen, L., Donato, J., Jr., Xia, J., et al. (2011). Leptin does not directly affect CNS serotonin neurons to influence appetite. Cell Metab. *13*, 584–591.

Li, J., Chen, K., Zhu, L., and Pollard, J.W. (2006). Conditional deletion of the colony stimulating factor-1 receptor (c-fms proto-oncogene) in mice. Genesis *44*, 328–335.

Liang, J., Xu, W., Hsu, Y.-T., Yee, A.X., Chen, L., and Südhof, T.C. (2015). Conditional neuroligin-2 knockout in adult medial prefrontal cortex links chronic changes in synaptic inhibition to cognitive impairments. Mol. Psychiatry *20*, 850–859.

Liput, D.J. (2018). Cre-Recombinase Dependent Germline Deletion of a Conditional Allele in the Rgs9cre Mouse Line. Front. Neural Circuits *12*, 68.

Liu, J., Willet, S.G., Bankaitis, E.D., Xu, Y., Wright, C.V.E., and Gu, G. (2013). Non-parallel recombination limits Cre-LoxP-based reporters as precise indicators of conditional genetic manipulation. Genesis *51*, 436–442.

Liu, Z., Brown, A., Fisher, D., Wu, Y., Warren, J., and Cui, X. (2016). Tissue Specific Expression of Cre in Rat Tyrosine Hydroxylase and Dopamine Active Transporter-Positive Neurons. PLoS ONE *11*, e0149379.

Liu, C., Kershberg, L., Wang, J., Schneeberger, S., and Kaeser, P.S. (2018a). Dopamine Secretion Is Mediated by Sparse Active Zone-like Release Sites. Cell *172*, 706–718.

Liu, Y., Chen, C., Liu, Y., Li, W., Wang, Z., Sun, Q., Zhou, H., Chen, X., Yu, Y., Wang, Y., and Abumaria, N. (2018b). TRPM7 Is Required for Normal Synapse Density, Learning, and Memory at Different Developmental Stages. Cell Rep. *23*, 3480–3491.

Long, M.A., and Rossi, F.M.V. (2009). Silencing inhibits Cre-mediated recombination of the Z/AP and Z/EG reporters in adult cells. PLoS ONE *4*, e5435.

Lukassen, S., Bosch, E., Ekici, A.B., and Winterpacht, A. (2018a). Characterization of germ cell differentiation in the male mouse through single-cell RNA sequencing. Sci. Rep. *8*, 6521.

Lukassen, S., Bosch, E., Ekici, A.B., and Winterpacht, A. (2018b). Single-cell RNA sequencing of adult mouse testes. Sci. Data *5*, 180192.

MacPherson, D., Sage, J., Crowley, D., Trumpp, A., Bronson, R.T., and Jacks, T. (2003). Conditional mutation of Rb causes cell cycle defects without apoptosis in the central nervous system. Mol. Cell. Biol. *23*, 1044–1053.

Madisen, L., Zwingman, T.A., Sunkin, S.M., Oh, S.W., Zariwala, H.A., Gu, H., Ng, L.L., Palmiter, R.D., Hawrylycz, M.J., Jones, A.R., et al. (2010). A robust and high-throughput Cre reporting and characterization system for the whole mouse brain. Nat. Neurosci. *13*, 133–140.

Madisen, L., Mao, T., Koch, H., Zhuo, J.M., Berenyi, A., Fujisawa, S., Hsu, Y.-W.A., Garcia, A.J., 3rd, Gu, X., Zanella, S., et al. (2012). A toolbox of Cre-dependent optogenetic transgenic mice for light-induced activation and silencing. Nat. Neurosci. *15*, 793–802.

Martins-Silva, C., De Jaeger, X., Guzman, M.S., Lima, R.D.F., Santos, M.S., Kushmerick, C., Gomez, M.V., Caron, M.G., Prado, M.A.M., and Prado, V.F. (2011). Novel strains of mice deficient for the vesicular acetylcholine transporter: insights on transcriptional regulation and control of locomotor behavior. PLoS ONE *6*, e17611.

Martyn, A.C., De Jaeger, X., Magalhães, A.C., Kesarwani, R., Gonçalves, D.F., Raulic, S., Guzman, M.S., Jackson, M.F., Izquierdo, I., Macdonald, J.F., et al. (2012). Elimination of the vesicular acetylcholine transporter in the forebrain causes hyperactivity and deficits in spatial memory and long-term potentiation. Proc. Natl. Acad. Sci. USA *109*, 17651–17656.

Matsuda, K., Budisantoso, T., Mitakidis, N., Sugaya, Y., Miura, E., Kakegawa, W., Yamasaki, M., Konno, K., Uchigashima, M., Abe, M., et al. (2016). Transsynaptic Modulation of Kainate Receptor Functions by C1q-like Proteins. Neuron *90*, 752–767.

Matsuoka, T., Ahlberg, P.E., Kessaris, N., Iannarelli, P., Dennehy, U., Richardson, W.D., McMahon, A.P., and Koentges, G. (2005). Neural crest origins of the neck and shoulder. Nature *436*, 347–355.

McMinn, J.E., Liu, S.-M., Liu, H., Dragatsis, I., Dietrich, P., Ludwig, T., Boozer, C.N., and Chua, S.C., Jr. (2005). Neuronal deletion of Lepr elicits diabesity in mice without affecting cold tolerance or fertility. Am. J. Physiol. Endocrinol. Metab. *289*, E403–E411.

Minichiello, L., Korte, M., Wolfer, D., Kühn, R., Unsicker, K., Cestari, V., Rossi-Arnaud, C., Lipp, H.-P., Bonhoeffer, T., and Klein, R. (1999). Essential role for TrkB receptors in hippocampus-mediated learning. Neuron *24*, 401–414.

Misawa, H., Nakata, K., Toda, K., Matsuura, J., Oda, Y., Inoue, H., Tateno, M., and Takahashi, R. (2003). VAChT-Cre. Fast and VAChT-Cre.Slow: postnatal expression of Cre recombinase in somatomotor neurons with different onset. Genesis *37*, 44–50.

Miyazaki, T., Yamasaki, M., Hashimoto, K., Yamazaki, M., Abe, M., Usui, H., Kano, M., Sakimura, K., and Watanabe, M. (2012). Cav2.1 in cerebellar Purkinje cells regulates competitive excitatory synaptic wiring, cell survival, and cerebellar biochemical compartmentalization. J. Neurosci. *32*, 1311–1328.

Miyoshi, G., Young, A., Petros, T., Karayannis, T., McKenzie Chang, M., Lavado, A., Iwano, T., Nakajima, M., Taniguchi, H., Huang, Z.J., et al. (2015). Prox1 Regulates the Subtype-Specific Development of Caudal Ganglionic Eminence-Derived GABAergic Cortical Interneurons. J. Neurosci. *35*, 12869–12889.

Mu, X., Fu, X., Beremand, P.D., Thomas, T.L., and Klein, W.H. (2008). Gene regulation logic in retinal ganglion cell development: Isl1 defines a critical branch distinct from but overlapping with Pou4f2. Proc. Natl. Acad. Sci. USA *105*, 6942–6947.

Murray, S.A., Eppig, J.T., Smedley, D., Simpson, E.M., and Rosenthal, N. (2012). Beyond knockouts: cre resources for conditional mutagenesis. Mamm. Genome *23*, 587–599.

Muzumdar, M.D., Tasic, B., Miyamichi, K., Li, L., and Luo, L. (2007). A global double-fluorescent Cre reporter mouse. Genesis *45*, 593–605.

Nakazawa, K., Quirk, M.C., Chitwood, R.A., Watanabe, M., Yeckel, M.F., Sun, L.D., Kato, A., Carr, C.A., Johnston, D., Wilson, M.A., and Tonegawa, S. (2002). Requirement for hippocampal CA3 NMDA receptors in associative memory recall. Science *297*, 211–218.

Nishida, H., Miyagawa, S., Vieux-Rochas, M., Morini, M., Ogino, Y., Suzuki, K., Nakagata, N., Choi, H.-S., Levi, G., and Yamada, G. (2008). Positive regulation of steroidogenic acute regulatory protein gene expression through the interaction between Dlx and GATA-4 for testicular steroidogenesis. Endocrinology *149*, 2090–2097.

Nishiyama, J., Miura, E., Mizushima, N., Watanabe, M., and Yuzaki, M. (2007). Aberrant membranes and double-membrane structures accumulate in the axons of Atg5-null Purkinje cells before neuronal death. Autophagy *3*, 591–596.

Nouri, N., and Awatramani, R. (2017). A novel floor plate boundary defined by adjacent En1 and Dbx1 microdomains distinguishes midbrain dopamine and hypothalamic neurons. Development *144*, 916–927.

Ozkan, E.D., Creson, T.K., Kramár, E.A., Rojas, C., Seese, R.R., Babyan, A.H., Shi, Y., Lucero, R., Xu, X., Noebels, J.L., et al. (2014). Reduced cognition in Syngap1 mutants is caused by isolated damage within developing forebrain excitatory neurons. Neuron *82*, 1317–1333.

Pai, E.L.-L., Vogt, D., Clemente-Perez, A., McKinsey, G.L., Cho, F.S., Hu, J.S., Wimer, M., Paul, A., Fazel Darbandi, S., Pla, R., et al. (2019). Mafb and c-Maf Have Prenatal Compensatory and Postnatal Antagonistic Roles in Cortical Interneuron Fate and Function. Cell Rep. *26*, 1157–1173.

Pettem, K.L., Yokomaku, D., Luo, L., Linhoff, M.W., Prasad, T., Connor, S.A., Siddiqui, T.J., Kawabe, H., Chen, F., Zhang, L., et al. (2013). The specific α-neurexin interactor calsyntenin-3 promotes excitatory and inhibitory synapse development. Neuron *80*, 113–128.

Potter, G.B., Petryniak, M.A., Shevchenko, E., McKinsey, G.L., Ekker, M., and Rubenstein, J.L.R. (2009). Generation of Cre-transgenic mice using Dlx1/Dlx2 enhancers and their characterization in GABAergic interneurons. Mol. Cell. Neurosci. *40*, 167–186.

Puñal, V.M., Paisley, C.E., Brecha, F.S., Lee, M.A., Perelli, R.M., Wang, J., O'Koren, E.G., Ackley, C.R., Saban, D.R., Reese, B.E., and Kay, J.N. (2019). Large-scale death of retinal astrocytes during normal development is non-apoptotic and implemented by microglia. PLoS Biol. *17*, e3000492.

Ray, T.A., Roy, S., Kozlowski, C., Wang, J., Cafaro, J., Hulbert, S.W., Wright, C.V., Field, G.D., and Kay, J.N. (2018). Formation of retinal direction-selective circuitry initiated by starburst amacrine cell homotypic contact. eLife *7*. Published online April 3, 2018. https://doi.org/10.7554/eLife.34241.

Rempe, D., Vangeison, G., Hamilton, J., Li, Y., Jepson, M., and Federoff, H.J. (2006). Synapsin I Cre transgene expression in male mice produces germline recombination in progeny. Genesis *44*, 44–49.

Rios, M., Fan, G., Fekete, C., Kelly, J., Bates, B., Kuehn, R., Lechan, R.M., and Jaenisch, R. (2001). Conditional deletion of brain-derived neurotrophic factor in the postnatal brain leads to obesity and hyperactivity. Mol. Endocrinol. *15*, 1748–1757.

Rock, J.R., Barkauskas, C.E., Cronce, M.J., Xue, Y., Harris, J.R., Liang, J., Noble, P.W., and Hogan, B.L.M. (2011). Multiple stromal populations contribute to pulmonary fibrosis without evidence for epithelial to mesenchymal transition. Proc. Natl. Acad. Sci. USA *108*, E1475–E1483.

Ross, S.E., Mardinly, A.R., McCord, A.E., Zurawski, J., Cohen, S., Jung, C., Hu, L., Mok, S.I., Shah, A., Savner, E.M., et al. (2010). Loss of inhibitory interneurons in the dorsal spinal cord and elevated itch in Bhlhb5 mutant mice. Neuron *65*, 886–898.

Rossi, J., Balthasar, N., Olson, D., Scott, M., Berglund, E., Lee, C.E., Choi, M.J., Lauzon, D., Lowell, B.B., and Elmquist, J.K. (2011). Melanocortin-4 receptors expressed by cholinergic neurons regulate energy balance and glucose homeostasis. Cell Metab. *13*, 195–204.

Rowitch, D.H., S-Jacques, B., Lee, S.M., Flax, J.D., Snyder, E.Y., and McMahon, A.P. (1999). Sonic hedgehog regulates proliferation and inhibits differentiation of CNS precursor cells. J. Neurosci. *19*, 8954–8965.

Rupp, A.C., Allison, M.B., Jones, J.C., Patterson, C.M., Faber, C.L., Bozadjieva, N., Heisler, L.K., Seeley, R.J., Olson, D.P., and Myers, M.G., Jr. (2018). Specific subpopulations of hypothalamic leptin receptor-expressing neurons mediate the effects of early developmental leptin receptor deletion on energy balance. Mol. Metab. *14*, 130–138.

Saher, G., Brügger, B., Lappe-Siefke, C., Möbius, W., Tozawa, R., Wehr, M.C., Wieland, F., Ishibashi, S., and Nave, K.-A. (2005). High cholesterol level is essential for myelin membrane growth. Nat. Neurosci. *8*, 468–475.

Saijo, K., Schmedt, C., Su, I.-H., Karasuyama, H., Lowell, C.A., Reth, M., Adachi, T., Patke, A., Santana, A., and Tarakhovsky, A. (2003). Essential role of Src-family protein tyrosine kinases in NF-kappaB activation during B cell development. Nat. Immunol. *4*, 274–279.

Saito, H., Tsumura, H., Otake, S., Nishida, A., Furukawa, T., and Suzuki, N. (2005). L7/Pcp-2-specific expression of Cre recombinase using knock-in approach. Biochem. Biophys. Res. Commun. *331*, 1216–1221.

Sanchis-Segura, C., Borchardt, T., Vengeliene, V., Zghoul, T., Bachteler, D., Gass, P., Sprengel, R., and Spanagel, R. (2006). Involvement of the AMPA receptor GluR-C subunit in alcohol-seeking behavior and relapse. J. Neurosci. *26*, 1231–1238.

Sanz, E., Yang, L., Su, T., Morris, D.R., McKnight, G.S., and Amieux, P.S. (2009). Cell-type-specific isolation of ribosome-associated mRNA from complex tissues. Proc. Natl. Acad. Sci. USA *106*, 13939–13944.

Sauer, B., and Henderson, N. (1988). Site-specific DNA recombination in mammalian cells by the Cre recombinase of bacteriophage P1. Proc. Natl. Acad. Sci. USA *85*, 5166–5170.

Schmidt, E.E., Taylor, D.S., Prigge, J.R., Barnett, S., and Capecchi, M.R. (2000). Illegitimate Cre-dependent chromosome rearrangements in transgenic mouse spermatids. Proc. Natl. Acad. Sci. USA *97*, 13702–13707.

Schwenk, F., Baron, U., and Rajewsky, K. (1995). A cre-transgenic mouse strain for the ubiquitous deletion of loxP-flanked gene segments including deletion in germ cells. Nucleic Acids Res. *23*, 5080–5081.

Shimshek, D.R., Jensen, V., Celikel, T., Geng, Y., Schupp, B., Bus, T., Mack, V., Marx, V., Hvalby, Ø., Seeburg, P.H., and Sprengel, R. (2006). Forebrain-specific glutamate receptor B deletion impairs spatial memory but not hippocampal field long-term potentiation. J. Neurosci. *26*, 8428–8440.

Silberberg, S.N., Taher, L., Lindtner, S., Sandberg, M., Nord, A.S., Vogt, D., Mckinsey, G.L., Hoch, R., Pattabiraman, K., Zhang, D., et al. (2016). Subpallial Enhancer Transgenic Lines: a Data and Tool Resource to Study Transcriptional Regulation of GABAergic Cell Fate. Neuron *92*, 59–74.

Simmons, A.B., Bloomsburg, S.J., Billingslea, S.A., Merrill, M.M., Li, S., Thomas, M.W., and Fuerst, P.G. (2016). Pou4f2 knock-in Cre mouse: A multifaceted genetic tool for vision researchers. Mol. Vis. *22*, 705–717.

Song, A.J., and Palmiter, R.D. (2018). Detecting and Avoiding Problems When Using the Cre-lox System. Trends Genet. *34*, 333–340.

Soriano, P. (1999). Generalized lacZ expression with the ROSA26 Cre reporter strain. Nat. Genet. *21*, 70–71.

Sousa, V.H., Miyoshi, G., Hjerling-Leffler, J., Karayannis, T., and Fishell, G. (2009). Characterization of Nkx6-2-derived neocortical interneuron lineages. Cereb. Cortex *19* (19, Suppl 1), i1–i10.

Steinmetz, N.A., Buetfering, C., Lecoq, J., Lee, C.R., Peters, A.J., Jacobs, E.A.K., Coen, P., Ollerenshaw, D.R., Valley, M.T., de Vries, S.E.J., et al. (2017). Aberrant Cortical Activity in Multiple GCaMP6-Expressing Transgenic Mouse Lines. eNeuro. Published online September 6, 2017. https://doi.org/10.1523/ENEURO.0207-17.2017.

Sternberg, N., and Hamilton, D. (1981). Bacteriophage P1 site-specific recombination. I. Recombination between loxP sites. J. Mol. Biol. *150*, 467–486.

Stogsdill, J.A., Ramirez, J., Liu, D., Kim, Y.H., Baldwin, K.T., Enustun, E., Ejikeme, T., Ji, R.-R., and Eroglu, C. (2017). Astrocytic neuroligins

control astrocyte morphogenesis and synaptogenesis. Nature *551*, 192–197.

Tabor, K.M., Marquart, G.D., Hurt, C., Smith, T.S., Geoca, A.K., Bhandiwad, A.A., Subedi, A., Sinclair, J.L., Rose, H.M., Polys, N.F., and Burgess, H.A. (2019). Brain-wide cellular resolution imaging of Cre transgenic zebrafish lines for functional circuit-mapping. eLife *8*. Published online February 8, 2019. https://doi.org/10.7554/eLife.42687.

Tachibana, N., Touahri, Y., Dixit, R., David, L.A., Adnani, L., Cantrup, R., Aavani, T., Wong, R.O., Logan, C., Kurek, K.C., and Schuurmans, C. (2018). Hamartoma-like lesions in the mouse retina: an animal model of *Pten* hamartoma tumour syndrome. Dis. Model. Mech. *11*, 11.

Takada, Y., Beyer, L.A., Swiderski, D.L., O'Neal, A.L., Prieskorn, D.M., Shivatzki, S., Avraham, K.B., and Raphael, Y. (2014). Connexin 26 null mice exhibit spiral ganglion degeneration that can be blocked by BDNF gene therapy. Hear. Res. *309*, 124–135.

Taniguchi, H., He, M., Wu, P., Kim, S., Paik, R., Sugino, K., Kvitsiani, D., Fu, Y., Lu, J., Lin, Y., et al. (2011). A resource of Cre driver lines for genetic targeting of GABAergic neurons in cerebral cortex. Neuron *71*, 995–1013.

Terauchi, A., Johnson-Venkatesh, E.M., Bullock, B., Lehtinen, M.K., and Umemori, H. (2016). Retrograde fibroblast growth factor 22 (FGF22) signaling regulates insulin-like growth factor 2 (IGF2) expression for activity-dependent synapse stabilization in the mammalian brain. eLife *5*, e12151.

Terauchi, A., Gavin, E., Wilson, J., and Umemori, H. (2017). Selective Inactivation of Fibroblast Growth Factor 22 (FGF22) in CA3 Pyramidal Neurons Impairs Local Synaptogenesis and Affective Behavior Without Affecting Dentate Neurogenesis. Front. Synaptic Neurosci. *9*, 17.

Tolson, K.P., Gemelli, T., Gautron, L., Elmquist, J.K., Zinn, A.R., and Kublaoui, B.M. (2010). Postnatal Sim1 deficiency causes hyperphagic obesity and reduced Mc4r and oxytocin expression. J. Neurosci. *30*, 3803–3812.

Traka, M., Podojil, J.R., McCarthy, D.P., Miller, S.D., and Popko, B. (2016). Oligodendrocyte death results in immune-mediated CNS demyelination. Nat. Neurosci. *19*, 65–74.

Traunmüller, L., Bornmann, C., and Scheiffele, P. (2014). Alternative splicing coupled nonsense-mediated decay generates neuronal cell type-specific expression of SLM proteins. J. Neurosci. *34*, 16755–16761.

Tronche, F., Kellendonk, C., Kretz, O., Gass, P., Anlag, K., Orban, P.C., Bock, R., Klein, R., and Schütz, G. (1999). Disruption of the glucocorticoid receptor gene in the nervous system results in reduced anxiety. Nat. Genet. *23*, 99–103.

Trumpp, A., Depew, M.J., Rubenstein, J.L., Bishop, J.M., and Martin, G.R. (1999). Cre-mediated gene inactivation demonstrates that FGF8 is required for cell survival and patterning of the first branchial arch. Genes Dev. *13*, 3136–3148.

Tsai, P.T., Hull, C., Chu, Y., Greene-Colozzi, E., Sadowski, A.R., Leech, J.M., Steinberg, J., Crawley, J.N., Regehr, W.G., and Sahin, M. (2012). Autistic-like behaviour and cerebellar dysfunction in Purkinje cell *Tsc1* mutant mice. Nature *488*, 647–651.

Tsien, J.Z., Chen, D.F., Gerber, D., Tom, C., Mercer, E.H., Anderson, D.J., Mayford, M., Kandel, E.R., and Tonegawa, S. (1996a). Subregion- and cell type-restricted gene knockout in mouse brain. Cell *87*, 1317–1326.

Tsien, J.Z., Huerta, P.T., and Tonegawa, S. (1996b). The essential role of hippocampal CA1 NMDA receptor-dependent synaptic plasticity in spatial memory. Cell *87*, 1327–1338.

Vong, L., Ye, C., Yang, Z., Choi, B., Chua, S., Jr., and Lowell, B.B. (2011). Leptin action on GABAergic neurons prevents obesity and reduces inhibitory tone to POMC neurons. Neuron *71*, 142–154.

Wang, Y., Rattner, A., Zhou, Y., Williams, J., Smallwood, P.M., and Nathans, J. (2012). Norrin/Frizzled4 signaling in retinal vascular development and blood brain barrier plasticity. Cell *151*, 1332–1344.

Wende, H., Lechner, S.G., Cheret, C., Bourane, S., Kolanczyk, M.E., Pattyn, A., Reuter, K., Munier, F.L., Carroll, P., Lewin, G.R., and Birchmeier, C. (2012). The transcription factor c-Maf controls touch receptor development and function. Science *335*, 1373–1376.

Weng, D.Y., Zhang, Y., Hayashi, Y., Kuan, C.-Y., Liu, C.-Y., Babcock, G., Weng, W.-L., Schwemberger, S., and Kao, W.W.-Y. (2008). Promiscuous recombination of LoxP alleles during gametogenesis in cornea Cre driver mice. Mol. Vis. *14*, 562–571.

Witten, I.B., Steinberg, E.E., Lee, S.Y., Davidson, T.J., Zalocusky, K.A., Brodsky, M., Yizhar, O., Cho, S.L., Gong, S., Ramakrishnan, C., et al. (2011). Recombinase-driver rat lines: tools, techniques, and optogenetic application to dopamine-mediated reinforcement. Neuron *72*, 721–733.

Wojcinski, A., Morabito, M., Lawton, A.K., Stephen, D.N., and Joyner, A.L. (2019). Genetic deletion of genes in the cerebellar rhombic lip lineage can stimulate compensation through adaptive reprogramming of ventricular zone-derived progenitors. Neural Dev. *14*, 4.

Xu, Q., Tam, M., and Anderson, S.A. (2008). Fate mapping Nkx2.1-lineage cells in the mouse telencephalon. J. Comp. Neurol. *506*, 16–29.

Yang, L., Cai, C.-L., Lin, L., Qyang, Y., Chung, C., Monteiro, R.M., Mummery, C.L., Fishman, G.I., Cogen, A., and Evans, S. (2006). Isl1Cre reveals a common Bmp pathway in heart and limb development. Development *133*, 1575–1585.

Young, P., Qiu, L., Wang, D., Zhao, S., Gross, J., and Feng, G. (2008). Single-neuron labeling with inducible Cre-mediated knockout in transgenic mice. Nat. Neurosci. *11*, 721–728.

Yu, W.-M., Appler, J.M., Kim, Y.-H., Nishitani, A.M., Holt, J.R., and Goodrich, L.V. (2013). A Gata3-Mafb transcriptional network directs post-synaptic differentiation in synapses specialized for hearing. eLife *2*, e01341.

Zeller, A., Crestani, F., Camenisch, I., Iwasato, T., Itohara, S., Fritschy, J.M., and Rudolph, U. (2008). Cortical glutamatergic neurons mediate the motor sedative action of diazepam. Mol. Pharmacol. *73*, 282–291.

Zerucha, T., Stühmer, T., Hatch, G., Park, B.K., Long, Q., Yu, G., Gambarotta, A., Schultz, J.R., Rubenstein, J.L.R., and Ekker, M. (2000). A highly conserved enhancer in the Dlx5/Dlx6 intergenic region is the site of cross-regulatory interactions between Dlx genes in the embryonic forebrain. J. Neurosci. *20*, 709–721.

Zhang, J., Dublin, P., Griemsmann, S., Klein, A., Brehm, R., Bedner, P., Fleischmann, B.K., Steinhäuser, C., and Theis, M. (2013). Germ-line recombination activity of the widely used hGFAP-Cre and nestin-Cre transgenes. PLoS ONE *8*, e82818.

Zheng, B., Sage, M., Sheppeard, E.A., Jurecic, V., and Bradley, A. (2000). Engineering mouse chromosomes with Cre-loxP: range, efficiency, and somatic applications. Mol. Cell. Biol. *20*, 648–655.

Zheng, R., Yang, L., Sikorski, M.A., Enns, L.C., Czyzyk, T.A., Ladiges, W.C., and McKnight, G.S. (2013). Deficiency of the RIIβ subunit of PKA affects locomotor activity and energy homeostasis in distinct neuronal populations. Proc. Natl. Acad. Sci. USA *110*, E1631–E1640.

Zhou, Y.-X., Zhao, M., Li, D., Shimazu, K., Sakata, K., Deng, C.-X., and Lu, B. (2003). Cerebellar deficits and hyperactivity in mice lacking Smad4. J. Biol. Chem. *278*, 42313–42320.

Zhu, Y., Romero, M.I., Ghosh, P., Ye, Z., Charnay, P., Rushing, E.J., Marth, J.D., and Parada, L.F. (2001). Ablation of NF1 function in neurons induces abnormal development of cerebral cortex and reactive gliosis in the brain. Genes Dev. *15*, 859–876.

Zhuang, X., Masson, J., Gingrich, J.A., Rayport, S., and Hen, R. (2005). Targeted gene expression in dopamine and serotonin neurons of the mouse brain. J. Neurosci. Methods *143*, 27–32.

Zhuo, L., Theis, M., Alvarez-Maya, I., Brenner, M., Willecke, K., and Messing, A. (2001). hGFAP-cre transgenic mice for manipulation of glial and neuronal function in vivo. Genesis *31*, 85–94.

Zirlinger, M., Lo, L., McMahon, J., McMahon, A.P., and Anderson, D.J. (2002). Transient expression of the bHLH factor neurogenin-2 marks a subpopulation of neural crest cells biased for a sensory but not a neuronal fate. Proc. Natl. Acad. Sci. USA *99*, 8084–8089.

STAR★METHODS

KEY RESOURCES TABLE

REAGENT or RESOURCE	SOURCE	IDENTIFIER
Experimental Models: Organisms/Strains		
Mouse: *Adgrb3*^{tm1Ksak}	A gift from Dr. Kenji Sakimura	MGI:5708584
Mouse: B6-Tg(Adora2a-Cre)KG139GSat	Mutant Mouse Resource & Research Centers (MMRRC)	MMRRC_036158-UCD
Mouse: *Atg5*^{tm1Myok}	Riken BioResource Center	MGI:3663625
Mouse: B6; *Bhlhe22*$^{tm3.1(cre)Meg}$	A gift from Dr. Sarah Ross (Michael E Greenberg Lab)	MGI:4440745
Mouse: *Cacna1a*^{tm1Kano}	A gift from Dr. Masanobu Kano	MGI:5140539
Mouse: Tg(Camk2a-cre)159Kln	A gift from Klein lab (Minichiello et al., 1999)	MGI:2176753
Mouse: B6-Tg(Camk2a-cre)T29-1Stl	The Jackson Laboratory	IMSR_JAX:005359
Mouse: B6;129S6-*Chat*$^{tm2(cre)Lowl}$/J	The Jackson Laboratory	IMSR_JAX:006410
Mouse: B6,129-*Chat*/*Slc18a3*$^{tm1.2Vpra}$	Prado lab (Martins-Silva et al., 2011)	MGI:1101061
Mouse: *Clstn3*^{tm1Amcr}/J	Craig lab (Pettem et al., 2013)	MGI:5521371
Mouse: B6.Cg-*Csf1r*$^{tm1.2Jwp}$/J	The Jackson Laboratory	IMSR_JAX:021212
Mouse: B6.Cg-*Cux2*$^{tm3.1(cre/ERT2)Mull}$/Mmmh	MMRRC	MMRRC_032779-MU
Mouse: *Cx3cr1*$^{tm2.1(cre/ERT2)Litt}$/WganJ	The Jackson Laboratory	IMSR_JAX:021160
Mouse: B6-Tg(dlx5a-cre)1Mekk/J	The Jackson Laboratory	IMSR_JAX:008199
Mouse: *Dnmt3a*$^{tm3.1Enl}$	Dr. Margaret Goodell, Baylor College of Medicine (Can be purchased from Riken BRC)	IMSR_RBRC03731
Mouse: B6-Tg(Drd1-Cre)EY262GSat	MMRRC	MMRRC_017264-UCD
Mouse: Tg(Drd2-cre)ER44Gsat/Mmucd	MMRC	MMRRC_017263-UCD
Mouse: B6.129S2-*Emx1*$^{tm1(cre)Krj}$/J	The Jackson Laboratory	IMSR_JAX:005628
Mouse: *En1*$^{tm2(cre)Wrst}$/J	The Jackson Laboratory	IMSR_JAX: 007916
Mouse: *Epas1*^{tm1Mcs}/J	The Jackson Laboratory	IMSR_JAX: 008407
Mouse: *Erc2*$^{tm1.1Sud}$/J	Generated by P.S. Kaeser and T.C. Sudhof, available at the Jackson Laboratory	IMSR_JAX:015831
Mouse: *Fdft1*^{tm1Kan}	Saher lab (Saher et al., 2005)	MGI:3579504
Mouse: *Fgf22*$^{tm1a(EUCOMM)Hmgu}$	European Conditional Mouse Mutagenesis Program (EUCOMM)	IMSR_EM:06822
Mouse: *Flrt2*$^{tm1c(EUCOMM)Wtsi}$	EMMA repository	MGI:6119416
Mouse: B6;129S4-*Foxd1*$^{tm1(GFP/cre)Amc}$/J	The Jackson Laboratory	IMSR_JAX:012463
Mouse: 129(Cg)-*Foxg1*$^{tm1(cre)Skm}$/J	The Jackson Laboratory	IMSR_JAX: 006084
Mouse: B6N.Cg-*Gad2*$^{tm2(cre)Zjh}$/J	The Jackson Laboratory	IMSR _JAX:019022
Mouse: FVB-Tg(GFAP-cre)25Mes/J	The Jackson Laboratory	IMSR _JAX:004600
Mouse: B6.Cg-Tg(Gfap-cre)77.6Mvs/2J	The Jackson Laboratory	IMSR _JAX:024098
Mouse: B6-Tg(Gpr26-cre) KO250Gsat/Mmucd	MMRRC	MMRRC_036915-UCD
Mouse: *Gria1*^{tm2Rsp}	A gift from Dr. Rolf Sprengel	IMRS_JAX: 019012
Mouse: *Gria2*^{tm3Rsp}	A gift from Dr. Rolf Sprengel	MGI:3611335
Mouse: *Gria3*^{tm1Rsp}	A gift from Dr. Rolf Sprengel	MGI:3611328
Mouse: *Grik2*$^{tm1.1Ksak}$	A gift from Dr. Kenji Sakimura	MGI:6117330
Mouse: B6-Tg(Grik4-cre)G32-4Stl/J	The Jackson Laboratory	IMSR_JAX:006474

(*Continued on next page*)

Continued

REAGENT or RESOURCE	SOURCE	IDENTIFIER
Mouse: *Grik4*$^{tm1(cre)Ksak}$	Sakimura lab (Akashi et al., 2009)	MGI: 4360478
Mouse: *Grin1*^{tm2Stl}	The Jackson Laboratory	IMRS_JAX:005246
Mouse: *Grin2c*$^{tm2(icre)Mwa}$	A gift from Dr. Masahiko Matanabe	MGI:5306941
Mouse: CBy.B6-*Gt(ROSA) 26Sor*$^{tm1(HBEGF)Awai}$/J	The Jackson Laboratory	IMRS_JAX: 007900
Mouse: *Gt(ROSA) 26Sor*$^{tm1.1(CAG-EGFP)Fsh}$/Mmjax	The Jackson Laboratory	MMRRC_ 32037-JAX
Mouse: *Gt(ROSA)26Sor*$^{tm2(CAG-tdTomato)Fawa}$	Dr. Fan Wang (Duke)	MGI:5305341
Mouse: *Gt(ROSA) 26Sor*$^{tm4(ACTB-tdTomato,-EGFP)Luo}$/J	The Jackson Laboratory	IMRS_JAX:007676
Mouse: B6.Cg-*Gt(ROSA) 26Sor*$^{tm9(CAG-tdTomato)Hze}$/J	The Jackson Laboratory	IMSR_JAX: 007909
Mouse: Ai14: B6.Cg-*Gt(ROSA) 26Sor*$^{tm14(CAG-tdTomato)Hze}$/J	The Jackson Laboratory	IMSR_JAX:007914
Mouse: Ai32: B6;129S-*Gt(ROSA) 26Sor*$^{tm32(CAG-COP4*H134R/EYFP)Hze}$/J	A gift from Dr. Timothy Murphy, originally from The Jackson Laboratory	IMSR_JAX:012569
Mouse: *Gt(ROSA)26Sor*$^{tm32(CAG-tdTomato)Hze}$	The Jackson Laboratory	IMSR_JAX:007908
Mouse: Ai34: 129S-*Gt(ROSA) 26Sor*$^{tm34.1(CAG-Syp/tdTomato)Hze}$/J	Gift from Dr. David Ginty, available at the Jackson Laboratory	IMSR_JAX:012570
Mouse: B6.Cg-*H2afv*$^{Tg(Wnt1-cre)11Rth}$	The Jackson Laboratory	IMSR_JAX:009107
Mouse: Tg(hs799-cre/ERT2,-GFP)405Jlr	N/A	MMRRC: 037574-UCD
Mouse: Tg(Htr3a-cre)NO152Gsat/Mmucd	MMRRC	MMRRC_036680
Mouse: Tg(I12b–cre)1Jlr	N/A	MMRRC_031698-UCD
Mouse: B6;129S6-*Igs7*$^{tm93.1(tetO-GCaMP6f)Hze}$/J	The Jackson Laboratory	IMSR_JAX:024103
Mouse: *Isl1*$^{tm1(cre)Sev}$/J	The Jackson Laboratory	IMSR_Jax:024242
Mouse: *Isl1*$^{tm1.1Whk}$	Xiuqian Mu	MGI:3837972
Mouse: *Khdrbs3*$^{tm1.1Schei}$/J	Generated in the Scheiffele Laboratory (deposited at Jackson)	IMSR_JAX:029273
Mouse: B6;129P-*Klf3*$^{tm1(cre/ERT2)Pzg}$/J	The Jackson Laboratory	IMSR_JAX:010985
Mouse: *Maf*$^{tm2.1Cbm}$	Gift from Dr. Carmen Birchmeier	MGI:5316895
Mouse: *Mafb*$^{tm1.1Good}$	Gift from Dr. Lisa Goodrich	MGI:5581684
Mouse: *Megf10*$^{tm1c(KOMP)Jrs}$	Josh Sanes lab	MGI:6194031
Mouse: *Neo1*$^{tm1.1Jfcl}$	Cloutier lab (Kam et al., 2016)	MGI:6285614
Mouse: B6.Cg-Tg(Nes-cre)1Kln/J	The Jackson Laboratory	IMSR_JAX: 003771
Mouse: *Neurod6*$^{tm1(cre)Kan}$	Goebbels lab (Goebbels et al., 2006)	MGI:2668659
Mouse: *Neurog2*$^{tm1(cre/Esr1)And}$	MMRRC	MGI:2652037
Mouse: Tg(Nkx2-1-cre)2Sand	Gift from Dr. Stewart Anderson	IMSR_JAX:008661
Mouse: B6;SJL-*Nlgn2*$^{tm1.1Sud}$/J	The Jackson Laboratory	IMSR_JAX:025544
Mouse: B6.Cg-Tg(Ntsr1-cre) GN220Gsat/Mmucd	MMRRC	MMRRC_030648-UCD
Mouse: B6.129-*Pcp2*$^{tm1(cre)Nobs}$	A gift from Dr. Noboru Suzuki	MGI:3578623
Mouse: B6.129-Tg(Pcp2-cre)2Mpin/J	The Jackson Laboratory	IMSR_JAX:004146
Mouse: PhotonSABER-LSL	Generated by S. Matsuda and M. Yuzaki	N/A
Mouse: *Ptf1a*^{tm3Cvw}	Christopher Wright	MGI:5788429
Mouse: B6.129P2-*Pvalb*$^{tm1(cre)Arbr}$/J	The Jackson Laboratory	IMSR_JAX:017320

(*Continued on next page*)

Continued

REAGENT or RESOURCE	SOURCE	IDENTIFIER
Mouse: B6.129S1(Cg)-*Rai1*$^{tm2.1Luo}$/J	Luo lab (Huang et al., 2016)	IMSR_JAX:029103
Mouse: B6.FVB(Cg)-Tg(Rbp4-cre) KL100Gsat/Mmucd/GENSAT	MMRRC	MMRRC_037128-UCD
Mouse: *Rims1*^{tm3Sud}/J	Generated by P.S. Kaeser and T.C. Sudhof, available at the Jackson Laboratory	IMSR_JAX:015832
Mouse: *Rims2*$^{tm1.1Sud}$/J	Generated by P.S. Kaeser and T.C. Sudhof, available at the Jackson Laboratory	IMSR_JAX:015833
Mouse: B6.129S-*Rorb*$^{tm1.1(cre)Hze}$/J	The Jackson Laboratory	IMSR_JAX_023526
Mouse: *Rpl22*$^{tm1.1Psam}$/J	The Jackson Laboratory	IMSR_JAX:011029
Mouse: B6;C3-Tg(Scnn1a-cre)2Aibs/J	The Jackson Laboratory	IMSR_JAX_009613
Mouse: Tg(Scx-GFP/cre)1Stzr	A gift from Dr. Jenna Lauren Galloway (Clifford Tabin Lab)	MGI:5317938
Mouse: Tg(Sim1-cre)1Lowl/J	A gift from Dr. Bradford Lowell	IMSR_JAX:006395
Mouse: Tg(Six3-cre)69Frty/GcoJ	A gift from Dr. Guillermo Oliver. Available at The Jackson Laboratory	IMSR_JAX: 019755
Mouse: Tg(Slc1a3-cre/ERT)1Nat/J	The Jackson Laboratory	IMSR_JAX: 012586
Mouse: *Slc6a3*$^{tm1.1(cre)Bkmn}$/J	A gift from Dr. Thomas Hnasko, originally from The Jackson Laboratory	IMRS_JAX: 006660
Mouse: B6.129(Cg)-*Slc6a4*$^{tm1(cre)Xz}$/J	Available at the Jackson Laboratory	IMRS_JAX# 014554
Mouse: *Slc16a1*$^{lox/lox}$	Rothstein lab (Jha et al., 2019)	N/A
Mouse: *Slc17a6*$^{tm2(cre)Lowl}$/J	The Jackson Laboratory	IMSR _JAX: 016963
Mouse: B6;129S-*Slc17a7*$^{tm1.1(cre)Hze}$/J	The Jackson Laboratory	IMSR _JAX: 023527
Mouse: Tg(Slc17a8-icre)1Edw/SealJ	A gift from Dr. Robert Edward. Available at The Jackson Laboratory	IMSR_JAX: 018147
Mouse: B6;129- Tg(Slc18a3-cre)KMisa/0	Riken BioResource Center	RBRC_No.RBRC01515
Mouse: B6.FVB-Tg(Slc32a1-cre) 2.1Hzo/FrkJ/	The Jackson Laboratory	IMSR_JAX:017535
Mouse: B6J.129S6(FVB)-*Slc32a1*$^{tm2(cre)Lowl}$/MwarJ	The Jackson Laboratory	IMSR _JAX: 028862
Mouse: B6;CBA-Tg(Sox10-cre)1Wdr/J	The Jackson Laboratory	IMSR _JAX: 025807
Mouse: *Sst*$^{tm2.1(cre)Zjh}$	The Jackson Laboratory	IMSR_JAX:013044
Mouse: *Stxbp1*^{tm1Mver}	Verhage lab (Heeroma et al., 2004)	MGI:5509149
Mouse: *Syk*$^{tm1.2Tara}$	The Jackson Laboratory	IMSR_JAX:017309
Mouse: B6.Cg-Tg(Syn1-cre)671Jxm/J	Gift from Dr. Lisa Goodrich, available at the Jackson Laboratory	IMSR_JAX:00396
Mouse: *Tgfb3*^{tm1Moaz}	The Jackson Laboratory	IMSR_JAX:024931
Mouse: Tg(Thy1-cre/ERT2,-EYFP) HGfng/PyngJ	The Jackson Laboratory	IMSR_JAX:012708
Mouse: *Trpm7*^{tm1Clph}/J	The Jackson Laboratory	IMRS_JAX:018784
Mouse: B6-*Vip*$^{tm1(cre)Zjh}$/J	The Jackson Laboratory	IMSR_JAX:031628
Mouse: *Wwp1*$^{tm1.1Hkb}$/N	Kawabe lab (Ambrozkiewicz et al., 2018)	MGI:6281946
Mouse: *Wwp2*$^{tm1.1Hkb}$/N	Kawabe lab (Ambrozkiewicz et al., 2018)	MGI:6281948
Zebrafish *D. rerio*: Et(REX2-SCP1-Ocu.Hbb2:Cre-2A-Cerulean)y492	Burgess lab (Tabor et al., 2019)	ZFIN:ZDB-ALT-180717–56
Zebrafish *D. rerio*: Et(REX2-SCP1-Ocu.Hbb2:Cre)y547	Burgess lab (Tabor et al., 2019)	ZFIN:ZDB-ALT-180717–80
Zebrafish *D. rerio*: Et(REX2-SCP1-Ocu.Hbb2:Cre)y549	Burgess lab (Tabor et al., 2019)	ZFIN:ZDB-ALT-180717–82

(*Continued on next page*)

Continued

REAGENT or RESOURCE	SOURCE	IDENTIFIER
Zebrafish *D. rerio*: Et(REX2-SCP1-Ocu.Hbb2:Cre)y559	Burgess lab (Tabor et al., 2019)	ZFIN:ZDB-ALT-180717–92
Zebrafish *D. rerio*: Et(REX2-SCP1-Ocu.Hbb2:Cre-2A-Cerulean)y546	Burgess lab (Tabor et al., 2019)	ZFIN:ZDB-ALT-180717–79
Zebrafish *D. rerio*: Et(REX2-SCP1-Ocu.Hbb2:Cre)y555	Burgess lab (Tabor et al., 2019)	ZFIN:ZDB-ALT-180717–88
Oligonucleotides		
Primers, see Table S1		

LEAD CONTACT AND MATERIALS AVAILABILITY

Further information and requests for resources and reagents should be directed to and will be fulfilled by the Lead Contact, Dr. Ann Marie Craig (acraig@mail.ubc.ca). Inquiries concerning the e-mail addresses of the investigators who contributed information regarding specified Cre driver lines in Table 1 should be directed to the Lead Contact.

EXPERIMENTAL MODEL AND SUBJECT DETAILS

All mice used and agencies approving procedures are as follows: the Canadian Council for Animal Care and the University of British Columbia Animal Care Committee: *Clstn3*^{tm1Amcr}/J (Pettem et al., 2013), Ai32 (Madisen et al., 2012), B6-Tg(dlx5a-cre)1Mekk/J (Zerucha et al., 2000), B6-Tg(Gpr26-cre)KO250Gsat/Mmucd (GENSAT Project); Association for the Assessment and Accreditation of Laboratory Animal Care and Stanford University's Administrative Panel on Laboratory Animal Care: Tg(Sim1-cre)1Lowl/J (Balthasar et al., 2005), B6.129S1(Cg)-*Rai1*$^{tm2.1Luo}$/J (Huang et al., 2016), B6.129S2-*Emx1*$^{tm1(cre)Krj}$/J (Gorski et al., 2002), B6N.Cg-*Gad2*$^{tm2(cre)Zjh}$/J (Taniguchi et al., 2011), B6.Cg-Tg(Nes-cre)1Kln/J (Tronche et al., 1999), B6J.129S6(FVB)-*Slc32a1*$^{tm2(cre)Lowl}$/MwarJ (Vong et al., 2011), B6;129S-*Slc17a7*$^{tm1.1(cre)Hze}$/J (Harris et al., 2014), *Slc17a6*$^{tm2(cre)Lowl}$/J (Vong et al., 2011); University of California San Francisco Laboratory Animal Research Center: Tg(Nkx2-1-cre)2Sand (Xu et al., 2008), Tg(hs799-cre/ERT2,-GFP)405Jlr (Silberberg et al., 2016), *Tg(I12b–cre)1Jlr* (Potter et al., 2009), *Mafb*$^{tm1.1Good}$ (Yu et al., 2013), *Maf*$^{tm2.1Cbm}$ (Wende et al., 2012), *Gt(ROSA)26Sor*$^{tm32(CAG-tdTomato)Hze}$, B6.Cg-*Gt(ROSA)26Sor*$^{tm14(CAG-tdTomato)Hze}$/J (Madisen et al., 2010), *Sst*$^{tm2.1(cre)Zjh}$ (Taniguchi et al., 2011); The Canadian Council for Animal Care and the University Western Ontario Animal Care Committee: Tg(Drd2-cre)ER44Gsat/Mmucd (Gong et al., 2007), *En1*$^{tm2(cre)Wrst}$/J (Kimmel et al., 2000), 129(Cg)-*Foxg1*$^{tm1(cre)Skm}$/J (Hébert and McConnell, 2000), C57BL/6J-Tg(Nkx2-1-cre)2Sand/J (Xu et al., 2008), Tg(Six3-cre)69Frty/GcoJ (Furuta et al., 2000), B6;129- Tg(SLC18A3-cre)KMisa/0 (Misawa et al., 2003), Tg(Slc17a8-icre)1Edw/SealJ (Divito et al., 2015), B6,129-*Chat/Slc18a3*$^{tm1.2Vpra}$ (Martins-Silva et al., 2011); Fudan University and Tsinghua University Committees on Animal Care and Use: *Trpm7*^{tm1Clph}/J (Jin et al., 2008), B6-Tg(Camk2a-cre)T29-1Stl (Tsien et al., 1996b), B6.129P2-*Pvalb*$^{tm1(cre)Arbr}$/J (Hippenmeyer et al., 2005); The NINDS Animal Care and Use Committee: *Gria1*^{tm2Rsp} (Engblom et al., 2008), *Gria2*^{tm3Rsp} (Shimshek et al., 2006), *Gria3*^{tm1Rsp} (Sanchis-Segura et al., 2006), *Grin1*^{tm2Stl} (Tsien et al., 1996b), B6.Cg-*Gt(ROSA)26Sor*$^{tm14(CAG-tdTomato)Hze}$/J (Madisen et al., 2010), *Slc6a3*$^{tm1.1(cre)Bkmn}$/J (Bäckman et al., 2006); Niedersächsisches Landesamt für Verbraucherschutz und Lebensmittelsicherheit: *Wwp1*$^{tm1.1Hkb}$/N (Ambrozkiewicz et al., 2018), *Wwp2*$^{tm1.1Hkb}$/N (Ambrozkiewicz et al., 2018), B6.129S2-*Emx1*$^{tm1(cre)Krj}$/J (Gorski et al., 2002), *Neurod6*$^{tm1(cre)Kan}$ (Goebbels et al., 2006), Tg(Camk2a-cre)159Kln (Minichiello et al., 1999), *Fdft1*^{tm1Kan} (Saher et al., 2005); The Kobe University Animal Care and Use Committee: *Grik4*$^{tm1(cre)Ksak}$ (Akashi et al., 2009), B6.Cg-*Gt(ROSA)26Sor*$^{tm9(CAG-tdTomato)Hze}$/J (Madisen et al., 2010); Institutional Animal Care and Use Committee of Harvard Medical School: Tg(Six3-cre)69Frty/GcoJ (Furuta et al., 2000), B6.SJL-*Slc6a3*$^{tm1.1(cre)Bkmn}$/J (Bäckman et al., 2006), *Rims1*^{tm3Sud}/J (Kaeser et al., 2008), *Rims2*$^{tm1.1Sud}$/J (Kaeser et al., 2011), Ai34 (MGI Direct Data Submission, J:170755), Tg(Nes-cre)1Kln/J (Tronche et al., 1999), B6.Cg-Tg(Syn1-cre)671Jxm/J (Zhu et al., 2001), *Erc2*$^{tm1.1Sud}$/J (Kaeser et al., 2009), *Slc17a7*$^{tm1.1(cre)Hze}$/J (Harris et al., 2014), B6.Cg-*Gt(ROSA)26Sor*$^{tm9(CAG-tdTomato)Hze}$/J (Madisen et al., 2010), B6; *Bhlhe22*$^{tm3.1(cre)Meg}$ (Ross et al., 2010), B6;129P-*Klf3*$^{tm1(cre/ERT2)Pzg}$/J (GenitoUrinary Development Molecular Anatomy Project (GUDMAP)), *Neurog2*$^{tm1(cre/Esr1)And}$ (Zirlinger et al., 2002), Tg(Scx-GFP/cre)1Stzr (Blitz et al., 2009), B6;129S4-*Foxd1*$^{tm1(GFP/cre)Amc}$/J (Humphreys et al., 2010); The Canadian Council for Animal Care and the Montreal Neurological Institute Animal Care Committee: *Neo1*$^{tm1.1Jfcl}$ (Kam et al., 2016), B6.Cg-*H2afv*$^{Tg(Wnt1-cre)11Rth}$ (Danielian et al., 1998; Rowitch et al., 1999); Stanford University's Administrative Panel on Laboratory Animal Care: B6.SJL-*Slc6a3*$^{tm1.1(cre)Bkmn}$/J (Bäckman et al., 2006), B6-Tg(Drd1-Cre)EY262GSat (Gong et al., 2003), B6-*Gad2*$^{tm2(cre)Zjh}$/J (Taniguchi et al., 2011), *Slc17a6*$^{tm2(cre)Lowl}$/J (Vong et al., 2011), B6-Tg(Adora2a-Cre)KG139GSat (Gong et al., 2007), B6.Cg-*Gt(ROSA)26Sor*$^{tm14(CAG-tdTomato)Hze}$/J ; the National Institutes of Health: B6.Cg-*Gt(ROSA)26Sor*$^{tm14(CAG-tdTomato)Hze}$/J (Madisen et al., 2010), *Gt(ROSA)26Sor*$^{tm1.1(CAG-EGFP)Fsh}$/Mmjax (Sousa et al., 2009), C57BL/6J-Tg(Nkx2-1-cre)2Sand/J (Xu et al., 2008), Tg(Slc17a8-icre)1Edw/SealJ (Grimes et al., 2011), Tg(Htr3a-cre)NO152Gsat/Mmucd (Chittajallu et al., 2013); Boston Children's Hospital: C57BL/6-Tg(Grik4-cre)G32-4Stl/J (Nakazawa et al., 2002), B6.FVB(Cg)-Tg(Adora2a-cre)

KG139Gsat/Mmucd/GENSAT, B6.FVB(Cg)-Tg(Drd1-cre)EY262Gsat/Mmucd/GENSAT, B6.FVB(Cg)-Tg(Rbp4-cre)KL100Gsat/Mmucd/GENSAT (Gong et al., 2007), B6.SJL-*Slc6a3*$^{tm1.1(cre)Bkmn}$/J/JAX (Bäckman et al., 2006), Tg(Thy1-cre/ERT2,-EYFP)HGfng/PyngJ (Young et al., 2008), *Gt(ROSA)26Sor*$^{tm2(CAG-tdTomato)Fawa}$ (Rock et al., 2011), *Fgf22*$^{tm1a(EUCOMM)Hmgu}$ (Terauchi et al., 2016); Cantonal Veterinary Office of Basel-Stadt, Switzerland: B6-Tg(Camk2a-cre)T29-1Stl, B6.Cg-*Cux2*$^{tm3.1(cre/ERT2)Mull}$/Mmmh (Franco et al., 2012), B6-Tg(Grik4-cre)G32-4Stl/J (Nakazawa et al., 2002), B6.Cg-Tg(Ntsr1-cre)GN220Gsat/Mmucd (Gong et al., 2003), B6.129-*Pcp2*$^{tm1(cre)Nobs}$ (Saito et al., 2005), B6.Cg-*Gt(ROSA)26Sor*$^{tm9(CAG-tdTomato)Hze}$/J (Madisen et al., 2010), B6.129P2-*Pvalb*$^{tm1(cre)Arbr}$/J, B6.Cg-Tg(Rbp4-cre)KL100Gsat/Mmucd (Gong et al., 2003), B6.129S-*Rorb*$^{tm1.1(cre)Hze}$/J (Harris et al., 2014), B6;C3-Tg(Scnn1a-cre)2Aibs/J (Madisen et al., 2010), B6-*Sst*$^{tm2.1(cre)Zjh}$, B6-*Vip*$^{tm1(cre)Zjh}$/J (Taniguchi et al., 2011), *Khdrbs3*$^{tm1.1Schei}$/J (Traunmüller et al., 2014), *Rpl22*$^{tm1.1Psam}$/J (Sanz et al., 2009); Institutional Animal Care and Use Committee at Duke University: B6;129S6-*Chat*$^{tm2(cre)Lowl}$/J (Rossi et al., 2011), B6.Cg-*Csf1r*$^{tm1.2Jwp}$/J (Li et al., 2006), B6.129P2(Cg)-*Cx3cr1*$^{tm2.1(cre/ERT2)Litt}$/WganJ (MGI Direct Data Submission MGI: J:190965), *Epas1*^{tm1Mcs}/J (Gruber et al., 2007), B6;129-*Flrt2*$^{tm1c(EUCOMM)Wtsi}$/RobH (Del Toro et al., 2017), FVB-Tg(GFAP-cre)25Mes/J (Zhuo et al., 2001), *Isl1*$^{tm1(cre)Sev}$/J (Yang et al., 2006), *Megf10*$^{tm1c(KOMP)Jrs}$ (Kay et al., 2012), *Tgfb3*^{tm1Moaz} (Doetschman et al., 2012), *Ptf1a*^{tm3Cvw} (Krah et al., 2015), *Isl1*$^{tm1.1Whk}$ (Mu et al., 2008), Tg(Six3-cre)69Frty/GcoJ, B6.129P2-*Syk*$^{tm1.2Tara}$/J (Saijo et al., 2003), CBy.B6-*Gt(ROSA)26Sor*$^{tm1(HBEGF)Awai}$/J (Buch et al., 2005), B6.129(Cg)-*Gt(ROSA)26Sor*$^{tm4(ACTB-tdTomato,-EGFP)Luo}$/J (Muzumdar et al., 2007), B6.Cg-*Gt(ROSA)26Sor*$^{tm14(CAG-tdTomato)Hze}$/J (Madisen et al., 2010); the Animal Resource Committee of Keio University: *Grin2c*$^{tm2(icre)Mwa}$ (Miyazaki et al., 2012), *Cacna1a*^{tm1Kano} (Hashimoto et al., 2011), *Grik4*$^{tm1(cre)Ksak}$ (Akashi et al., 2009), *Grik2*$^{tm1.1\ Ksak}$ (Matsuda et al., 2016), *Adgrb3*^{tm1Ksak} (Kakegawa et al., 2015), *Atg5*^{tm1Myok} (Hara et al., 2006), B6.129-Tg(Pcp2-cre)2Mpin/J (Barski et al., 2000), PhotonSABER-LSL; The Institutional Animal Care and Use Committee and the Duke Division of Laboratory Animal Resources oversight: Tg(Slc1a3-cre/ERT)1Nat/J (Wang et al., 2012), *Nlgn2*$^{tm1.1Sud}$/J (Liang et al., 2015), *Gt(ROSA)26Sor*$^{tm14(CAG-tdTomato)Hze}$/J (Madisen et al., 2010); the nstitutional and Dutch governmental guidelines for animal welfare: B6.129(Cg)-*Slc6a4*$^{tm1(cre)Xz}$/J (Zhuang et al., 2005), *Stxbp1*^{tm1Mver} (Heeroma et al., 2004), B6-*Gad2*$^{tm2(cre)Zjh}$/J (Taniguchi et al., 2011), Baylor College of Medicine Institutional Animal Care and Use Committee: *Dnmt3a*$^{tm3.1Enl}$ (Kaneda et al., 2004), B6.FVB-Tg(Slc32a1-cre)2.1Hzo/FrkJ/ (Chao et al., 2010), the Johns Hopkins University Institutional Animal Care and Use Committee: B6.Cg-Tg(Gfap-cre)77.6Mvs/2J (Gregorian et al., 2009), *Slc16a1*$^{lox/lox}$ (Jha et al., 2019), B6;CBA-Tg(Sox10-cre)1Wdr/J (Matsuoka et al., 2005). Genotyping was performed using primers and tissues described in Table S1.

Procedures involving zebrafish were approved by the *Eunice Kennedy Shriver* National Institute of Child Health and Human Development Animal Care and Use Committee and are described in Tabor et al. (2019).

METHOD DETAILS

Brain slice imaging

Offspring from Ai32 crosses were euthanized at P14-16, brains extracted and sectioned in ice cold artificial cerebrospinal fluid (ACSF) containing (in mM): 124 NaCl, 3 KCl, 1.25 NaH_2PO_4, 1 $MgSO_47H_2O$, 2 $CaCl_2$, 26 $NaHCO_3$ and 15 D-glucose which was bubbled continuously with carbogen (95% O2/ 5% CO2) to adjust the pH to 7.3. Slices (300μm) were then recovered in 31°C ACSF for 20 min and fixed in 4% paraformaldehyde + 4% sucrose in PBS (pH 7.4) for 12 min. They were then washed in PBS containing the nuclear counterstain DAPI (4',6 diamidino-2- phenylindole), and mounted in elvanol (Tris-HCl, glycerol, and polyvinyl alcohol with 2% 1,4-diazabicyclo[2,2,2]octane). Tiled and individual images were captured on a Zeiss LSM 700 confocal microscope.

DATA AND CODE AVAILABILITY

Information from Table 1 will be incorporated in the Mutation details section for each Cre line in the MGI webpage, tagged in bold as "Germline Recombination." This particular Mutation details field is already exported to various resources, including mutant mouse repositories for display on strain data pages.